UNIVERSITY OF CALIFORNIA,
IRVINE

Performance Analysis and Enhancements for In-Band Full-Duplex Wireless Networks

DISSERTATION

submitted in partial satisfaction of the requirements
for the degree of

DOCTOR OF PHILOSOPHY

in Electrical Engineering

by

Murad Rida Q Murad

Dissertation Committee:
Professor Ahmed M. Eltawil, Chair
Professor Ender Ayanoglu
Professor A. Lee Swindlehurst

2019

DEDICATION

To those who never give up on their dreams for inspiring me not to give up on mine

TABLE OF CONTENTS

LIST OF FIGURES

LIST OF TABLES

ACKNOWLEDGMENTS

All research in this dissertation was made possible by the keen mentoring of my advisor and Dissertation Committee Chair, Dr. Ahmed M. Eltawil. His sincere guidance and genuine interest in my success are unparalleled. He has been dedicated to support me in every way during my PhD career. Every discussion I had with Dr. Eltawil has shown a new side of his brilliance. He challenged me throughout my research career, but he never doubted me. Dr. Eltawil always treated me with respect, and being extremely respectful is one his many exceptional attributes. The few words I mention here are not sufficient to describe his expertise or character.

I would like to thank Dr. Ender Ayanoglu and Dr. A. Lee Swindlehurst for serving on my Dissertation Committee. The insights they provided me since the early stages of my research have been useful in refining my initial work to construct meaningful results.

The knowledge I obtained in classrooms makes the building blocks for this dissertation. I would like to thank Dr. Ender Ayanoglu for his Digital Communications I & II courses, Dr. Thomas Ketseoglou for his Random Processes course, and Dr. Hamid Jafarkhani for his Engineering Probability course.

Developing teaching skills was a valuable part of my PhD career. I would like to thank both Dr. Franco De Flaviis and Dr. Peter Burke for giving me the opportunities to assist in their courses. I would like to thank Dr. Matthew Mahavongtrakul at the UCI Division of Teaching Excellence and Innovation for his valuable feedback and discussions about pedagogical skills. I am grateful for the kind and honest teaching evaluations I received from hundreds of undergraduate students who helped me improve my practices.

I am thankful for many professors who taught me since the time of my undergraduate education and encouraged me to pursue graduate degrees. Dr. Hen-Geul (Henry) Yeh at California State University, Long Beach taught me MATLAB programming in his Digital Signal Processing courses. I used MATLAB to generate all results in this dissertation. Dr. Melvin Lax at California State University, Long Beach excelled in teaching his mathematics courses, and he taught me how to think logically and appreciate applied mathematics. Dr. John Veillette at Vanderbilt University made every effort to ease the transition to college life, and I am grateful for the brief but precious time he supported me to succeed academically.

I would not have been able to complete any of this work without the support of my family. My wife, Rua, and kids, Yusuf and Ammar, have been loving, understanding, and patient during my PhD career. They are the reason I aspire to be the best in everything I do.

Several groups at UCI were on-board during my PhD journey. I would like to thank the staff of the Electrical Engineering and Computer Science Department for their support over the past years. I would like to thank the staff of the Graduate Resource Center for the amazing programming they create. I would like to thank the members of Zotspeak Toastmasters club for creating a positive atmosphere to develop public speaking and leadership skills.

CURRICULUM VITAE

Murad Rida Q Murad

EDUCATION

Doctor of Philosophy (PhD) in Electrical Engineering 2019
University of California, Irvine (UCI)
Wireless Systems and Circuits Laboratory

Master of Engineering in Electrical and Computer Engineering 2011
University of British Columbia (UBC)
Concentration in Communications
Additional sub-specialization in Engineering Management

Bachelor of Science in Electrical Engineering, *Summa Cum Laude* 2003
California State University, Long Beach (CSULB)
Emphasize in Digital Signal Processing (DSP)

Preparatory Academics for Vanderbilt Engineers (PAVE) 1999
Vanderbilt University

PUBLICATIONS AND PRE-PRINTS

M. Murad and A. M. Eltawil, "Power consumption and energy-efficiency for in-band full-duplex wireless systems," April 2019. [Online]. Available: https://arxiv.org/abs/1904.10426

M. Murad and A. M. Eltawil, "Performance analysis and enhancements for in-band full-duplex wireless local area networks," March 2019. [Online]. Available: https://arxiv.org/abs/1903.11720

M. Murad and A. M. Eltawil, "Collision tolerance and throughput gain in full-duplex IEEE 802.11 DCF," *IEEE International Conference on Communications (ICC)*, Kansas City, MO, 2018.

M. Murad and A. M. Eltawil, "A simple full-duplex MAC protocol exploiting asymmetric traffic loads in WiFi systems," *IEEE Wireless Communications and Networking Conference (WCNC)*, San Francisco, CA, 2017.

TEACHING EXPERIENCE

University of California, Irvine 2018-2019
Department of Electrical Engineering and Computer Science
Teaching Assistant
Undergraduate course in DC and AC electric circuits (Network Analysis I)

PROFESSIONAL SERVICE

Reviewer for IEEE Communications Letters.
Reviewer for IEEE Wireless Communications and Networking Conference.

INDUSTRY EXPERIENCE

Saudi Aramco 2011-2014
Information Technology - Data Networks and Communications Operations
Supervisor
Managed teams, processes, projects, and infrastructure to provide secure, reliable, efficient, and cost-effective data network and communications services.

Saudi Aramco 2003-2009
Information Technology - Communications Operations
Communications Engineer
Handled design review, installation, testing, commissioning, operation, maintenance, and troubleshooting for communications systems and projects.

PEDAGOGICAL & PROFESSIONAL DEVELOPMENT

Center for the Integration of Research, Teaching and Learning (CIRTL) Associate
Summer Institute, Scientific Teaching Fellow
Certificate in Teaching Excellence
Mentoring Excellence Program
Excellence in Engineering Communication
Improv for Teaching

TECHNICAL TRAINING COURSES

Wireless Networks & Plant Applications
Terrestrial Trunked Radio Systems
Radio Trunking Concepts
Accelerated HP Network Technologies
Interconnecting Cisco Networking Devices
Hands-on Network Convergence
Endpoint Security & Network Access Control
Transmission Systems & Applications
Alcatel Synchronous Digital Hierarchy Operations & Maintenance
Nokia-Siemens Open Transport Networks
Huawei Telephone Exchange
Fiber Optic Cable Installation & Measurement
Outside Plant Engineering
Value Engineering

LEADERSHIP TRAINING COURSES

The 7 Habits of Highly Effective People
What Matters Most
Business Communication
Communicating Openly & Effectively
Interpersonal Communication
The 7 Innovation Tools
Leadership Challenge
Supervisory Skills for Success
Basics of Supervision
Mentor Certification Program
Coaching Others for Top Performance

PROFESSIONAL AFFILIATIONS

Institute of Electrical and Electronics Engineers (IEEE)
IEEE Communications Society
IEEE Education Society
American Society for Engineering Education (ASEE)
Toastmasters International (Distinguished Toastmaster)

ABSTRACT OF THE DISSERTATION

Performance Analysis and Enhancements for In-Band Full-Duplex Wireless Networks

By

Murad Rida Q Murad

Doctor of Philosophy in Electrical Engineering

University of California, Irvine, 2019

Professor Ahmed M. Eltawil, Chair

Traditional solutions based on Modulation and Coding Schemes (MCSs) have been exhaustively used to improve the performance of wireless systems, striving to reach close to the maximum theoretical limits for channel capacity. In-Band Full-Duplex (IBFD) is an emerging technique that enables a wireless node to transmit and receive at the same time and on the same assigned frequency. Consequently, IBFD wireless communications can potentially double the channel capacity compared to contemporary Half-Duplex (HD) wireless systems. Therefore, IBFD techniques provide new insights into how available resources can be exploited.

In this dissertation, a novel IBFD Medium Access Control (MAC) protocol is presented for Wireless Local Area Networks (WLANs) using IEEE 802.11 Distributed Coordination Function (DCF). The concept of IBFD communications is examined from an unconventional perspective to propose a mechanism that increases the symmetry between uplink (UL) and downlink (DL) traffic loads in order to maximize the utilization of the channel. This dissertation also provides matching analytical and simulation results to show how frame collisions are reduced and how throughput increases when IBFD schemes are implemented for WLANs. Additionally, a collision-free mode enabled by IBFD communications is presented.

In order to study the feasibility and benefits of IBFD networks, this dissertation presents an

accurate analytical model based on Discrete-Time Markov Chain (DTMC) analysis for IEEE 802.11 DCF with IBFD capabilities. The model captures all parameters necessary to calculate important performance metrics including latency and link utilization, which quantify enhancements introduced as a result of IBFD solutions. Moreover, two frame aggregation schemes for WLANs with IBFD features are proposed to increase the efficiency of data transmission. The dissertation also presents an analytical model for power consumption in IBFD-WLANs. Energy-efficiency is compared for both HD and IBFD networks. The results via the presented analytical model closely match the results generated by simulation.

Generated results show an increase in the aggregate throughput of the system. While a simple IBFD MAC protocol alone improves the aggregate throughput by an average increase of ∼85% compared to standard IEEE 802.11 DCF, introducing the proposed IBFD-MAC scheme to increase traffic symmetry in the system improves the aggregate throughput by an additional average factor of up to ∼20%. When using both the analyses presented in this dissertation and the simulator constructed to study the performance in IBFD systems, matching analytical and simulation results with less than 1% average errors confirm that the proposed frame aggregation schemes further improve the overall throughput by up to 24% and reduce latency by up to 47% in practical IBFD-WLANs. The results assert that IBFD transmission can only reduce latency to a suboptimal point in WLANs, but frame aggregation is necessary to minimize it. Power and energy analyses show that IBFD-WLANs consume more power but also have higher energy-efficiency in terms of transmitted data compared to contemporary HD WLANs.

Chapter 1

Introduction

Wireless systems have traditionally been Half-Duplex (HD) in that resources are divided between uplink (UL) and downlink (DL) transmission directions. An HD system can either use Frequency Division Duplexing (FDD) or Time Division Duplexing (TDD). In FDD systems, a frequency band is divided into sub-bands, then the sub-bands are assigned to both UL and DL for concurrent transmission (see Fig. 1.1 for an illustration). In TDD systems, UL and DL transmissions alternate in time to occupy a frequency band as shown in Fig. 1.2.

Deviating from FDD and TDD was discouraged even beyond mid 2000's. For example, it is common for advanced wireless communications textbooks to include statements like "it is generally not possible for radios to receive and transmit on the same frequency band because of the interference that results" [1]. Another example is mentioned in [2] where it is stated that "full duplex radio [is] capable of transmitting and receiving at the same time, an approach that would increase the cost significantly." Ultimately, those statements and many similar ones have been challenged by introducing the concept of In-Band Full-Duplex (IBFD) communications.

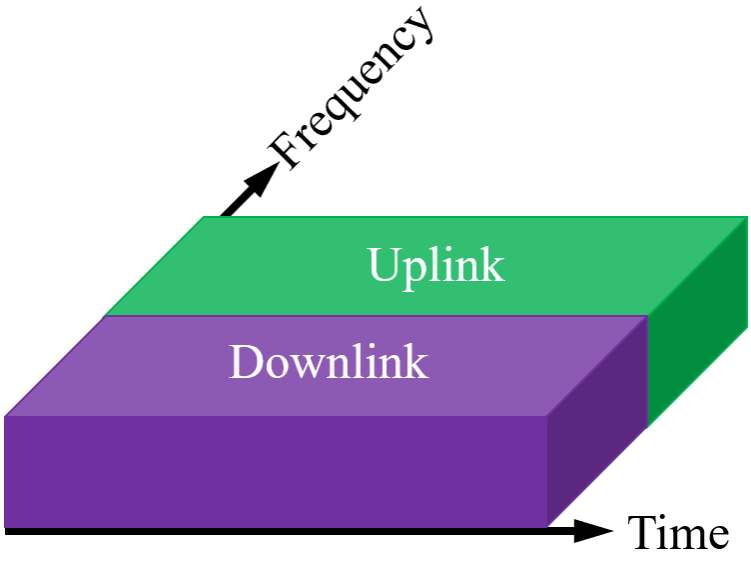

Figure 1.1: Frequency Division Duplexing (FDD).

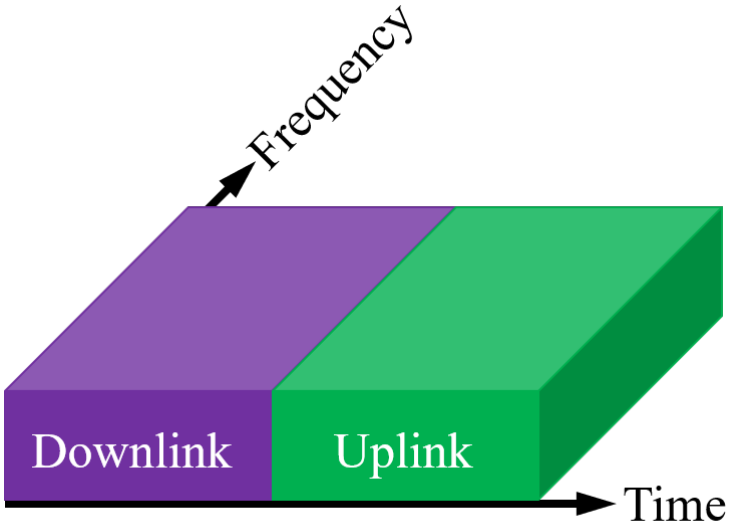

Figure 1.2: Time Division Duplexing (TDD).

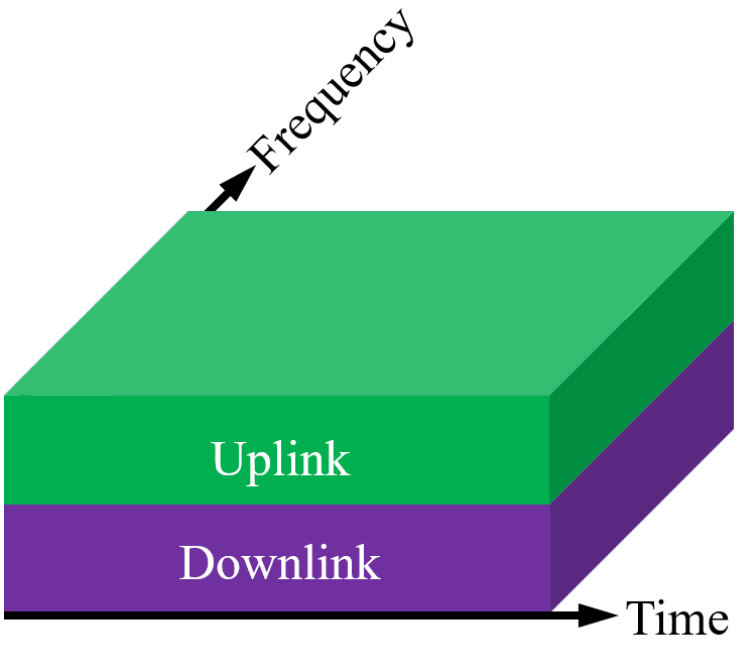

Figure 1.3: In-Band Full-Duplex (IBFD).

1.1 In-Band Full-Duplex (IBFD) Communications

IBFD (frequently referenced to as simply FD in technical literature) is a powerful technique to make an efficient use of the wireless channel. IBFD communications can theoretically double channel capacity by allowing each wireless node to transmit and receive at the same time and over the same frequency band (see Fig. 1.3). Historically, IBFD has been implemented since the 1940s, but its use was limited to radar systems [3]. IBFD was disqualified in the past due to high self-interference at the terminal's own receiving antenna. However, recent advancements in Self-Interference Cancellation (SIC) solutions enabled the implementation of IBFD systems. A comprehensive coverage of IBFD communications can be found in [3, 4, 5, 6].

1.2 Self-Interference Cancellation (SIC) Solutions

Prior advancements in SIC affirm that IBFD is possible, and the legacy assumption of a single transmission over a frequency is no longer a necessity. SIC can be implemented at different levels and in numerous ways as detailed in [7]. A possible SIC solution can purely take place in the analog domain at both the transmitter and receiver sides [8]. On the other hand, SIC can be treated in the digital domain at the transceiver like in [9]. An innovative method can extract the Self-Interference (SI) signal from the analog domain and cancel it at the digital domain like in [10]. Alternatively, the SI signal can be extracted from the digital domain and cancelled at the analog domain to enable proper reception for the Signal of Interest (SOI) [11]. A combination of SIC techniques at various levels is often necessary to reduce SI below the noise floor in order to make the received SOI decodable (a recent collection of comprehensive SIC methods can be found in [12]). SIC is possible for WiFi signals due to the lower transmit power, which makes WiFi under IEEE 802.11 standard a strong candidate for IBFD techniques. As a result, IBFD platforms utilizing IEEE 802.11 standard are used to establish operational Wireless Local Area Networks (WLANs) such as [13], [14], and [15].

1.3 IBFD Medium Access Control (MAC) Challenges

According to [15], "The most interesting possible benefits of full duplex occur above the physical layer." Additionally, [5] affirms that "the most interesting FD benefits may occur at the higher layer protocols such as MAC-layer protocols." However, Implementing IBFD systems comes with many challenges. In the MAC sub-layer, several considerations must be taken into account when IBFD systems are designed. Some of those challenges are summarized in this section as follows:

Backward Compatibility: it is necessary to ensure that new IBFD MAC protocols can operate within contemporary HD systems [4]. Implementing IBFD should not assume that existing HD systems will all be replaced in one step. New implementations for IBFD must accommodate existing HD wireless nodes and operate in a hybrid mode. The novel IBFD MAC protocol presented in this dissertation is backward-compatible with current IEEE 802.11 standard.

Handling Asymmetrical Traffic: an IBFD link becomes underutilized when the traffic is asymmetrical, and an open research question is about the effect of transmitting multiple short frames in order to efficiently utilize the link [5]. For example, measurements confirm that WiFi networks typically have higher downlink traffic than uplink traffic [16, 17]. This challenge is addressed in this dissertation from the perspective of the MAC sub-layer, and the effects of aggregation on throughput, latency, and utilization are quantified through both analysis and simulation results.

Performance Analysis and Limits: factors such as simultaneous transmission/reception, packet sizes, and overhead introduce complications when MAC protocols are examined in IBFD networks [18]. This dissertation provides a thorough and accurate analytical model that characterizes throughput and latency in IBFD-WLANs.

Reducing Energy Consumption: energy-efficiency is a crucial factor in designing MAC protocols in order to ensure longer battery life and proper mobility wherever needed for wireless nodes [5]. IBFD systems are expected to consume more power for simultaneous operations of transmitters and receivers. In this dissertation, an analytical model is provided to compute power consumption and energy-efficiency. The model is used to show that IBFD-WLANs are energy-efficient in terms of transmitting more bits per unit of energy compared to contemporary HD systems.

Fairness: when IBFD takes place between two nodes, both transmitters use the same chan-

nel. The quality of the channel at each transmitter must be taken into consideration in order to ensure proper utilization and fair allocation of resources [18]. In addition, when designing MAC protocols in hybrid systems, IBFD nodes should not be given a higher priority than HD nodes even though they increase the overall utilization, which can create unfair distribution of resources if this issue is not addressed properly [5].

1.4 Dissertation Contributions

Clearly, many open questions exist in the MAC-sublayer for IBFD systems. Unless MAC challenges are properly resolved, IBFD implementations will not be practical. This dissertation examines IBFD-WLANs at the MAC-sublayer. The contributions of the dissertation are summarized as follows:

- Proposing a novel MAC protocol for WLANs to increase the symmetry between UL and DL traffic loads in order to maximize the utilization of an IBFD link.
- Presenting results to show how frame collisions are reduced and how throughput increases when IBFD schemes are implemented for WLANs.
- Formulating an accurate analytical model based on Discrete-Time Markov Chain (DTMC) analysis for IEEE 802.11 Distributed Coordination Function (DCF) with IBFD capabilities. The model is used to calculate key performance metrics like throughput and latency.
- Using distributed frame aggregation schemes for WLANs with IBFD features to reduce end-to-end delay in data transmission.
- Examining energy-efficiency in IBFD-WLANs by formulating an analytical model to calculate average power consumption per wireless node.

The benefits of IBFD in WLANs are quantified in terms of increasing throughout, reducing collisions, minimizing latency, enhancing utilization, and improving energy-efficiency. Reported results are confirmed by closely matching simulation and analytical results.

1.5 Dissertation Organization

A novel IBFD-MAC protocol for WLANs with asymmetrical traffic is presented to illustrate how IBFD can provide new perspectives. In addition, a collision-free mode of operation is introduced to show maximum throughput gain resulting from IBFD schemes. Furthermore, mathematical analyses for throughput, latency, link utilization, power consumption, and energy-efficiency are presented for IBFD-WLANs adopting IEEE 802.11 DCF mechanisms. The benefits of IBFD solutions are presented by comparing IBFD and HD networks. All analytical work is confirmed by matching simulation results. Exciting future work is highlighted at the end of the dissertation.

Chapter 2

A Novel IBFD MAC Protocol for WLANs with Asymmetrical Traffic

2.1 Motivation

IEEE 802.11 Distributed Coordination Function (DCF) [19] enables a WiFi Access Point (AP) and associated Stations (STAs) to gain access to a channel based on Carrier Sense Multiple Access with Collision Avoidance (CSMA/CA). With IEEE 802.11 DCF, an AP and each STA have equal probability of winning the contention for the channel. However, the downlink (DL) traffic load from an AP to an STA is usually much higher than the uplink (UL) traffic load in the reverse direction and can be up to 10 times as large [20], which creates an inevitable traffic asymmetry between UL and DL traffic loads. Consequently, a well-known inherited problem of contemporary WiFi systems is the underserved DL traffic load at the AP.

2.2 Related Work

Prior work, similar to [20], [21], [22], and [23], alleviates the problem of underserved DL traffic by giving the AP a higher priority to use the channel while keeping UL traffic demands in mind. However, considerations for node starvation restricted classic solutions since an STA cannot transmit on the channel if it does not win the contention in an HD system, which became an obsolete assumption for IBFD systems. A basic yet frequently overseen benefit of IBFD communications is that an STA can get an opportunity to transmit over a channel even without competing to access the channel. Whenever an AP wins the contention and has traffic to a specific STA, the STA can make use of an IBFD communications opportunity and transmit UL traffic.

More recent research proposed solutions to resolve asymmetric transmission using IBFD MAC protocols. The authors of [23] proposed a new IBFD MAC protocol to serve asymmetric transmission scenarios. However, the proposed protocol requires interrupting transmission to alert neighboring STAs of an opportunity to use IBFD communications, and it can only accommodate IBFD transmission for STAs with limited traffic loads. The IBFD MAC solution proposed in [24] identifies STAs hidden from a particular STA receiving DL traffic, which provides IBFD transmission opportunities for the hidden STAs to send UL traffic. This solution significantly aids UL traffic but is not always useful for DL traffic as it is noted in the reported results. Asymmetric Transmission MAC (AT-MAC) proposed as an IBFD scheme in [25] attempts to serve STAs with mixed requirements in either UL or DL directions, but the protocol assumes that the AP has global knowledge of the channel among STAs, which defeats the purpose of IEEE 802.11 DCF as a distributed protocol.

2.3 Contribution

In this chapter, an IBFD-MAC protocol with busytone proposed in [15] is adopted to IEEE 802.11 DCF. Busytone is used to alert neighboring STAs that the channel is occupied by concurrent communications when an STA finishes its own transmission but is still engaged in IBFD transmission with the AP. While transmitting busytone consumes time and power resources with no contribution to sending useful data, it can provide backward compatibility for IBFD systems with existing WiFi networks by avoiding modifications to IEEE 802.11 MAC standard.

The contribution is to introduce a Symmetry Ratio (SR) at each WiFi STA based on how similar its UL traffic load is to the incoming DL load from the AP. SR is then used by each STA to decide if the STA will enter the contention for the channel according to a minimum required SR threshold (SR_{th}). If an STA is out of contention, it accumulates traffic until it meets the minimum SR_{th}. Complete node starvation does not occur in this IBFD system since the node has the opportunity to send its UL traffic load whenever it receives a DL load from the AP. By mandating a minimum SR_{th}, busytone transmissions used by STAs are reduced. As a result, the aggregate throughput (useful transmitted data in both UL and DL traffic directions) of the system is improved.

2.4 Proposed Symmetry Ratio (SR) Scheme

A WiFi Basic Service Set (BSS) is assumed with a single AP and n associated STAs. Without loss of generality, a single IBFD channel is assumed, and the channel can be used to connect the AP to a single STA at a time. When the AP gains access to the channel and transmits to an STA, the STA makes use of the IBFD opportunity to transmit UL traffic. Conversely, when an STA wins the contention and transmits to the AP, the AP sends its DL traffic to

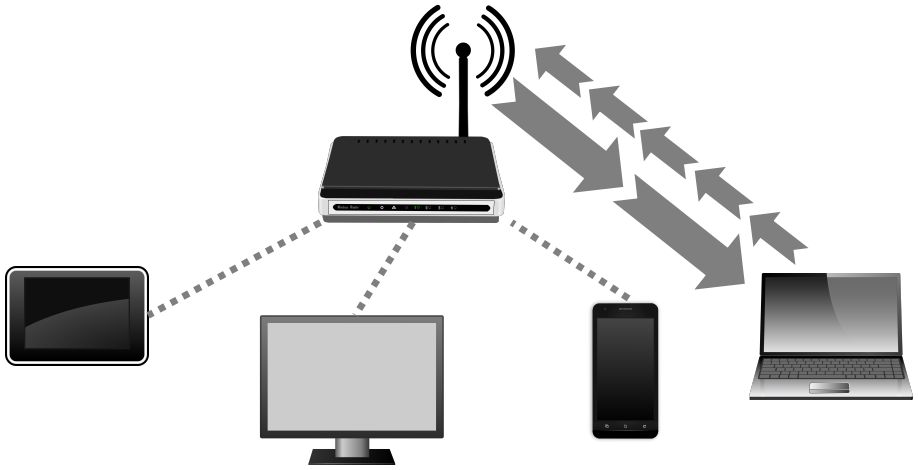

Figure 2.1: A typical IBFD WiFi system with a single AP and multiple STAs.

the STA. UL traffic is assumed to always be smaller than DL traffic, and STAs transmit busytone once they finish transmitting UL load until the AP finishes transmitting its load. A typical WiFi system employing UL/DL IBFD transmission is shown in Fig. 2.1.

The proposed scheme starts by establishing an SR value at each STA. If traffic load is designated as (L) and transmission time as (T), $\mathrm{SR_n}$ at $\mathrm{STA_n}$ can be defined as follows

$$\mathrm{SR_n} = \frac{L_{UL}}{L_{DL}} = \frac{T_{UL}}{T_{DL}} = \left.\frac{T_{UL}}{T_{UL} + T_{\mathrm{busytone}}}\right|_{\mathrm{IBFD}}. \tag{2.1}$$

Thus, each STA can calculate its own SR in a distributed manner. A small SR value indicates high asymmetry while a large SR value indicates high symmetry (SR of 1 indicates perfect symmetry).

The proposed scheme sets a minimum required $\mathrm{SR_{th}}$ needed for each STA to enter IEEE 802.11 DCF contention. If $\mathrm{SR_n}$ is greater than $\mathrm{SR_{th}}$, then $\mathrm{STA_n}$ is in *contention mode* and can transmit its load either if it wins the contention or if the AP wins the contention and transmits DL traffic to the STA. If an STA does not meet the required $\mathrm{SR_{th}}$ value, then it is in *partial starvation mode* and can transmit if the AP is transmitting DL traffic to the STA.

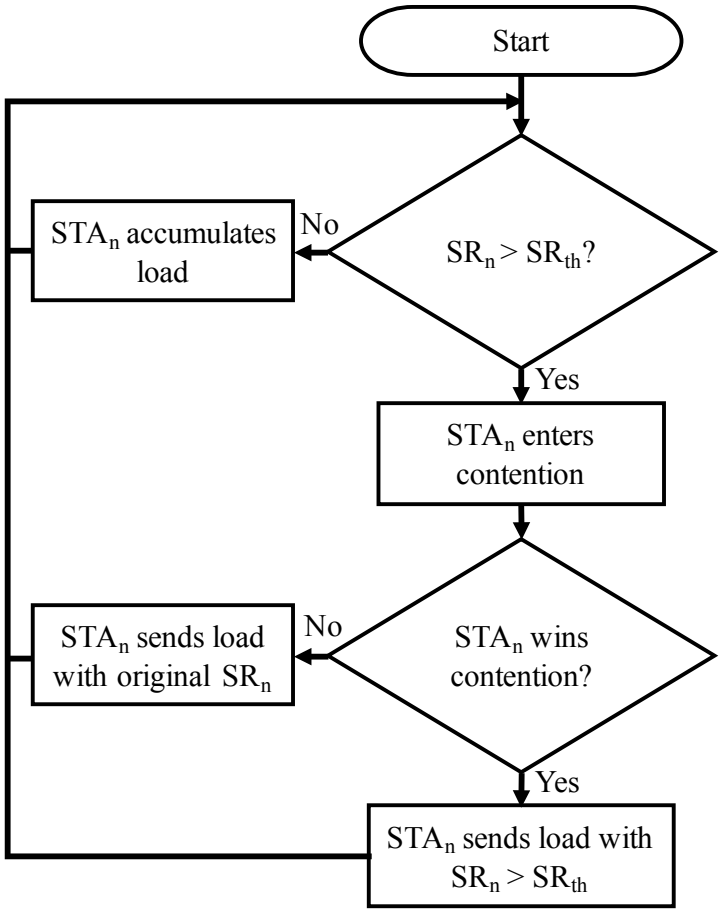

Figure 2.2: Flow chart for the proposed SR scheme.

While an STA is in a partial starvation mode, it accumulates traffic at a rate of λ Mbps. Once accumulated traffic becomes high enough to meet the minimum SR_{th}, the STA can exit partial starvation mode and enter contention mode.

When STA_n transmits on the channel by gaining access through contention mode, it transmits its traffic with its $SR_n > SR_{th}$. On the other hand, if the AP gains access to the channel and is connected to STA_n, then STA_n sends traffic based on its original SR_n value. Fig. 2.2 shows a flow chart for the proposed SR mechanism.

There are several anticipated benefits which can be realized by implementing the SR scheme. When there are STAs in partial starvation mode, the number of STAs contending for the channel is reduced, and the AP has a higher probability to access the channel to serve the

Table 2.1: Simulation parameters

Parameter	Value
$MPDU_{max}$	11,454 bytes
MAC header size	36 bytes
ACK size	14 bytes
Slot time	9 μs
SIFS time	16 μs
DIFS time	34 μs
PLCP time	40 μs
CW_{min}	15
CW_{max}	1,023
Data rate (UL and DL)	100 Mbps
Simulated run time	5 minutes/run

larger DL traffic load. Moreover, dictating a larger payload size to compete for the channel not only reduces signaling overhead but also reduces busytone used in IBFD communications. Consequently, the combined UL/DL aggregate throughput is expected to increase by setting a minimum SR_{th}. Such benefits are realized while preventing total node starvation and ensuring backward compatibility with current IEEE 802.11 WiFi networks.

2.5 System Model

IEEE 802.11 DCF without RTS/CTS is simulated. Each STA can only communicate with the AP, and transmission always occurs as IBFD communications using IBFD-MAC with busytone. Collisions can occur if more than a single WiFi device (either the AP or an associated STA) wins the contention for the channel. Furthermore, complete frame loss is assumed in case of a collision (i.e., no capture effect). No transmission errors are assumed, and all STAs are close enough to one another to detect channel occupancy and busytone transmission (i.e., no hidden terminals). The values of MAC Protocol Data Unit (MPDU), overhead, and Inter Frame Spacing (IFS) durations are based on IEEE 802.11ac standard [26]. Table 2.1 shows the parameters used in the simulation and corresponding values.

Every time either the AP or an STA gets an opportunity to use the channel, it transmits a single MPDU without fragmentation or aggregation. The AP and STAs always have MPDUs to transmit, and the AP has $\text{MPDU}_{\text{AP}} = \text{MPDU}_{\text{max}}$. Each STA has a fixed SR throughout each simulation run. Consequently, the MPDU size at STA_n is

$$\text{MPDU}_{\text{STA}_\text{n}} = \text{SR}_\text{n} \times \text{MPDU}_{\text{AP}}. \tag{2.2}$$

SR_{th} is globally set by the network administrator and kept fixed throughout each simulation run. When an STA is in partial starvation mode, it accumulates traffic at an assumed rate of $\lambda \approx 10$ Mbps. This value is constant as long as the STA is accumulating traffic regardless of its SR_n value.

2.6 Results and Evaluation

A simulator was constructed using MATLAB. An HD system based on standard IEEE 802.11 DCF is simulated to establish a solid reference for comparison. The SR scheme is then introduced, and the aggregate throughput and average Busytone per Transmission $(\text{BT/TX})_{\text{avg}}$ are analyzed in terms of how they are affected by dictating an SR_{th} policy. Since each STA has a different MPDU size, there is no need to compare how channel occupancy per STA is affected when the SR scheme is implemented. Instead, Access Opportunity (AcOp) is introduced as the percentage of times each STA has the opportunity to transmit on the channel, which can occur either by winning the contention or while receiving transmission from the AP. AcOp per STA is analyzed as the SR_{th} value increases. AcOp is only analyzed for UL transmission since the AP has 100% AcOp in IBFD communications. The behavior of the system is studied at minimum SR_{th} values of 0, 0.2, 0.4, 0.6, and 0.8. When $\text{SR}_{\text{th}} = 0$, this case corresponds to IBFD-MAC with busytone but with no SR_{th} policy in place.

To explain the results clearly, 3 scenarios are simulated: predefined deterministic SR_n values, random SR_n values, and varying values for number of STAs with random SR_n values.

2.6.1 Deterministic SR_n values

In this first scenario, 5 STAs (STA_1 through STA_5) are assumed with deterministic SR values of $SR_1 = 0.1$, $SR_2 = 0.3$, $SR_3 = 0.5$, $SR_4 = 0.7$, and $SR_5 = 0.9$. Fig. 2.3 shows how the aggregate throughput of the system changes when an SR_{th} policy is enforced. The case of HD IEEE 802.11 DCF simulation is shown for comparison. Additionally, the case of $SR_{th} = 0$ is taken as the baseline case, which represents a 78% gain in aggregate throughput compared to IEEE 802.11 DCF. As SR_{th} increases, the aggregate throughput increases since STAs with lower SR values leave the contention for the AP and other STAs with higher payloads. When $SR_{th} = 0.8$, the aggregate throughput experiences an 18% increase compared to the case when $SR_{th} = 0$. In addition to the apparent benefit the proposed SR scheme adds in terms of requiring each STA to have a higher load of useful data and giving the AP more opportunities to transmit, requiring a larger payload decreases the overall signaling overhead, which allows more transmission opportunities for useful data. Moreover, increasing SR_{th} decreases the number of STAs in contention for the channel, which decreases the number of collisions. Nevertheless, when collisions actually happen while transmitting large loads, the number of wasted time slots due to each collision is high, which limits observed improvements in aggregate throughput.

Fig. 2.4 shows $(BT/TX)_{avg}$ versus SR_{th}. When $SR_{th} = 0$, all STAs equally contribute to the overall busytone regardless of individual SR values. In this case, the simulated $(BT/TX)_{avg}$ value of 50.08% coincides with the theoretical value of

$$(BT/TX)_{avg}\Big|_{n\,=\,5} = \frac{1}{5}\sum_{i=1}^{5}(1 - SR_i) = 50\%. \tag{2.3}$$

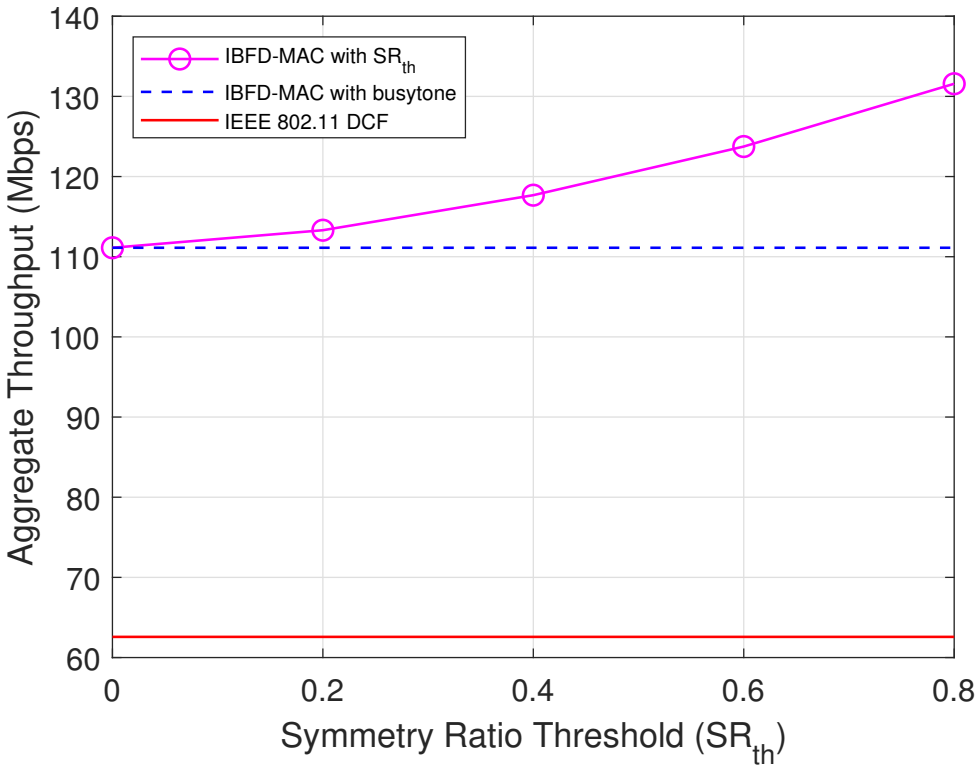

Figure 2.3: Aggregate throughput vs. $\mathrm{SR_{th}}$ (deterministic $\mathrm{SR_n}$, $n = 5$).

It is noted that $(\mathrm{BT/TX})_{\mathrm{avg}}$ decreases as stricter $\mathrm{SR_{th}}$ values are required to enter contention. $(\mathrm{BT/TX})_{\mathrm{avg}}$ decreases to 26% when $\mathrm{SR_{th}}$ is increased to 0.8.

Fig. 2.5 shows how each STA is affected in terms of AcOp by implementing the minimum $\mathrm{SR_{th}}$ policy. When $\mathrm{SR_{th}} = 0$, all STAs have very close AcOp values to transmit on the channel. This value coincides with the shown theoretical value of AcOp for UL traffic using IEEE 802.11 DCF, which is $\frac{1}{5} = 20\%$ per STA (approximately 20% per STA is also the simulated but not shown results for AcOp under IEEE 802.11 DCF). As the system becomes more conservative in admitting STAs to compete for the channel, STAs with lower SR values than $\mathrm{SR_{th}}$ lose opportunities to transmit. The further away from $\mathrm{SR_{th}}$ an STA is, the more opportunities it loses. Also, the closer to $\mathrm{SR_{th}}$ an STA is, the higher AcOp it has because it needs less time to accumulate traffic in partial starvation mode. STAs with SR values above $\mathrm{SR_{th}}$ get approximately an equal increase per STA in AcOp. It is worth noting that even though an STA may be out of contention initially, no drastic decrease in AcOp occurs since

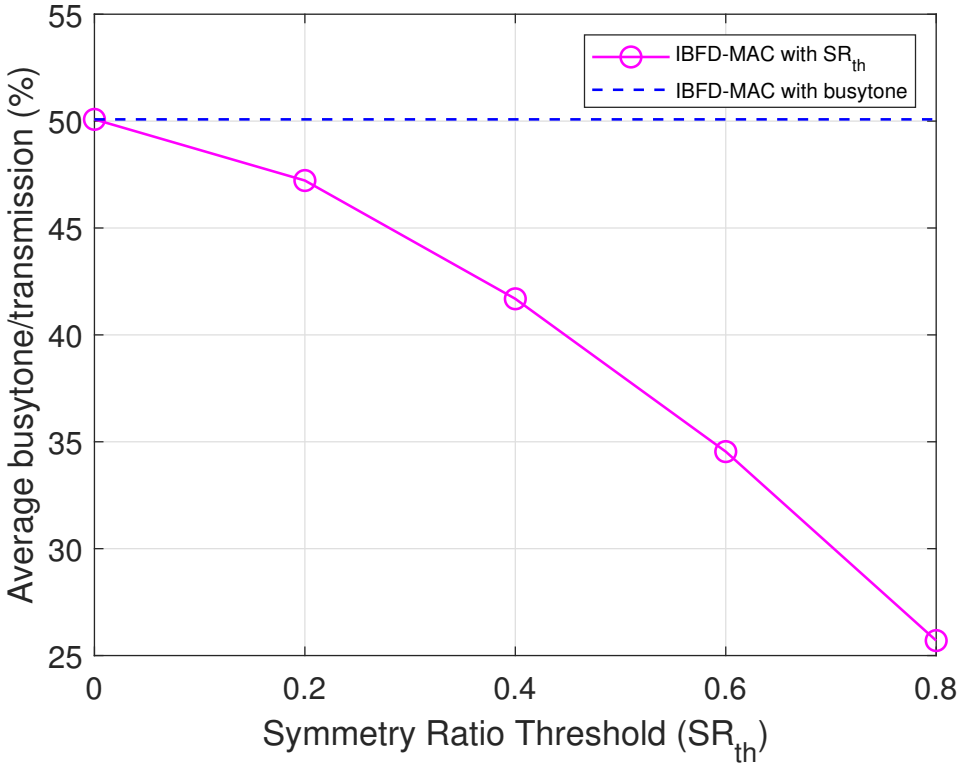

Figure 2.4: Average busytone/transmission vs. $\mathrm{SR_{th}}$ (deterministic $\mathrm{SR_n}$, $n = 5$).

the STA gets IBFD opportunities when the AP is communicating with it. Based on delay requirements of each STA, degradation in AcOp may or may not be tolerable.

2.6.2 Random $\mathrm{SR_n}$ values

To study the scalability and usefulness of the proposed SR scheme, a scaled up simulation scenario was implemented. The number of STAs was increased to $n = 10$ STAs. Each STA was assigned a random SR value between 0.1 and 0.9, and the SR values are kept fixed throughout each simulation run. Five independent runs constituted a Monte Carlo simulation, and the average results of all runs were plotted.

The aggregate throughput versus varying values of $\mathrm{SR_{th}}$ is shown in Fig. 2.6. The average simulated aggregate throughput under IEEE 802.11 DCF using the random SR values of this

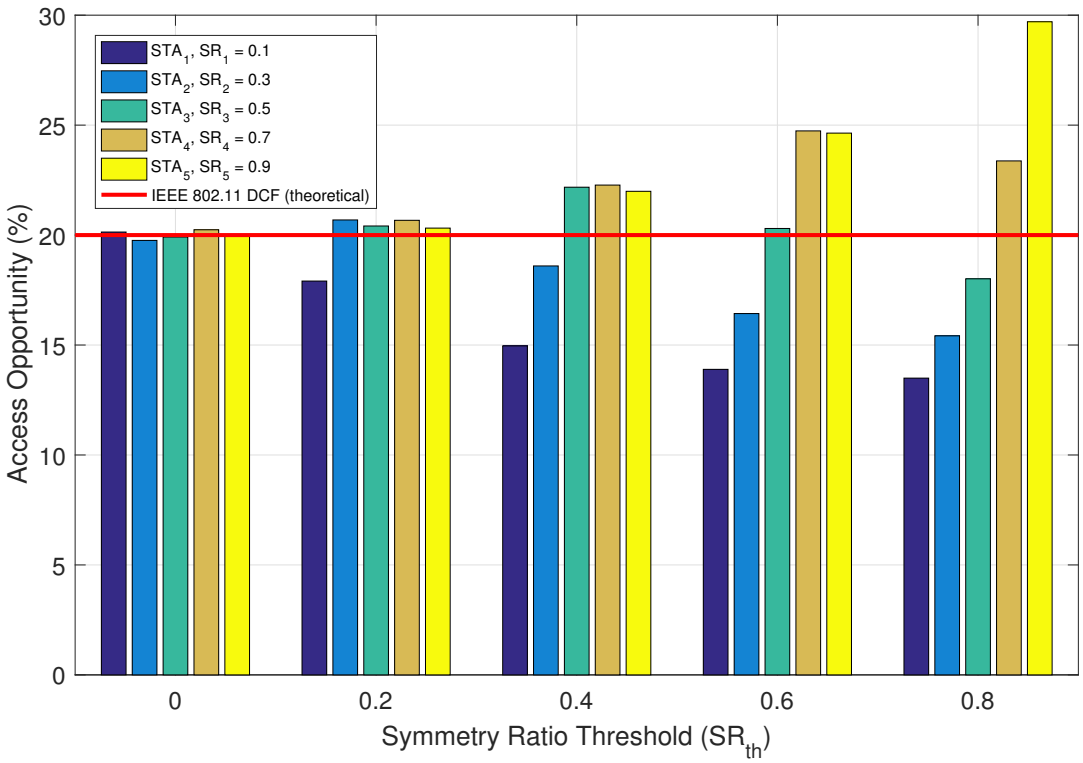

Figure 2.5: Access Opportunity vs. SR_{th} (deterministic SR_n, $n = 5$).

scenario is plotted to show an HD system for comparison. The first case of $SR_{th} = 0$ indicates implementing the simple IBFD-MAC with busytone in the system, which yields an 86% gain in aggregate throughput compared to IEEE 802.11 DCF. Similar to the simulated case with deterministic SR values, an increase in aggregate throughput as SR_{th} increases is observed. An improvement of 22% in aggregate throughput is noted when SR_{th} increases from 0 to 0.8. It is noted that lower throughput values are observed throughout the simulation compared to the case with deterministic SR values, which is expected since doubling the number of STAs has the adverse effect of increasing the number of collisions.

Fig. 2.7 shows $(BT/TX)_{avg}$ against varying SR_{th} values. In a similar fashion to equation (2.3), the overall average of $(BT/TX)_{avg}$ values was numerically calculated based on SR values from the 10 STAs in all 5 simulation runs to represent the case when $SR_{th} = 0$. Calculated $(BT/TX)_{avg}$ was found to be 56.40% compared to the simulated $(BT/TX)_{avg}$ of 56.24%. The increase of initial $(BT/TX)_{avg}$ from 50% in the case of deterministic SR values

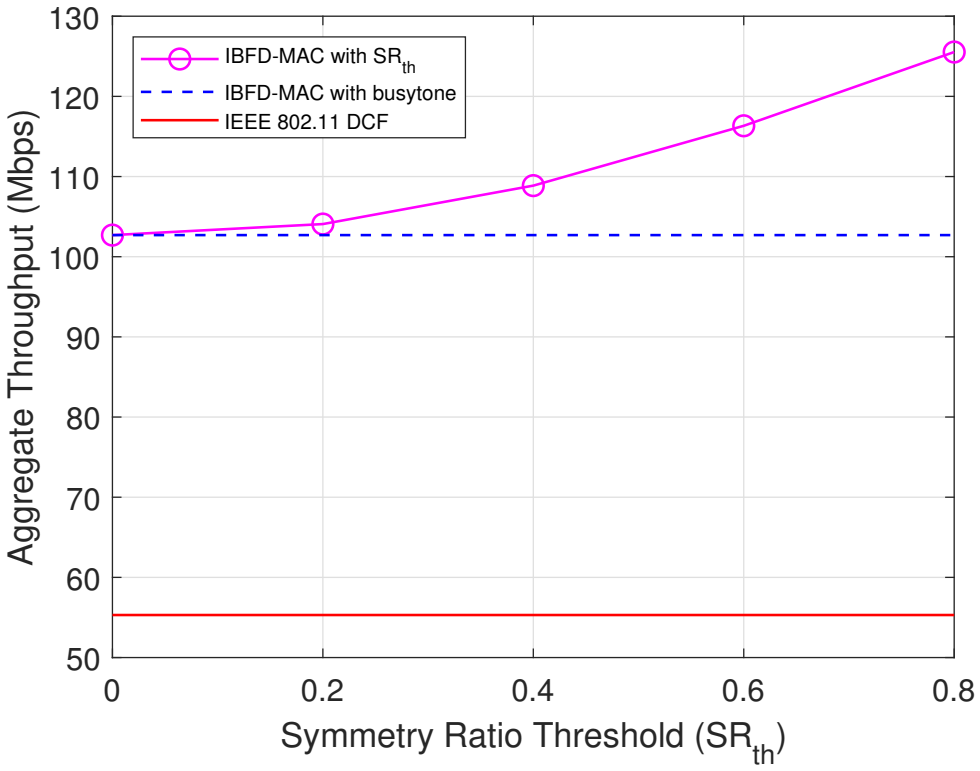

Figure 2.6: Aggregate throughput vs. SR_{th} (random SR_n, $n = 10$).

to 56% in the case of random SR values contributed to the lower throughput values observed throughout the simulation in Fig. 2.6. When $SR_{th} = 0.8$ is enforced, $(BT/TX)_{avg}$ decreases to 26%.

Since SR values were not deterministic and due to the higher number of STAs in this scenario, studying AcOp per STA was omitted in the case of random SR values. However, no deviation from the results obtained in the case of deterministic SR values is expected.

2.6.3 Varying values for number of STAs with random SR_n values

In this scenario, aggregate throughput is analyzed in several cases with a different number of STAs in each case. Each STA is assigned a random SR value between 0.1 and 0.9. Fig. 2.8 shows the results of each case using 4 schemes: IEEE 802.11 DCF, IBFD-MAC with

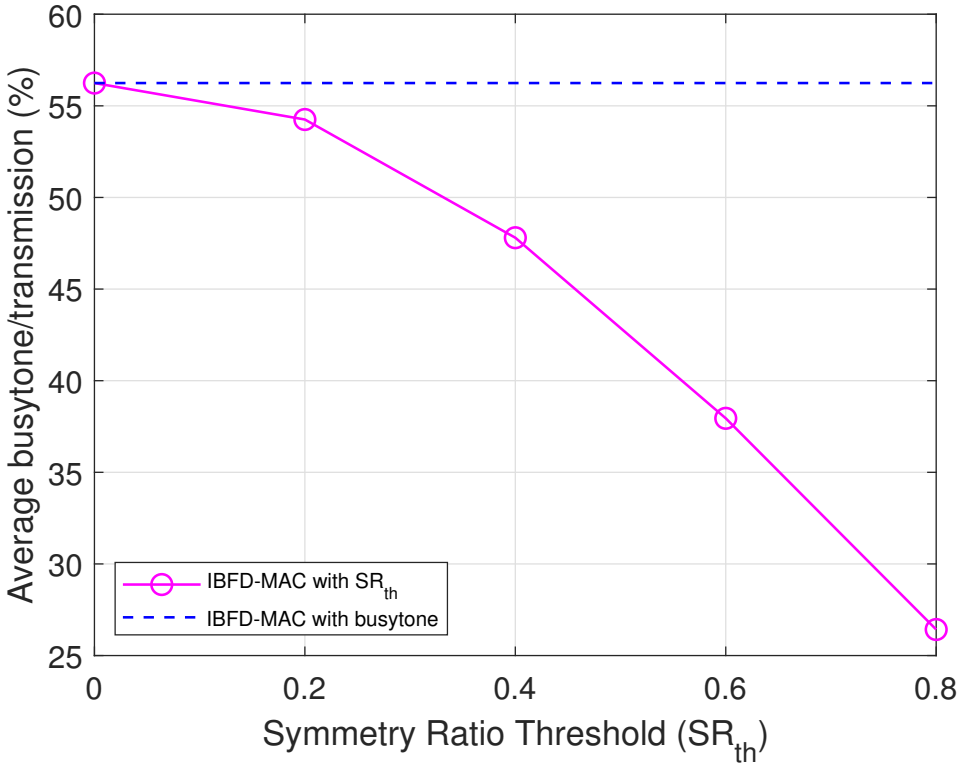

Figure 2.7: Average busytone/transmission vs. $\mathrm{SR_{th}}$ (random $\mathrm{SR_n}$, $n = 10$).

busytone, IBFD-MAC with $\mathrm{SR_{th}} = 0.6$, and IBFD-MAC with $\mathrm{SR_{th}} = 0.8$. As a general trend observed in all schemes, throughput values decrease as the number of STAs increases, which is expected since there are more collisions with larger values for the number of STAs. IBFD-MAC with busytone produces an average of approximately 85% improvement in throughput compared to the case of the HD system using IEEE 802.11 DCF. When IBFD-MAC with $\mathrm{SR_{th}} = 0.6$ is introduced, there is an average of about 8% increase in throughput over the case of IBFD-MAC with busytone. By increasing $\mathrm{SR_{th}}$ to 0.8, the average improvement in throughput increases to about 20% compared to the case of IBFD-MAC with busytone since the stricter SR policy reduces the overall busytone experienced in the system.

The results in this scenario show that the proposed IBFD-MAC with $\mathrm{SR_{th}}$ is scalable to cases with higher numbers of STAs. Consistent results appear throughout the range of simulated values for the number of STAs with random $\mathrm{SR_n}$ assignments.

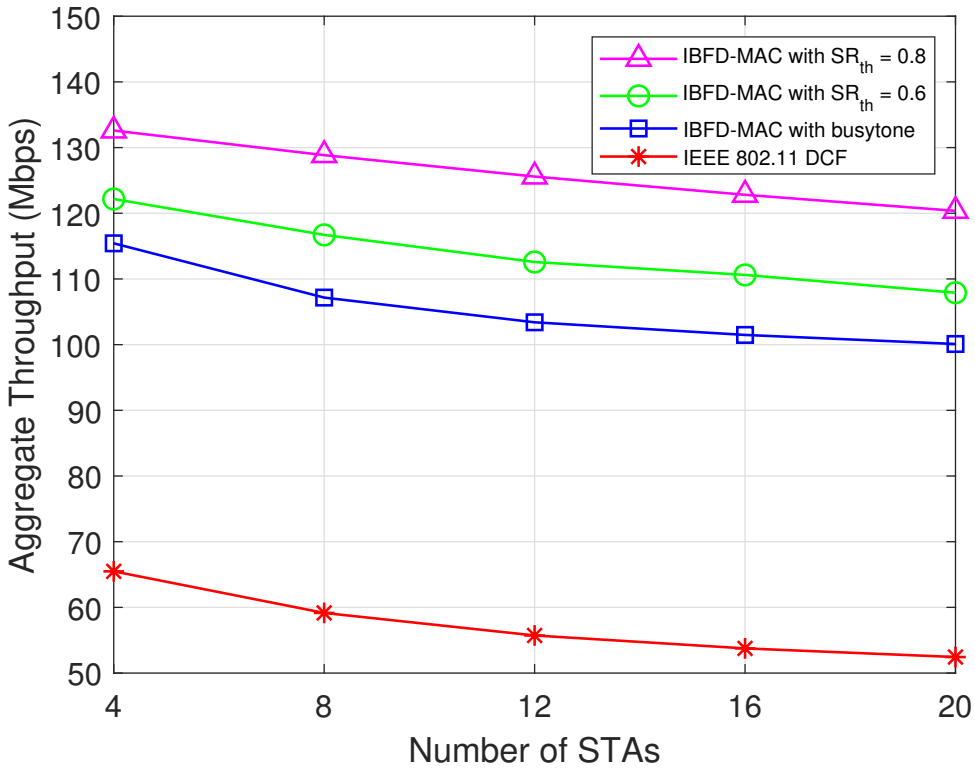

Figure 2.8: Aggregate throughput vs. Number of STAs (random SR_n).

2.7 Conclusion

The concept of IBFD communications is used to ensure no node starves when extreme measures are enforced by setting a strict policy on contention to increase the performance of a WiFi system. A simple yet backward compatible IBFD-MAC with busytone is adopted to IEEE 802.11 DCF. Wasting resources is limited by reducing the average busytone per transmission through inducing partial starvation in some STAs. The proposed IBFD-MAC can be easily adopted to future WiFi standards currently under development.

This chapter represents a first look at the proposal for the SR scheme in WiFi networks with asymmetric traffic. The realized benefits of this scheme are apparent and scalable, and this chapter aims to validate the concept and show initial implementation for an IBFD solution.

Chapter 3

Collision Tolerance and Throughput Gain for IBFD WLANs

3.1 Motivation

There are currently more than eight billion operational WiFi devices in the world, and the production in 2017 is about three billion new devices [27]. As there is increasing reliance on WiFi, future WiFi standards are expected to handle greater levels of traffic loads, transmission rates, and reliability. Innovative approaches are needed to cope with the demand for peak-performance WiFi systems.

3.2 Contribution

In this chapter, a modified analytical framework to study IBFD IEEE 802.11 Distributed Coordination Function (DCF) is introduced. Using IBFD for IEEE 802.11 reduces packet collisions and increases throughput gain. Special cases where a collision-free transmission

mode can be realized in a WiFi network are introduced. The proposed analytical model still produces accurate results for random simulation scenarios.

3.3 Overview of IEEE 802.11 DCF

IEEE 802.11 DCF standardized in [19] is the basic building block for MAC in WiFi systems. IEEE 802.11 is based on CSMA with Collision Avoidance (CSMA/CA). Each WiFi node randomly selects a number of time slots within its current Contention Window (CW) size as its Backoff Counter (BC) to wait before transmitting. The node senses the medium to check if there is an active transmission in the current time slot. If the medium is busy, the node freezes its BC. When the node senses the medium as idle, it decrements its BC. When the BC reaches zero, the node starts its transmission. A collision occurs when two or more nodes start transmitting in the same time slot. The collision is then detected by the absence of an acknowledgement (ACK) frame from the receiving node. By adopting the Binary Exponential Backoff (BEB) mechanism, a node experiencing a collision doubles its CW (i.e. increments its backoff stage) and randomly selects a new BC value in order to retransmit its current traffic load. If the node continues to experience collisions, the node continues to double its CW value until it reaches a CW_{max} value (i.e. maximum backoff stage) set by the standard. Once the node successfully transmits its load, it resets its CW value back to CW_{min} and resumes contending for the medium whenever it has data to transmit. Further details about IEEE 802.11 MAC are clarified in [28].

3.4 Overview of the Bianchi Model

The Bianchi Model published in [29] provides a widely celebrated analytical model for IEEE 802.11 DCF. The significance of the model is rooted in providing closed-form expressions for

both the probability of collision and maximum throughput. The size of the CW at each node is modeled as a two-dimensional Discrete-Time Markov Chain based on the current values of both BC and backoff stage. Assuming that each node always has a load to transmit (i.e. saturated traffic), the *probability of transmitting* (τ) is given by (see [29] for complete derivation)

$$\tau = \frac{2(1-2p)}{(1-2p)(W+1) + pW(1-(2p)^m)} \tag{3.1}$$

where W is the initial $\mathrm{CW}_{\min}$, m is the maximum backoff stage, and p is the *conditional collision probability* which occurs when at least one other node also transmits and is expressed as

$$p = 1 - (1-\tau)^{n-1} \tag{3.2}$$

where n is the total number of nodes. Equations (3.1) and (3.2) can be solved numerically to calculate the values of τ and p for each node.

Accordingly, the *probability of a successful transmission* (P_s) is the conditional probability there is exactly one transmission given there is at least one transmission, which simplifies to

$$P_s = \frac{n\tau(1-\tau)^{n-1}}{1-(1-\tau)^n}. \tag{3.3}$$

In the case of the basic access mode of DCF (i.e. no RTS/CTS), the amount of time used to successfully transmit useful data (i.e. without overhead) is given by the *normalized system throughput* (S) as

$$S = \frac{P_s P_{tr} E[P]}{(1-P_{tr})\sigma + P_{tr} P_s T_s + P_{tr}(1-P_s)T_c} \tag{3.4}$$

where P_{tr} is the *probability that there is at least a transmission*, and it is given by

$$P_{tr} = 1 - (1 - \tau)^n. \tag{3.5}$$

T_s is the *expected time needed for a successful transmission* which is expressed as

$$T_s = \mathrm{H} + E[P] + \mathrm{SIFS} + \mathrm{ACK} + \mathrm{DIFS} + 2\delta \tag{3.6}$$

and T_c is the *expected time spent during a collision* which is expressed as

$$T_c = \mathrm{H} + E[P^*] + \mathrm{DIFS} + \delta \tag{3.7}$$

where $E[P]$ is the expected payload time, $E[P^*]$ is the expected collision time, and H is the total time for both PHY and MAC headers. Values for headers, SIFS, ACK, DIFS, time slot duration (σ), and propagation delay (δ) are set by IEEE 802.11 standard.

3.5 CSMA with Collision Tolerance (CSMA/CT)

Both IEEE 802.11 and the Bianchi Model [29] are based on HD assumptions. This section shows how some quantities used in the Bianchi Model change when IBFD methods are assumed.

3.5.1 Conditional Collision Probability in IBFD WiFi

The concept of IBFD communications can be used to propose a scheme where certain collisions are tolerable. Namely, unlike contemporary HD WiFi systems, collision-free transmission in IBFD-enabled WiFi networks does not only happen when one node transmits while

all other nodes are silent. Two additional cases leading to successful transmission exist and are as follows:

1. The transmitting node is the Access Point (AP) *and* the corresponding client station (STA) is also transmitting back to the AP.

2. The transmitting node is a client STA *and* the AP is also transmitting back to it.

Therefore, by extending the analysis provided in [29], the expression for the conditional collision probability at each node under an IBFD assumption can be rewritten as

$$\begin{aligned} p^{IBFD} &= 1 - [(1-\tau)^{n-1} + \frac{1}{n} \cdot \frac{1}{n-1} \cdot \tau(1-\tau)^{n-2} + \frac{n-1}{n} \cdot \frac{1}{n-1} \cdot \tau(1-\tau)^{n-2}] \\ &= 1 - [\underbrace{(1-\tau)^{n-1}}_{\text{HD term}} + \underbrace{\frac{\tau(1-\tau)^{n-2}}{n-1}}_{\text{IBFD term}}]. \end{aligned} \tag{3.8}$$

The addition of an IBFD term decreases the probability of collision. When $n = 2$, $p^{IBFD} = 0$ leading to totally collision-free communications. When $n \to \infty$, the IBFD term approaches zero reducing the impact of IBFD term on p^{IBFD} as the number of nodes increases.

3.5.2 Probability of Successful Transmission in IBFD WiFi

When IBFD techniques are used, a successful transmission is no longer restricted to the case defined as the probability of exactly one transmission given that there is at least a transmission. Two additional cases exist and are as follows:

1. The probability of two transmissions, one is by the AP *and* the other is by the corresponding client STA back to the AP given that there is at least a transmission.

2. The probability of two transmissions, one is by a client STA *and* the other is by the AP back to the STA given that there is at least a transmission.

Therefore, the expression for the probability of a successful transmission under an IBFD assumption is

$$\begin{aligned} P_s^{IBFD} &= \frac{n\tau(1-\tau)^{n-1}}{1-(1-\tau)^n} + \frac{1}{n}\cdot\frac{1}{n-1}\cdot\frac{\tau^2(1-\tau)^{n-2}}{1-(1-\tau)^n} + \frac{n-1}{n}\cdot\frac{1}{n-1}\cdot\frac{\tau^2(1-\tau)^{n-2}}{1-(1-\tau)^n} \\ &= \underbrace{\frac{n\tau(1-\tau)^{n-1}}{1-(1-\tau)^n}}_{\text{HD term}} + \underbrace{\frac{\tau^2(1-\tau)^{n-2}}{(n-1)[1-(1-\tau)^n]}}_{\text{IBFD term}}. \end{aligned} \tag{3.9}$$

The addition of an IBFD term increases the probability of successful transmission. When $n = 2, P_s^{IBFD} = 1$ (all transmissions are successful). When $n \to \infty$, the IBFD term approaches zero reducing the impact of the IBFD term on P_s^{IBFD} as the number of nodes increases.

3.6 IBFD Throughput Gain Due to Full-Duplex Factor (FDF)

The concept of Symmetry Ratio (SR) defined in [30] is used here as the ratio of the UL load over the DL load. The UL load is assumed to be smaller than the DL load. If the traffic load is designated as (L) and transmission time as (T), $\mathrm{SR_i}$ at $\mathrm{STA_i}$ is

$$\mathrm{SR_i} = \frac{L_{UL}}{L_{DL}} = \frac{T_{UL}}{T_{DL}} < 1. \tag{3.10}$$

Full-Duplex Factor (FDF) is defined here as the average of all SR values of the client STAs in the network which can be calculated as

$$\mathrm{FDF} = \frac{\sum_{i=1}^{n-1} \mathrm{SR}_i}{n-1} < 1. \tag{3.11}$$

Therefore, the normalized system throughput under an IBFD assumption is modified as

$$S^{IBFD} = \frac{P_s^{IBFD} P_{tr} E[P] \cdot \overbrace{(1 + \text{FDF})}^{\text{IBFD Gain}}}{(1 - P_{tr})\sigma + P_{tr} P_s^{IBFD} T_s + P_{tr}(1 - P_s^{IBFD}) T_c}. \tag{3.12}$$

The throughput gain due to the bidirectional IBFD transmission is represented by the FDF term. In the next section, $E[P]$ and $E[P^*]$ values (which directly affect T_s and T_c quantities) are considered in both HD and IBFD cases.

3.7 Average Transmission Durations for Payload and Collision

3.7.1 E[P] and E[P*] in HD IEEE 802.11

An analytical expression for the average time to successfully transmit a payload is given by

$$(E[P])^{HD} = \frac{1}{n} \cdot E[P_{\text{AP}}] + \frac{n-1}{n} \cdot E[P_{\text{STA}}]. \tag{3.13}$$

The AP is assumed to always have a load of maximum MAC Protocol Data Unit ($\text{MPDU}_{\max}$) bytes as L_{DL}. Therefore,

$$E[P_{\text{AP}}] = \frac{\text{MPDU}_{\max}}{\text{Transmission rate}}. \tag{3.14}$$

As an assumption, $\text{L}_{\text{UL}} \in \{0.1 \times \text{MPDU}_{\max}, 0.2 \times \text{MPDU}_{\max}, ..., 0.9 \times \text{MPDU}_{\max}\}$. Therefore, the *average* payload duration when an STA transmits is

$$E[P_{\text{STA}}] = \frac{0.5 \times \text{MPDU}_{\max}}{\text{Transmission rate}}. \tag{3.15}$$

An expression for the average collision duration is

$$(E[P^*])^{HD} = (P_c)_{AP}^{HD} E[P_{\text{AP}}] + [100\% - (P_c)_{AP}^{HD}] E[(P_{\text{STA}}^*)] \tag{3.16}$$

where $(P_c)_{AP}^{HD}$ is the percentage of time the AP is involved in collisions and $E[P_{\text{STA}}^*]$ is the average collision duration when only STAs are involved in collisions without the AP. Following a similar analysis in [29] to express $(P_c)_{AP}^{HD}$, the conditional probability that both the AP and at least one other STA are transmitting given that there are least two transmissions is

$$(P_c)_{AP}^{HD} = \frac{\tau(1-(1-\tau)^{n-1})}{1-(1-\tau)^n - n\tau(1-\tau)^{n-1}} \times 100. \tag{3.17}$$

When $n = 2, (P_c)_{AP}^{HD} = 100\%$ (the AP is involved whenever there is a collision) as expected.

To calculate $E[P_{\text{STA}}^*]$, let X be a discrete random variable defined as

$$X = 10 \times max(\text{SR}_i \text{ in a collision}). \tag{3.18}$$

The probability mass function is

$$\text{Prob}(X = x) = \begin{cases} (\frac{1}{9})^k & \text{for} \quad x = 1 \\ \sum_{j=1}^{k} \binom{k}{j} (\frac{1}{9})^j (\frac{x-1}{9})^{k-j} & \text{for} \quad 2 \leq x \leq 9 \\ 0 & \text{otherwise} \end{cases} \tag{3.19}$$

where k is the number of colliding STAs. If $k = 2$, expression (3.19) simplifies to

$$\text{Prob}(X = x) = \begin{cases} \frac{2x-1}{81} & \text{for} \quad 1 \leq x \leq 9 \\ 0 & \text{otherwise} \end{cases} \tag{3.20}$$

As a result,

$$E[P^*_{\text{STA}}] = \sum_{j=1}^{9} \text{Prob}(X = j) \cdot \frac{j}{10} \cdot \frac{\text{MPDU}_{\max}}{\text{Transmission rate}} \approx \frac{0.6481 \times \text{MPDU}_{\max}}{\text{Transmission rate}}. \quad (3.21)$$

3.7.2 E[P] and E[P*] in IBFD IEEE 802.11

A saturated traffic condition is assumed. Since the transmission always occurs as IBFD between the AP and an STA, the AP is always transmitting. Consequently, when there is a collision, the AP is always involved. It follows that the duration of both a successful transmission and a collision is always equal to an AP transmission. Hence,

$$(E[P])^{IBFD} = (E[P^*])^{IBFD} = E[P_{\text{AP}}] = \frac{\text{MPDU}_{\max}}{\text{Transmission rate}}. \quad (3.22)$$

3.8 System Model

A WiFi network is assumed as shown in Fig. 3.1 with an AP and $n-1$ client STAs using IEEE 802.11ac release [26] to access a single channel. The basic mode without 4-way RTS/CTS handshake is assumed. Total packet loss occurs in case of a collision (i.e. no capture effect). No transmission errors occur at PHY, and there are no hidden terminals in the network (i.e. all nodes hear one another). Transmission always occurs with no fragmentation or aggregation. It is assumed that the AP always has a load of $\text{MPDU}_{\max}$, and each STA_i has $0.1 \leq \text{SR}_i \leq 0.9$. STAs keep SR values constant throughout each simulation run. For IBFD WiFi, all transmissions occur as IBFD between the AP and an STA, and each transmission lasts until the AP finishes transmitting its traffic. Table 3.1 shows the PHY and MAC parameters.

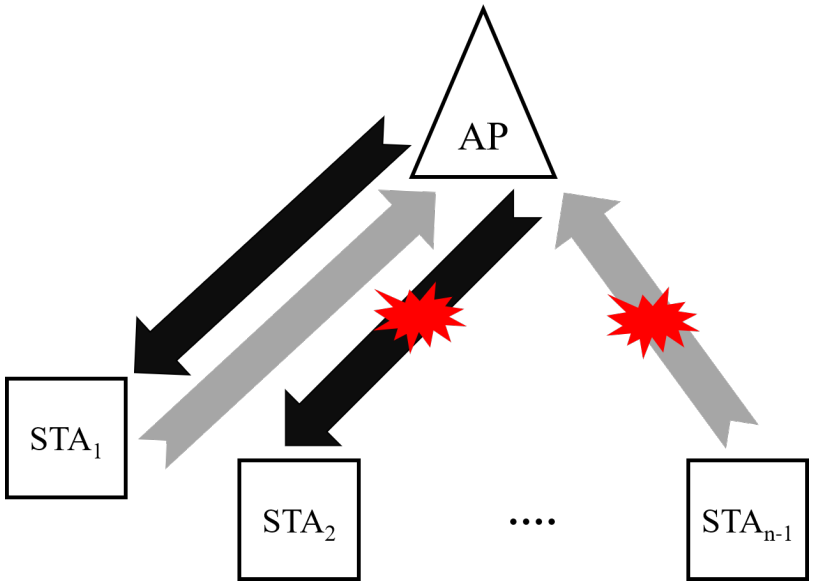

Figure 3.1: A collision in a typical WiFi network.

Table 3.1: IEEE 802.11ac PHY and MAC Parameters

Parameter	Value
Frequency	5 GHz band
Channel bandwidth	80 MHz
Modulation scheme	16-QAM
Code rate	1/2
Spatial streams	2×2 MIMO
PHY header duration	44 μs
Guard Interval (GI)	800 ns
Transmission rate	234 Mbps
Basic rate	24 Mbps
MAC header size	36 bytes
FCS size	4 bytes
ACK size	14 bytes
MPDU_{max} size	7,991 bytes
Slot duration (σ)	9 μs
SIFS duration	16 μs
DIFS duration	34 μs
CW_{min}	16
CW_{max}	1024

3.9 Results and Evaluation

3.9.1 Modified Collision and Transmission Probabilities

Establishing the IBFD assumption into a WiFi system directly introduces a change in the probability of collision p. Consequently, a change in transmission probability τ is also introduced. Analytical results for both p and τ are illustrated in Fig. 3.2. When CSMA/CT is introduced into the system, p decreases while τ increases. Intuitively, this is due to the fact that a node tends to transmit when its probability of collision decreases. It is also worth noting that when the number of nodes is 2, the probability of collision is zero, and the system is collision-free. This case is only possible due to the IBFD assumption which introduces CSMA/CT reaching its peak performance when the number of nodes is 2. The significance of CT on τ and p diminishes as the number of STAs gets larger. This is due to the fact that when there is a large number of STAs, the odds of a CT scenario happening approaches zero. Analytically, this was previously explained by noting that the IBFD term in the derived expression for p^{IBFD} in equation 3.8 becomes zero as the number of nodes approaches infinity.

3.9.2 Modified Probability of a Successful Transmission

Fig. 3.3 shows the effect of CT on the probability of a successful transmission P_s. Both analytical and simulation results are illustrated. The case of the standard HD IEEE 802.11 DCF is shown as a reference. The significance of the CSMA/CT scheme is that every transmission is successful when the number of nodes is 2. Similar to the results in the previous section, the influence of IBFD on the system diminishes as the number of STAs increases, which is explained by the same argument that when the number of STAs increases, the chances of CT cases happening decreases, and consequently the IBFD term in the derived

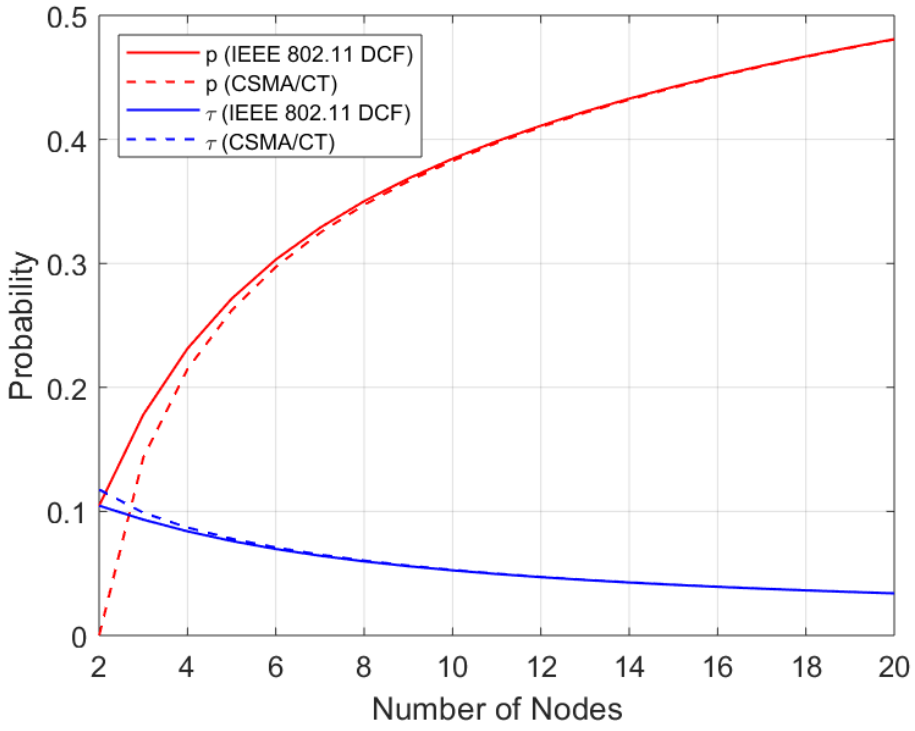

Figure 3.2: Analytical values for τ and p versus number of nodes.

expression 3.9 for P_s^{IBFD} disappears. This intuitive result is also confirmed by the matching analytical and simulation results.

3.9.3 IBFD Throughput Gain (Deterministic SR Values)

Fig. 3.4 shows both analytical and simulation results for normalized throughput versus the number of nodes. The case for standard IEEE 802.11 DCF is shown as a base case. The case when FDF equals to 0.5 (each STA has an SR = 0.5) is shown. IBFD throughput gain is due to both CT and the bidirectional flow of traffic represented by FDF. When the number of nodes is 2, there is a 41% gain in throughput compared to 35% when the number of nodes is 20. This is explained by the fact that when the number of nodes is 2, the gain is due to both CT (collision-free mode) and FDF, while the throughput gain is only dominated by FDF when the number of STAs is large. There is another reason for the lower improvement

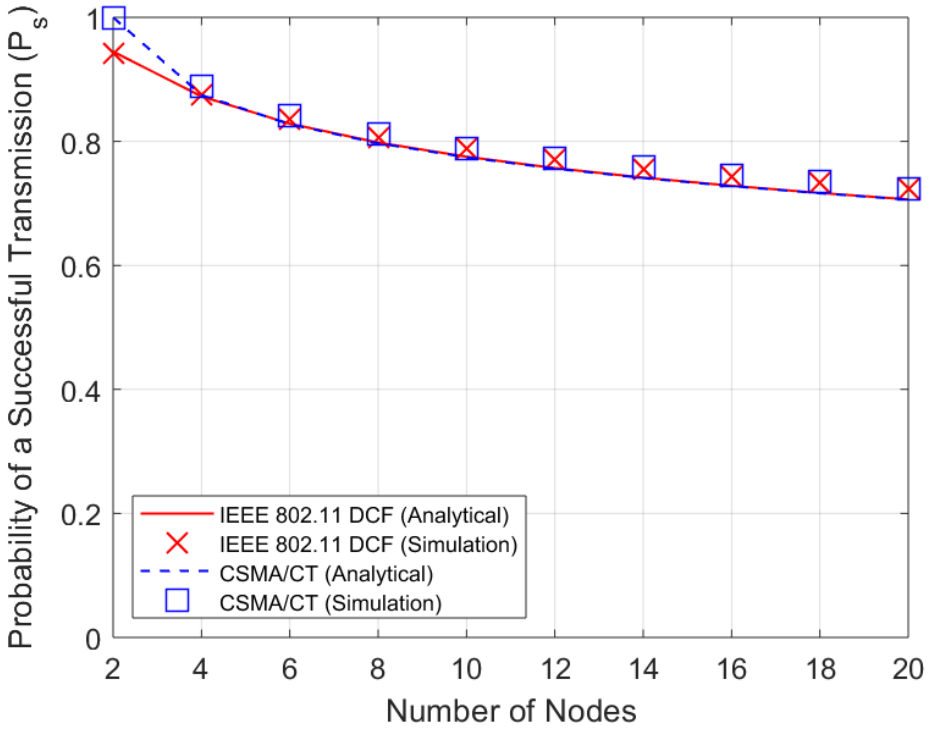

Figure 3.3: Probability of a successful transmission (P_s) versus number of nodes.

in throughput gain when the number of STAs increases. The high number of STAs leads to a higher number of collisions, which consequently decreases throughput.

3.9.4 Collision Metrics $(P_c)_{AP}$ and $E[P^*]$

In this section, metrics related to collisions are examined. Fig. 3.5 shows both analytical and simulation results for the percentage of time the AP is involved in collisions $(P_c)_{AP}$ against the number of nodes. Analytical results for the HD case is based on equation (3.17). For the standard IEEE 802.11 case, $(P_c)_{AP}^{HD} = 100\%$ when the number of nodes $= 2$ since the AP is always involved in every collision. $(P_c)_{AP}^{HD}$ decreases as the number of nodes increases since there are more client STAs colliding by contending for the channel. For the IBFD case, $(P_c)_{AP}^{IBFD} = 0$ when the number of nodes is 2 since this is the collision-free mode. Once there are more than 2 nodes, $(P_c)_{AP}^{IBFD} = 100\%$ since the AP is always involved in every collision.

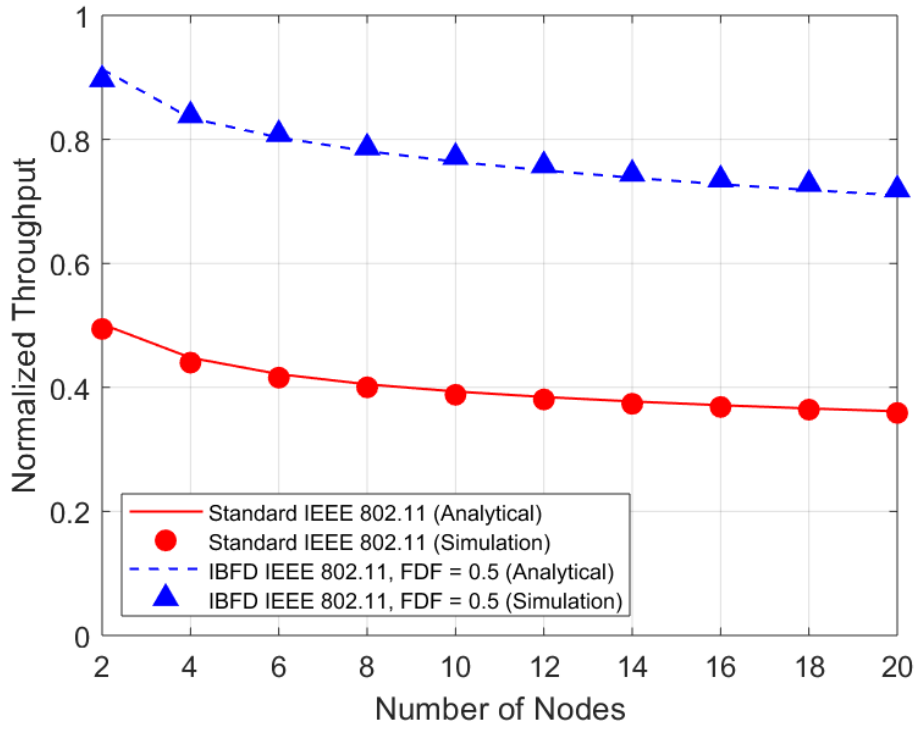

Figure 3.4: Normalized throughput versus number of nodes (all SRs = 0.5).

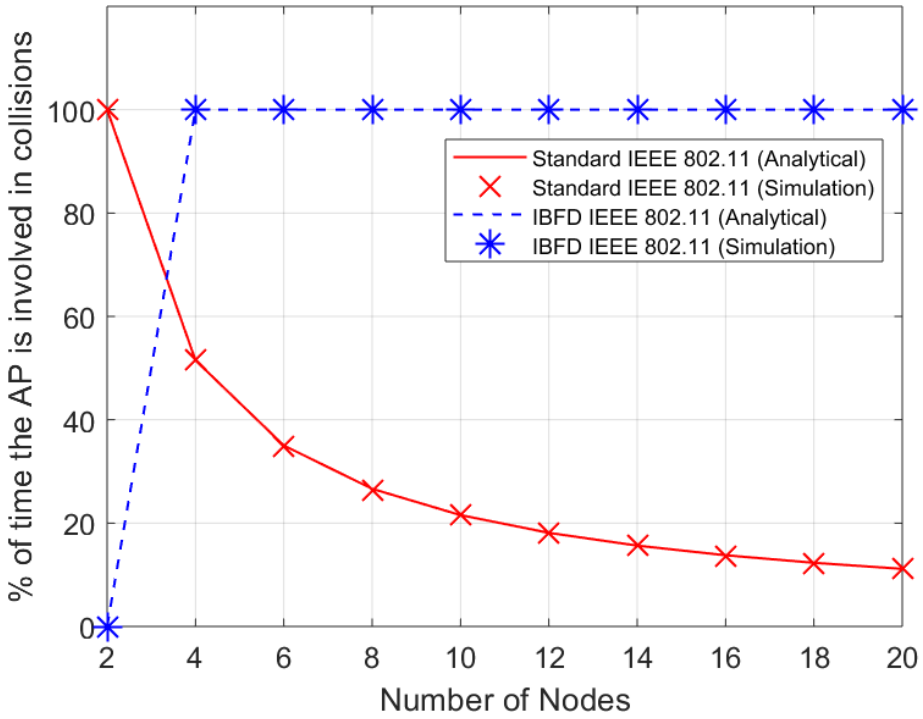

Figure 3.5: Percentage of time the AP is in collisions $(P_c)_{AP}$ versus number of nodes.

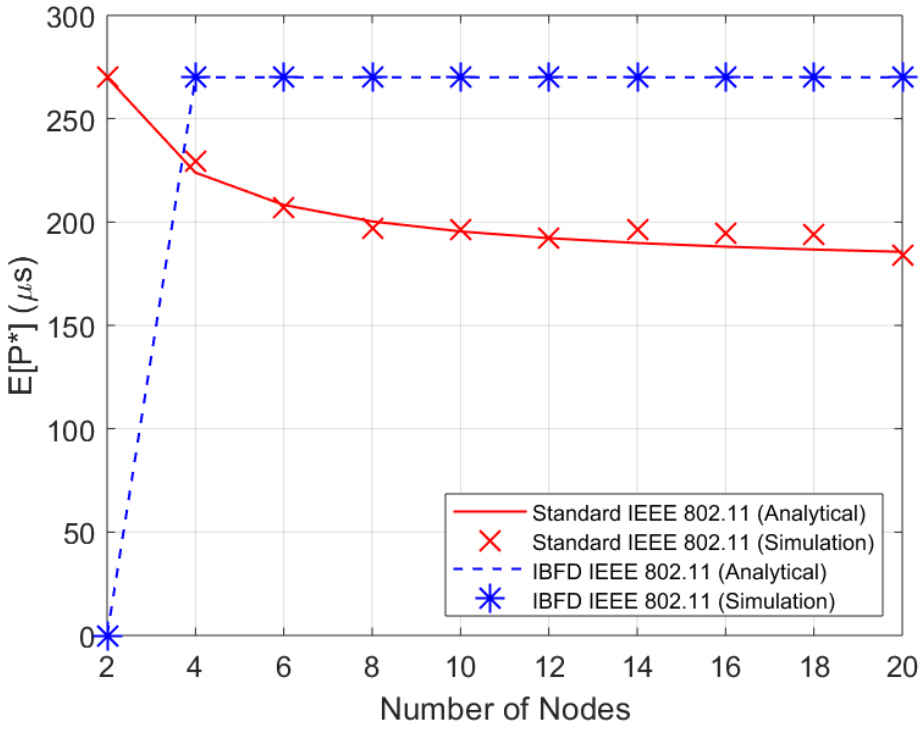

Figure 3.6: E[P*] versus number of nodes.

Fig. 3.6 shows both analytical and simulation results for $E[P^*]$ versus the number of nodes. The average of 20 simulation runs is taken. Analytical results for the HD case are plotted. For the standard IEEE 802.11 DCF, the value of $(E[P^*])^{HD}$ decreases as the number of nodes increases since there are more client STAs with smaller loads than that of the AP being involved in collisions. For the IBFD case, $(E[P^*])^{IBFD} = 0$ when the number of nodes equals 2 since this corresponds to the collision-free mode. Once the number of nodes is more than 2, $(E[P^*])^{IBFD}$ is constant and always equal to $E[P_{\text{AP}}]$ since AP is always involved in all collisions. Therefore, a drawback of introducing IBFD in IEEE 802.11 is that collisions always take longer. However, overall IBFD gain still introduces improvement in the system performance despite the longer collision durations.

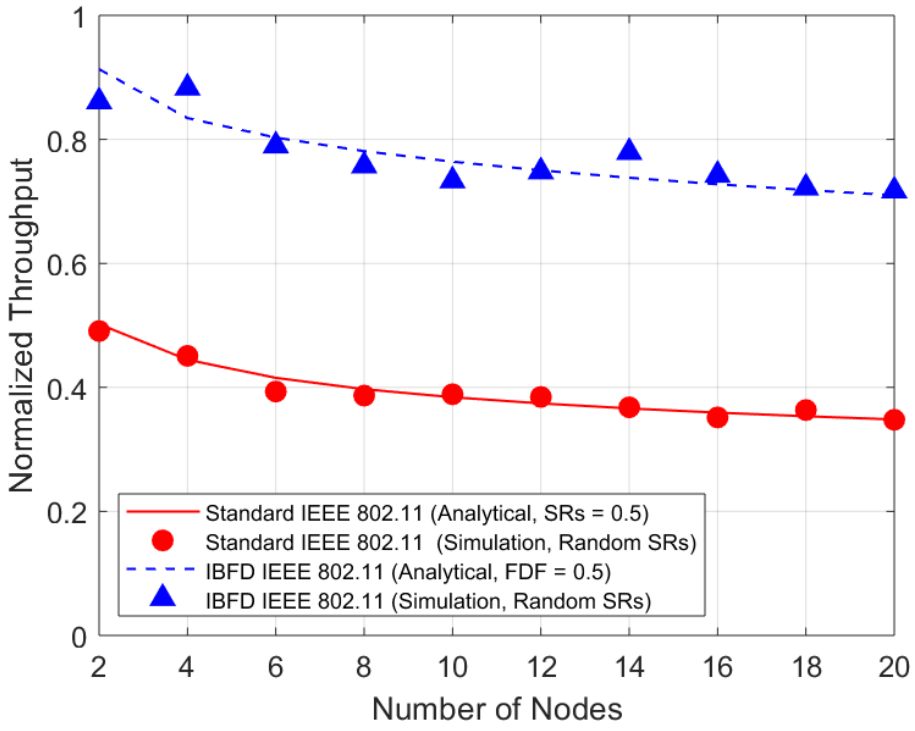

Figure 3.7: Normalized throughput versus number of nodes (5 runs).

3.9.5 IBFD Throughput Gain (Random SR Values)

A random SR value is assigned here to each client STA according to $0.1 \leq \mathrm{SR}_i \leq 0.9$. The SR values are kept constant throughout each simulation run. The expressions of average transmission durations for payload and collision ($E[P]$ and $E[P^*]$) were incorporated in the simulation and analysis to accurately capture the effect of random SR values. The average of only 5 runs is taken in a Monte Carlo simulation setup. The results of normalized throughput versus number of nodes are shown in Fig. 3.7. Simulation results are scattered around the trend of analytical results. The simulation results here lack accuracy due to the low number of simulation runs.

Fig. 3.8 displays the results of normalized throughput when SR values are still random but the number of independent simulation runs is increased to 200. Simulation results for both HD and IBFD systems coincide with the analytical results. There is a 41% IBFD throughput

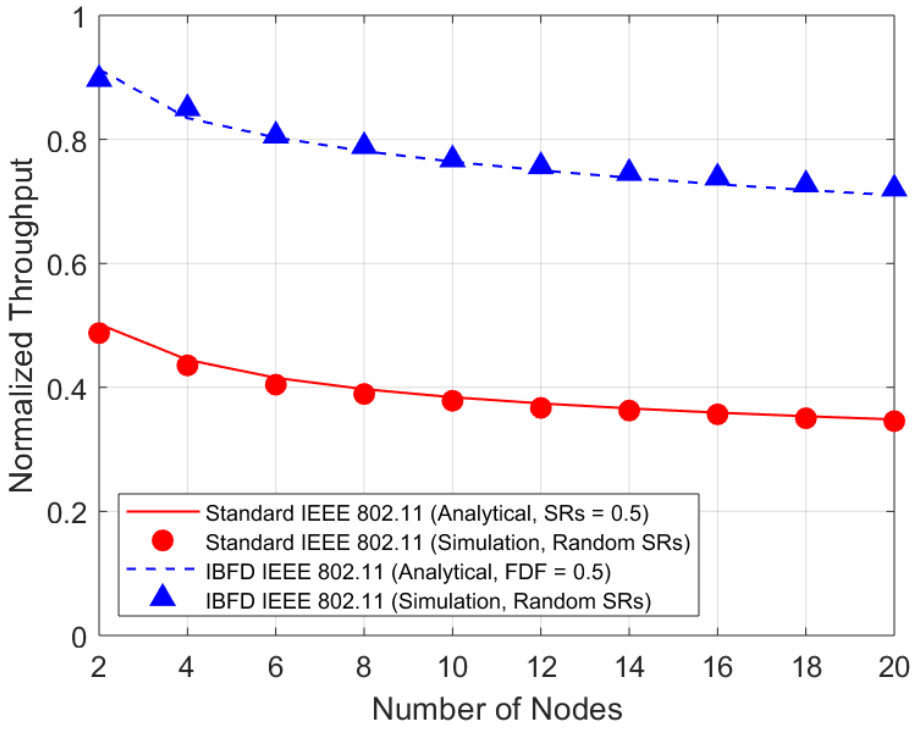

Figure 3.8: Normalized throughput versus number of nodes (200 runs).

gain when the number of nodes is 2. When the number of nodes is increased to 20, IBFD throughput gain drops to 36%. The results here are in agreement with the case of fixed SR values. Hence, the analyses for collision and throughput gain scale properly when random metrics are introduced into the system. Therefore, the analytical expressions presented in this chapter as an IBFD IEEE 802.11 model accurately represent the behavior of the system as confirmed by simulations.

3.10 Conclusion

This chapter demonstrates a modified analytical model for IBFD IEEE 802.11. Expressions for WiFi system metrics (represented by probabilities) are revised to incorporate IBFD into a WiFi network. An accurate analysis to capture the effect of IBFD communications on

packet collisions was shown by proposing CSMA/CT. IBFD gain in normalized throughput is illustrated by introducing the FDF term. A special case for collision-free communications due to IBFD is presented. Results show that the proposed analytical model for IBFD IEEE 802.11 is robust even when randomness is introduced in simulation scenarios.

The number of WiFi hotspots is expected to grow to more than 540 million by 2021 compared to 94 million in 2016, and WiFi traffic will represent about half of the global IP traffic by 2020 [31]. Therefore, IEEE 802.11 standard needs to implement new methods to increase WiFi system capacity, and IBFD is a strong candidate to improve performance.

Chapter 4

Analytical Modeling and Latency Reduction for IBFD WLANs

4.1 Motivation

The growth of video traffic led to larger data loads in the downlink (DL) direction to users as compared to uplink (UL) data from users. While Ethernet traffic is declining, WiFi traffic is growing [31]. Additionally, even with the prevalence of social networks, where users frequently upload content, the degree of viewership of video has continued to outpace upload leading to a pattern of asymmetric data traffic that is expected to continue for the upcoming years [32]. Therefore, data traffic in Wireless Local Area Networks (WLANs) is becoming more asymmetric, and this pattern of asymmetry is expected to continue to be the norm. IEEE 802.11 standard defined in [19] enables client Stations (STAs) to communicate with an Access Point (AP). IEEE 802.11 Distributed Coordination Function (DCF) constitutes the foundation of the Medium Access Control (MAC) protocol for WLANs. By design, IEEE 802.11 DCF does not consider the amount of traffic a node has when facilitating

access to the wireless channel. Thus, all WLAN nodes (i.e. the AP and client STAs) have an equal opportunity to access the channel despite the asymmetry between traffic loads in the UL and DL directions. Consequently, traffic asymmetry coupled with equal access to the channel leads to serving data traffic inefficiently in contemporary WLANs. As a result, there is increasing pressure to design future wireless networks that can cope with demands for higher data rates, lower latency, and efficient utilization of resources. Contemporary wireless communications systems are approaching performance limits set by classical analyses. Therefore, there is a need to innovatively design wireless systems that revolutionize the current perception of theoretical limits.

4.2 Contribution

In this chapter, two-dimensional Discrete-Time Markov Chain (DTMC) analysis is used to produce an accurate analytical model for IBFD-WLANs based on IEEE 802.11 DCF. In addition, to serve data traffic even more efficiently, two distributed aggregation solutions for IBFD-WLANs are proposed. Each STA can make an independent decision about the possibility and amount of aggregation based on knowing the size of the traffic it receives. Simulation results indicate that IBFD aggregation leads to both maximizing the throughput of the system and minimizing the average latency of frame delivery. The final contribution of this chapter is to formalize metrics in order to study the increase in efficiency that IBFD provides for WLANs. Fig. 4.1 illustrates a typical IBFD-WLAN network with asymmetric traffic and the possibility of frame aggregation.

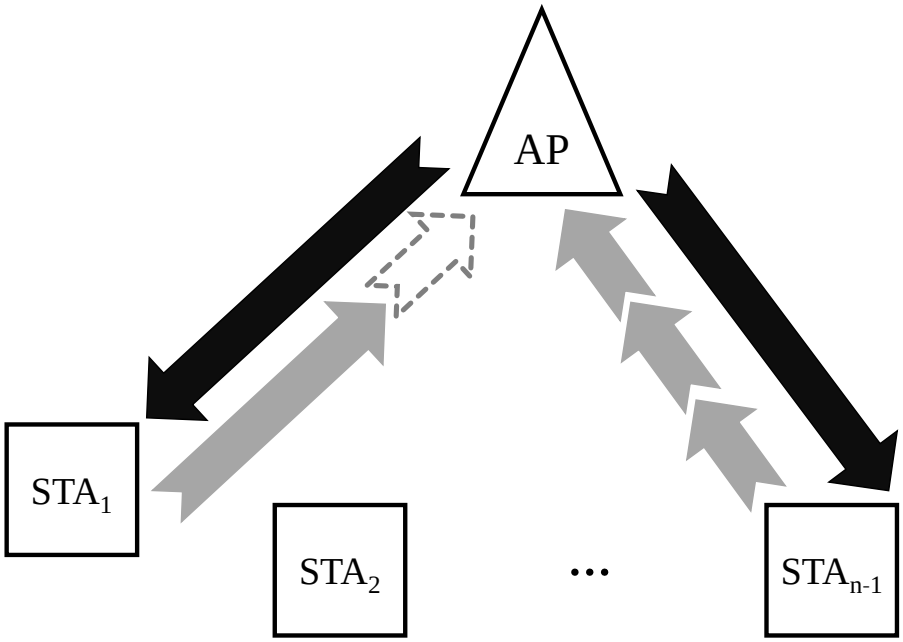

Figure 4.1: A typical IBFD-WLAN with asymmetric traffic loads.

4.3 Prior Work

There were several previously published research attempts to provide analytical models for IBFD MAC protocols. In [33], a MAC protocol for wireless ad hoc networks is studied based on a three-dimensional DTMC model, but the proposed protocol deviates from IEEE 802.11 DCF mechanism and neglects to derive IBFD-compatible expressions for the probability of transmission. The two-dimensional DTMC model outlined in [34] does not account for starting a new contention cycle after a node successfully gets an IBFD transmission opportunity, and the model does not follow IEEE 802.11 when it comes to an unsuccessful transmission at the maximum backoff stage. The IBFD MAC protocol in [35] focuses on simultaneous transmitting and sensing, but the analysis does not fully exploit IBFD benefits for increasing throughput and reducing latency. The authors of [36] model a new MAC protocol as a three-dimensional DTMC to use IBFD-synchronized transmission only after a successful HD transmission, but the model does not treat collisions accurately. While [37] addresses both throughput and delay in the three-dimensional DTMC analysis for a proposed distributed

MAC protocol, the work primarily focuses on multi-hop networks. The IBFD MAC protocol proposed in [38] limits IBFD capabilities to the AP only and substantially neglects to show the details of the theoretical work leading to a basic expression for the probability of transmission. An Embedded Markov Chain model is used in [39] to study a Carrier-Sense Multiple Access with Collision Avoidance (CSMA/CA) MAC protocol, but the proposed protocol uses a fixed contention window and does not follow IEEE 802.11 Binary Exponential Backoff in case of a collision. The reported results for throughput and delay in [40] show major mismatch between theoretical and simulation results, and the authors state that there was not enough space to include derived analytical expressions for delay calculations. Both inaccuracy of results and lack of a full model for IBFD-WLANs are resolved in this chapter. While references [41, 42, 43, 44, 45] all address IBFD MAC solutions, none of them look into producing an analytical expression for the probability of transmission, which is a substantial part of this chapter's contributions.

4.4 Background on HD IEEE 802.11 DCF Modeling

A well-celebrated analytical model for IEEE 802.11 DCF was presented in [29]. This model was subsequently revised a number of times, especially when it comes to the the *probability of transmitting* (τ). To generate highly accurate results for HD IEEE 802.11 DCF, τ is adopted from the refined model published in [46] as

$$\tau = \frac{1}{1 + \frac{1-p}{1-p^{R+1}} \sum_{i=0}^{R} p^i (2^i W - 1)/2 - \frac{1-p}{2}} \tag{4.1}$$

where W is the initial Contention Window ($\mathrm{CW}_{\min}$), R is the maximum number of retransmission attempts, and p is the *conditional collision probability*. A wireless node experi-

ences a collision when at least one other node concurrently transmits. Therefore,

$$p = 1 - (1 - \tau)^{n-1} \tag{4.2}$$

where n is the total number of nodes. Equations (4.1) and (4.2) can simply be solved numerically to calculate the values of τ and p for each node.

The *probability of a successful transmission* (P_s) is the conditional probability there is exactly one transmission given there is at least one transmission, which is equal to

$$P_s = \frac{n\tau(1-\tau)^{n-1}}{1-(1-\tau)^n}. \tag{4.3}$$

The *throughput* (S) in bits per second (bps) is calculated as

$$S = \frac{P_s P_{tr} \overline{E[P]}}{(1-P_{tr})\sigma + P_{tr} P_s \overline{T_s} + P_{tr}(1-P_s)\overline{T_c}} \tag{4.4}$$

where P_{tr} is the *probability that there is at least a transmission*, and it is given by

$$P_{tr} = 1 - (1-\tau)^n. \tag{4.5}$$

According to [46], an accurate characterization for the throughput is achieved if the *expected payload size* $\overline{E[P]}$, the *expected time needed for a successful transmission* ($\overline{T_s}$), and the *expected time spent during a collision* ($\overline{T_c}$) are respectively expressed as

$$\overline{E[P]} = P\frac{W}{W-1}, \tag{4.6}$$

$$\overline{T_s} = T_s \frac{W}{W-1} + \sigma, \tag{4.7}$$

and

$$\overline{T_c} = T_c + \sigma \tag{4.8}$$

where

$$T_s = \mathrm{H} + \text{payload time} + \mathrm{SIFS} + \mathrm{ACK} + \mathrm{DIFS} \tag{4.9}$$

and

$$T_c = \mathrm{H} + \text{collision time} + \mathrm{SIFS} + \mathrm{ACK} + \mathrm{DIFS}. \tag{4.10}$$

P is the payload size. H is the time for both PHY and MAC headers. Values for headers, SIFS, ACK, DIFS, and time slot (σ) are set by IEEE 802.11 standard. Table 3.1 shows the assumed values of PHY and MAC parameters based on the IEEE 802.11ac release [26].

Considering the system model detailed in the next section, analytical expressions for the expected size of successfully transmitted MAC Protocol Data Unit (MPDU) and the expected size of a collision are thoroughly derived in [47] and can respectively be simplified as

$$(E[P])^{HD} = \frac{n+1}{2n} \cdot \mathrm{MPDU}_{\max} \tag{4.11}$$

and

$$(E[P^*])^{HD} \approx \left[\frac{0.3519 \times \tau(1-(1-\tau)^{n-1})}{1-(1-\tau)^n - n\tau(1-\tau)^{n-1}} + 0.6481 \right] \mathrm{MPDU}_{\max}. \tag{4.12}$$

Latency is calculated as the average time from the instant a frame becomes Head-of-Line (HOL) until the frame is successfully delivered. The analytical expression for latency in HD IEEE 802.11 is derived in [48] directly from the well-known Little's Theorem (see [49] for further explanation) as

$$D = \frac{n}{S/E[P]}. \tag{4.13}$$

4.5 System Model

This chapter assumes a WLAN with an AP and $n-1$ client STAs using IEEE 802.11ac standard to communicate over a single channel. The basic mode of DCF without Request to Send/Clear to Send (RTS/CTS) handshake is assumed. In case of a collision, total frame loss occurs (no capture effect). Error-free PHY transmission is assumed, and all nodes can detect one another (no hidden terminals). The AP always has a load of $\text{MPDU}_{\max}$. A saturated buffer at each node is assumed (i.e. there is always traffic to transmit), and frame aggregation is possible by combining more than one MPDU to make a larger aggregated MPDU. Client STAs have Symmetry Ratio (SR) values where the value of SR at STA_i, indicated here as ρ_i, is defined in [30] as the ratio of the UL load over the DL load. If the traffic load is designated as (L) and transmission time as (T), then ρ is

$$\rho \triangleq \frac{L_{UL}}{L_{DL}} = \frac{T_{UL}}{T_{DL}}. \tag{4.14}$$

Each STA_i has $0.1 \leq \rho_i \leq 0.9$. STAs keep their original ρ values constant throughout each simulation run.

In IBFD-WLAN scenarios, all transmissions occur as IBFD between the AP and an STA. The Full-Duplex Factor (FDF) defined in [47] as the average of all ρ values of the client

STAs in the network can be calculated as

$$\Phi \triangleq \frac{\sum_{i=1}^{n-1} \rho_i}{n-1}. \tag{4.15}$$

For an HD system, $\Phi = 0$.

4.6 Analytical Model for IBFD-WLAN

Prior work to model contemporary IEEE 802.11 DCF was based on the assumption that all transmission takes place in a Time-Division Duplexing (TDD) fashion, which is an HD scheme. Therefore, the prominent model originally presented in [29] is no longer valid when the transmission is IBFD. In HD systems, two key parameters, namely the probability of transmitting (τ) and the conditional collision probability (p), determine the performance of a WLAN at the MAC sub-layer. However, when the system is IBFD, both τ and p must be revised. First, unlike the HD case where AP and STAs share equal τ and p values, there are τ_{AP}, τ_{STA}, p_{AP}, and p_{STA} values in an IBFD network. Second, in addition to the *direct* transmission probability, τ, which happens when a node wins the contention for the channel, there is potential for IBFD *reply-back* transmission when the node is not in direct transmission ($\overline{\tau}$). The probability of reply-back transmission (β) for a tagged node happens when another node is in direct transmission with the tagged node. Third, collisions are treated differently for IBFD systems compared to a contemporary HD WLAN, which is thoroughly explained in [47].

In this section, analytical work is carried out to construct a model for IBFD-WLAN based on IEEE 802.11 DCF protocol. Key parameters needed to calculate important performance metrics are defined. All parameters take into account IBFD and its effects on the behavior of wireless nodes at MAC-level operations.

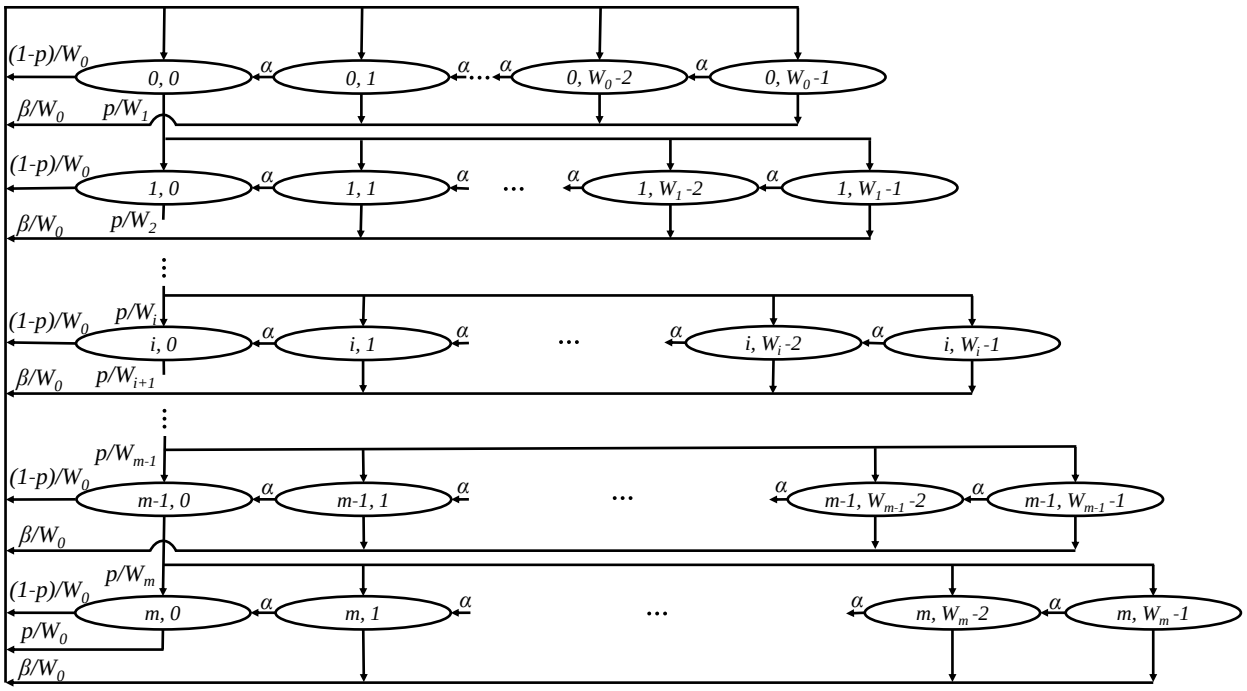

Figure 4.2: Two-dimensional DTMC representing backoff stage and backoff counter for each wireless node.

4.6.1 Revised Probability of Transmission

Fig. 4.2 shows the model adopted for IBFD-WLAN. The two-dimensional DTMC model represents each state in terms of backoff stage, i, and backoff counter, k. Unlike [40], the model in Fig. 4.2 resets its backoff stage to zero if a frame experiences a collision while the transmitting node is at the maximum backoff stage m.

The transition probabilities for the DTMC model are as follows

$$P\{0, k_0|i, 0\} = \frac{1-p}{W_0} \qquad i \in [0, m-1], \quad k_0 \in [0, W_0 - 1] \tag{4.16}$$

$$P\{i, k|i-1, 0\} = \frac{p}{W_i} \qquad i \in [1, m], \quad k \in [0, W_i - 1] \tag{4.17}$$

$$P\{0, k_0|m, 0\} = \frac{1}{W_0} \qquad k_0 \in [0, W_0 - 1] \tag{4.18}$$

$$P\{i, k-1|i, k\} = \alpha \qquad i \in [0, m], \quad k \in [1, W_i - 1] \tag{4.19}$$

$$P\{0, k_0|i, k\} = \frac{\beta}{W_0} \qquad i \in [0, m], \quad k \in [1, W_i - 1], \quad k_0 \in [0, W_0 - 1]. \tag{4.20}$$

The stationary distribution of the chain is represented as

$$b_{i,k} \triangleq \lim_{t \to \infty} P\{s(t) = i, b(t) = k\} \qquad i \in [0, m], \quad k \in [0, W_i - 1] \tag{4.21}$$

where $s(t)$ and $b(t)$ are respectively the stochastic processes for the backoff stage and backoff counter as in [29].

Direct transmission happens when a node is at any of the possible $b_{i,0}$ states. Therefore, the probability of direct transmission is

$$\tau \triangleq \sum_{i=0}^{m} b_{i,0}. \tag{4.22}$$

By applying the normalization condition, the following result can be directly obtained

$$\begin{aligned} 1 &= \sum_{i=0}^{m}\sum_{k=0}^{W_i-1} b_{i,k} = \sum_{i=0}^{m} b_{i,0} + \sum_{i=0}^{m}\sum_{k=1}^{W_i-1} b_{i,k} = \tau + \sum_{i=0}^{m}\sum_{k=1}^{W_i-1} b_{i,k} \\ &\Rightarrow \overline{\tau} \triangleq 1-\tau = \sum_{i=0}^{m}\sum_{k=1}^{W_i-1} b_{i,k} \end{aligned} \tag{4.23}$$

where $\overline{\tau}$ is the probability that there is potential for IBFD reply-back transmission when a node is not in direct transmission.

The expressions for both $b_{i,0}$ and $b_{0,0}$ are respectively as follows (see Appendix A for complete derivations)

$$b_{i,0} = b_{0,0}(\frac{p}{1-\alpha})^i \prod_{j=1}^{i} \frac{1-\alpha^{W_j}}{W_j}, 1 \leq i \leq m \tag{4.24}$$

and

$$b_{0,0} = \frac{\frac{1-\alpha^{W_0}}{W_0}\left[\frac{\alpha-p}{1-\alpha}\cdot\tau+1\right]}{1-(\frac{p}{1-\alpha})^{m+1}\prod_{j=0}^{m}\frac{1-\alpha^{W_j}}{W_j}}. \tag{4.25}$$

Thus, τ is readily calculated as

$$\tau = \sum_{i=0}^{m} b_{i,0} = b_{0,0} + \sum_{i=1}^{m} b_{i,0} = b_{0,0}\left[1+\sum_{i=1}^{m}(\frac{p}{1-\alpha})^i \prod_{j=1}^{i}\frac{1-\alpha^{W_j}}{W_j}\right]. \tag{4.26}$$

Given that calculating α and p is treated in the next two sub-sections, the value of τ can be numerically calculated using (4.25) and (4.26). While τ is the same for the AP and STAs in contemporary HD IEEE 802.11 DCF, its value in an IBFD-WLAN is different depending on if the transmitting node is the AP or an STA. τ_{AP} and τ_{STA} are calculated based on the corresponding α_{AP}, p_{AP}, α_{STA}, and p_{STA} values. Finally, the average probability

of transmission in the network is calculated as

$$\tau^{IBFD} = \frac{1}{n}\tau_{AP} + \frac{n-1}{n}\tau_{STA}. \tag{4.27}$$

4.6.2 Probability of reply-back IBFD transmission

In IBFD-WLAN, each node has an opportunity for indirect transmission. Whenever a node is not in any of the states represented by τ, the node can have the opportunity to transmit if another node is transmitting to it. There are two cases for this to happen as follows

1. When the AP is silent, it still has an opportunity to transmit whenever an STA is transmitting. This probability can be represented as

$$\beta_{AP} = (n-1)\tau_{STA}(1-\tau_{STA})^{n-2} = (n-1)\tau_{STA}(\overline{\tau}_{STA})^{n-2}. \tag{4.28}$$

2. When an STA is silent, it still has an opportunity to transmit whenever the AP is transmitting to that particular STA. This probability is represented as

$$\beta_{STA} = \frac{\tau_{AP}(1-\tau_{STA})^{n-2}}{n-1} = \frac{\tau_{AP}(\overline{\tau}_{STA})^{n-2}}{n-1}. \tag{4.29}$$

For the special case when $n = 2$, (4.28) and (4.29) respectively become $\beta_{AP} = \tau_{STA}$ and $\beta_{STA} = \tau_{AP}$, which is compatible with the intuition that the AP has a reply-back opportunity whenever the STA is transmitting and vice versa. Also, based on Fig. 4.2, the following equation can be used to calculate both α_{AP} and α_{STA} according to the corresponding β_{AP} and β_{STA} values

$$\alpha = 1 - \beta. \tag{4.30}$$

4.6.3 Revised Conditional Collision Probability

In HD IEEE 802.11 networks, collisions are treated in the same way for the AP and all STAs. As a result, conditional collision probability, p, is defined in [29] as previously stated (refer to equation (4.2)). However, in IBFD scenarios, the conditional collision probability for the AP ($p_{_{AP}}$) is different from that of an STA ($p_{_{STA}}$). For the AP, collision-free transmission happens in either of the following two cases

1. The AP is in direct transmission while all STAs are silent.
2. The AP is in direct transmission with a tagged STA, and this tagged STA is directly transmitting back to the AP while all other STAs are silent.

Therefore, the conditional collision probability for the AP can be expressed as

$$\begin{aligned} p_{_{AP}} &= 1 - \left[(1-\tau_{_{STA}})^{n-1} + \tau_{_{STA}}(1-\tau_{_{STA}})^{n-2} \right] \\ &= 1 - \left[(\overline{\tau}_{_{STA}})^{n-1} + \tau_{_{STA}}(\overline{\tau}_{_{STA}})^{n-2} \right]. \end{aligned} \tag{4.31}$$

For the conditional collision probability of an active STA, transmission without collision takes place when either one of the below scenarios is true

1. The AP is silent, and so are all other STAs.
2. The AP is directly transmitting back to the active STA while all other STAs are silent.

Consequently, the conditional collision probability of a tagged STA is

$$\begin{aligned} p_{STA} &= 1 - \left[(1-\tau_{AP})(1-\tau_{STA})^{n-2} + \frac{\tau_{AP}(1-\tau_{STA})^{n-2}}{n-1} \right] \\ &= 1 - \left[\overline{\tau}_{AP}(\overline{\tau}_{STA})^{n-2} + \frac{\tau_{AP}(\overline{\tau}_{STA})^{n-2}}{n-1} \right]. \end{aligned} \tag{4.32}$$

Similar to how it was detailed in [47] with simplified assumptions regarding τ, (4.31) and (4.32) indicate that a collision-free mode of IBFD transmission is achieved when $n = 2$ since both equations respectively evaluate to $p_{AP} = 0$ and $p_{STA} = 0$.

4.6.4 Revised Probability of Successful Transmission

The probability of successful transmission for an IBFD-WLAN, P_s^{IBFD}, happens during any one of the following four conditional probabilities

1. There is exactly one direct transmission by the AP and all STAs are silent given there is at least a direct transmission.
2. There is exactly one direct transmission by an STA while the AP and all other STAs are silent given there is at least a direct transmission.
3. There are exactly two direct transmissions, one is by the AP and the other is by the corresponding STA back to the AP given that there is at least a direct transmission.
4. There are exactly two direct transmissions, one is by an STA and the other is by the AP back to the STA given that there is at least a direct transmission.

Therefore, P_s^{IBFD} is expressed as (see Appendix B for complete derivation)

$$P_s^{IBFD} = \frac{\tau_{AP}(\overline{\tau}_{STA})^{n-1} + (n-1)\tau_{STA}(\overline{\tau}_{AP})(\overline{\tau}_{STA})^{n-2}}{1 - [(\overline{\tau}_{AP})(\overline{\tau}_{STA})^{n-1}]} + \frac{\tau_{AP}\tau_{STA}(\overline{\tau}_{STA})^{n-2}}{(n-1)\big\{1 - [(\overline{\tau}_{AP})(\overline{\tau}_{STA})^{n-1}]\big\}}. \tag{4.33}$$

When (4.33) is evaluated at $n = 2$, (4.33) becomes $P_s^{IBFD} = 1$ indicating that every transmission is successful, which is consistent with the result assuming $\tau_{AP} = \tau_{STA} = \tau$ reported in [47].

4.7 IBFD-WLAN System Performance Metrics

In this section, IBFD-compatible metrics are outlined. The purpose of composing a portfolio of metrics is to measure the enhancements added by IBFD to WLAN performance. The metrics will be used to generate the results in this chapter.

4.7.1 Network Throughput

Throughput gain by IBFD was previously addressed in [47]. However, the focus there was primarily on presenting how collisions are treated and consequently affect the performance of normalized aggregate throughput. Therefore, the value of τ was directly obtained from [29]. The analysis in [47] is revisited here to include a more accurate model that considers both τ_{AP} and τ_{STA} derived in this chapter. Additionally, the total network throughput is calculated in the absolute sense in terms of bits per second instead of the normalized value. Therefore, the *network throughput* can be expressed as

$$S^{IBFD} = \frac{P_s^{IBFD} P_{tr}^{IBFD} E[P](1+\Phi)}{\overline{P_{tr}^{IBFD}}\sigma + P_{tr}^{IBFD} P_s^{IBFD} T_s + P_{tr}^{IBFD} \overline{P_s^{IBFD}} T_c} \tag{4.34}$$

where the probability of transmitting is revised here to include both τ_{AP} and τ_{STA} as

$$P_{tr}^{IBFD} = 1 - [(1-\tau_{AP})(1-\tau_{STA})^{n-1}] = 1 - [(\overline{\tau}_{AP})(\overline{\tau}_{STA})^{n-1}]. \tag{4.35}$$

Note that

$$\overline{P_{tr}^{IBFD}} = 1 - P_{tr}^{IBFD} \tag{4.36}$$

and

$$\overline{P_{s}^{IBFD}} = 1 - P_{s}^{IBFD}. \tag{4.37}$$

Both T_s and T_c are already reported respectively as (4.9) and (4.10) in this chapter. As explained in [47], since UL < DL, both the expected size of successfully transmitted MPDU and the expected size of a collision are equal to the load of the AP as follows

$$(E[P])^{IBFD} = (E[P^*])^{IBFD} = E[P_{_{AP}}] = \text{MPDU}_{\max}. \tag{4.38}$$

4.7.2 Frame Aggregation

Frame aggregation at the MAC sub-layer was introduced in the legacy IEEE 802.11n release [50] as a way to increase the efficiency of utilizing the channel by reducing the overhead. Aggregation enables a node to concatenate several frames into a single transmission. As a result, the overhead is reduced since there is no need to allocate transmission time for more than a single header duration if the frames are combined into one transmission. Frame aggregation can be either Aggregated MAC Service Data Unit (A-MSDU) or Aggregated MPDU (A-MPDU). In this chapter, MPDUs are aggregated. Details about frame aggregation in IEEE 802.11 standard can be found in [51] and [52].

The goal of frame aggregation is to increase traffic symmetry between UL and DL data loads and consequently serve traffic more efficiently. This section introduces two aggregation schemes which significantly improve network throughput, average latency, and link utiliza-

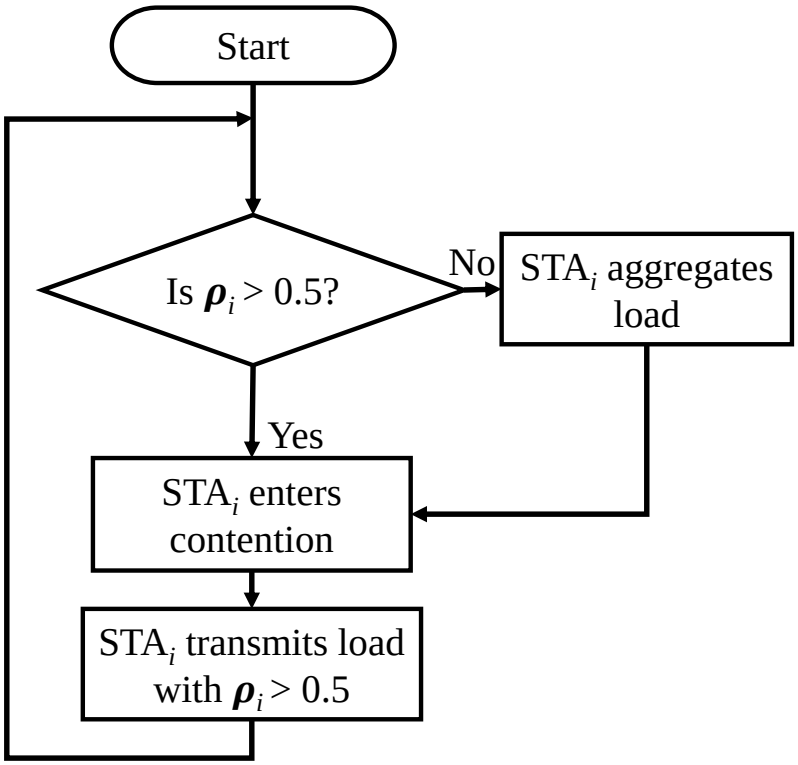

Figure 4.3: Flow chart of the proposed aggregation schemes.

tion. Fig. 4.3 shows a flow chart of how aggregation is performed based on the value of ρ at each STA. The frame aggregation schemes are namely *Dual-Frame Aggregation* and *Multi-Frame Aggregation*.

Dual-Frame Aggregation

In this aggregation scheme, any STA with $\rho \leq 0.5$ doubles its transmission load by aggregating two MPDUs. Thus,

$$\rho_{new}^{dual} := 2 \times \rho_{current}. \tag{4.39}$$

The *IBFD aggregation factor* (i.e. number of aggregated frames) for dual-frame aggregation is $\gamma^{dual} = 2$ if aggregation takes place. In this case, it is still guaranteed that each STA can fit

its transmission while the IBFD connection is established with the AP since UL $\leq$ DL even after frame aggregation. Dual-frame aggregation increases the utilization of the available UL transmission time that would be otherwise not used.

Multi-Frame Aggregation

Some STAs with $\rho < 0.5$ can aggregate more than two frames in a transmission. The following is a simple rule to calculate IBFD aggregation factor for multi-frame aggregation in order to determine how many frames each STA can aggregate based on its current ρ value

$$\gamma^{multi} \triangleq \texttt{floor}\left(\frac{1}{\rho}\right). \tag{4.40}$$

In this aggregation technique,

$$\rho_{new}^{multi} := \texttt{floor}\left(\frac{1}{\rho_{current}}\right) \times \rho_{current}. \tag{4.41}$$

The result of multi-frame aggregation is that STAs with very small ρ values can aggregate several frames, which increases both UL/DL traffic symmetry and utilization of available UL transmission time. For any STA with $\rho > 0.5$, no aggregation takes place ($\gamma^{dual} = \gamma^{multi} = 1$).

4.7.3 Average Latency

A similar analysis to the work in [48] is used to derive an analytical expression for average latency in IBFD-WLAN. According to [49], Little's Theorem classically states that the average number of customers in a system (N) is equal to the average arrival rate of the customers

(λ) multiplied by the average delay per customer in the system (T). Thus,

$$N = \lambda T \Rightarrow T = \frac{N}{\lambda}. \tag{4.42}$$

Since saturated traffic is assumed in the network, the number of customers in the system is always equal to the number of nodes n. Unlike the case of HD latency considered as equation (4.13), the case of IBFD transmission is more involved. The expected number of aggregated MPDUs, $E[\gamma]$, must be taken into consideration when calculating the frame arrival rate, which is equal to the frame departure rate since in a saturated buffer, a new (possibly aggregated) frame promptly arrives once the HOL frame is transmitted. Since one frame is transmitted in the DL direction and $E[\gamma]$ frames are transmitted in the UL direction, Little's Theorem can be applied to calculate the average latency per frame in an IBFD-WLAN as follows

$$D^{IBFD} = \frac{n}{(1 + E[\gamma]) \cdot S^{IBFD} \Big/ \Big[E[P_{AP}] \cdot (1 + \Phi)\Big]} = \frac{n \cdot E[P_{AP}] \cdot (1 + \Phi)}{(1 + E[\gamma]) \cdot S^{IBFD}}. \tag{4.43}$$

4.7.4 IBFD Link Utilization

Throughput quantifies successful transmission of data over the total time including successful, collision, and sensing durations while considering added overhead. A metric that is worth introducing is IBFD link utilization, η, in order to quantify the efficiency of using the link (in both UL and DL directions) for transmission of useful data loads without the overhead. Since UL transmission is less than or equal to DL transmission, IBFD link utilization can be defined as

$$\eta \triangleq \frac{1 + \Phi}{2} \times 100\%. \tag{4.44}$$

Ideally, if the channel is fully utilized in both UL and DL directions (i.e. $\rho = 1$ at each STA $\Rightarrow \Phi = 1$), then $\eta = 100\%$ indicating a fully utilized and symmetrical link. IBFD link utilization is particularly crucial when assessing the benefits of frame aggregation, and this becomes clear by the numerical results reported in the next section.

4.8 Results and Evaluation

In order to confirm the validity of the analytical model detailed in this chapter for IBFD-WLAN, results based on simulated IEEE 802.11ac standard are used as a baseline. Analytical and simulation results for both network throughput and average latency in standard HD IEEE 802.11, IBFD-WLAN, IBFD-WLAN with dual-frame aggregation, and IBFD-WLAN with multi-frame aggregation are presented. In all generated results, the IBFD-WLAN analytical model provides values that closely match the simulated results within 1% error or less. Throughput quantifies successfully transmitted data over the total time. Latency quantifies the average time needed to successfully deliver an MPDU frame from the time the frame becomes HOL until an ACK frame is received. IBFD link utilization is used as a new metric to measure the enhancements added by IBFD aggregation techniques.

Three sets of results are provided. First, both the IBFD-WLAN model proposed in this chapter and the analytical model published in [40] are compared to simulated results. Then, the performance of the network in terms of throughput, latency, and utilization when ρ values are deterministic is evaluated in order to illustrate the aggregation schemes and their benefits. Finally, the performance results are repeated when ρ values are random to show a more practical scenario for a typical network.

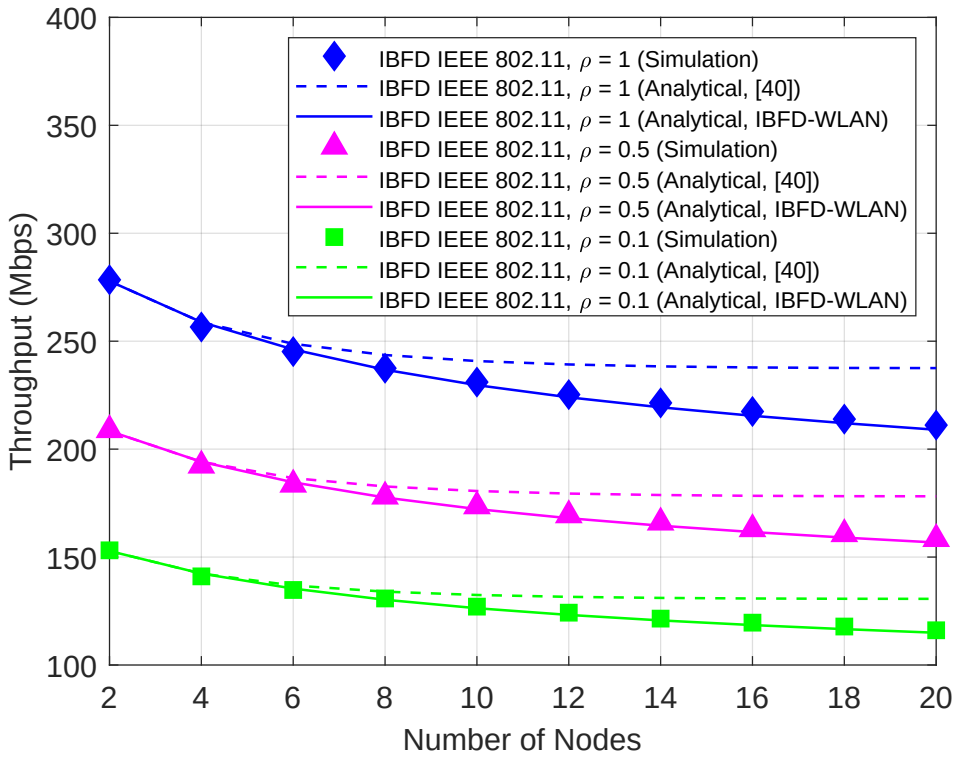

Figure 4.4: Comparison between the proposed model and a previously published model.

4.8.1 Accuracy of the proposed IBFD-WLAN model

The reported graphs in [40] show noticeable discrepancies between simulation and analytical results for the performance of the network. Therefore, there is a need for an accurate analytical model that realizes the impact of IBFD on WLANs. Fig. 4.4 shows simulation results for network throughput versus number of nodes (n) in a WLAN based on IEEE 802.11 standard for three deterministic ρ values. The corresponding analytical results based on the IBFD-WLAN framework proposed in this chapter are plotted. Additionally, the corresponding cases based on the analytical work reported in [40] are plotted for comparison. To make the comparison fair, the testing of the two analytical models was made closely similar by primarily using different formulas from the corresponding models for τ calculations while keeping all other parameters identical using the latest IEEE 802.11ac release (which [40] does not originally use). It is clear that at low n values, both analytical models match the

simulated results. However, at higher n values, the analytical model proposed in this chapter continues to match the simulation results while the model from [40] provides overly optimistic results. For each curve, the average error between the simulated scenario and analytical results based on IBFD-WLAN model is always less than 1% (matching the accuracy of the well-studied HD IEEE 802.11 model). On the other hand, the mismatch introduced by [40] consistently increases as the number of nodes increases until it reaches about 13% in all three cases when $n = 20$. The high error at high n values cannot be justified by the fact that the model in [40] assumes, unlike IEEE 802.11 standard, infinite re-transmission attempts at the maximum backoff stage until the frame is successfully delivered. This difference alone can only provide much smaller deviation between simulation and analytical cases. The inaccurate results at high n values are also apparent in the reported plots in [40]. Latency comparison is not performed here since no complete analytical model for latency was reported in [40].

4.8.2 Deterministic Symmetry Ratio Values

Fig. 4.5 shows both analytical and simulation results for network throughput versus the number of nodes when each client STA always has $\rho = 0.3$ originally. The AP always transmits a load of MPDU_{max}. The case for a standard HD IEEE 802.11 network is shown as a baseline case. When IBFD mode is enabled, the improvement in throughput depends on the number of nodes. For 2 nodes, the throughput increases by 72% compared to the case of HD IEEE 802.11 protocol. For 20 nodes, there is a 132% improvement in throughput when the IBFD mode is activated. The reason behind the difference in improvement is that the amount of transmitted data during each transmission opportunity in the HD mode is either MPDU_{max} (AP transmission) or $0.3 \times \text{MPDU}_{\text{max}}$ (STA transmission). Therefore, when the number of nodes is high, there is less likelihood that the AP transmits its larger load, which yields significantly lower throughput in the HD mode. On the other hand, each transmission opportunity in the IBFD mode results in transmitting an MPDU_{max} in the DL direction

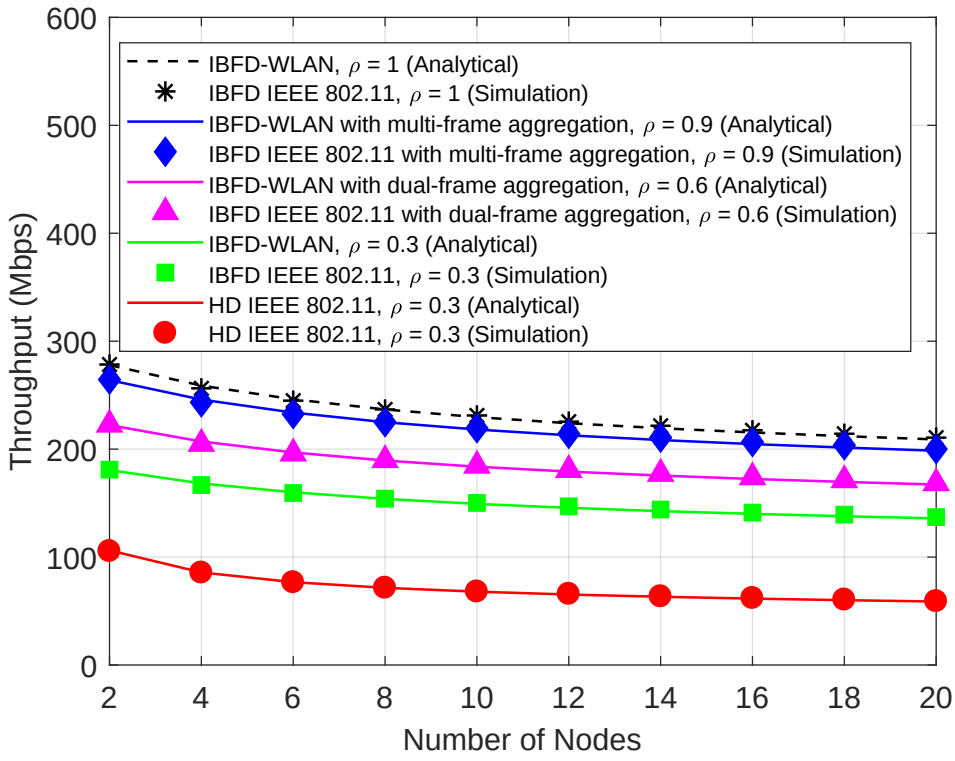

Figure 4.5: Throughput versus number of nodes ($\rho = 0.3$).

and $0.3 \times \text{MPDU}_{\text{max}}$ in the UL direction. When IBFD dual-frame aggregation is enabled, ρ_{new}^{dual} becomes 0.6. In this case, an increase of 23% is consistently realized in throughput compared to the case of IBFD without aggregation. The throughput is increased by 46% in each simulated case of n when IBFD multi-frame aggregation is employed in the network, which corresponds to $\rho_{new}^{multi} = 0.9$. The superior performance of IBFD multi-frame aggregation is expected since there is more data pushed in the UL direction. The upper limit for IBFD mode is indicated by the case when $\rho = 1$, and the increase in throughput from the case of IBFD without aggregation is 54%.

Fig. 4.6 displays the results for latency versus n. HD IEEE 802.11 exhibits the highest latency since in each transmission opportunity, either a DL or a UL frame is transmitted. Once IBFD transmission is implemented, there is reduction in latency since a DL frame *and* a UL frame are delivered in each transmission. When $n = 2$, there is a decrease of 42% in latency compared to HD IEEE 802.11. When n increases to 20, the reduction in latency

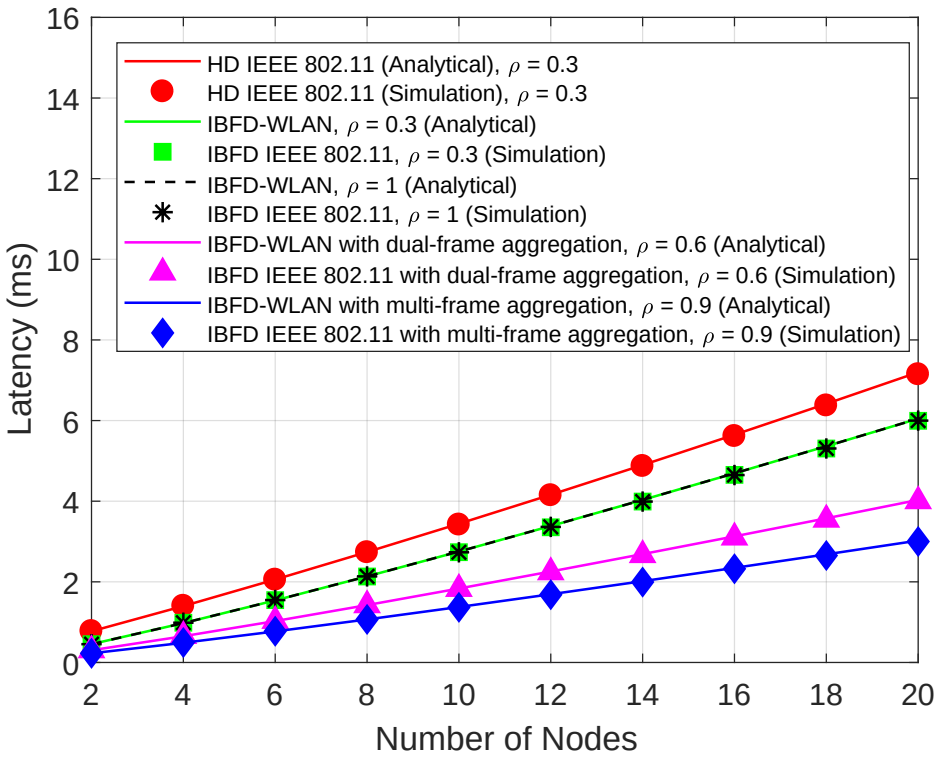

Figure 4.6: Latency versus number of nodes ($\rho = 0.3$).

is only 16% since there are more frames at silent STAs experiencing delay while an IBFD transmission takes place between the AP and an STA. The case for IBFD IEEE 802.11 with $\rho = 1$ (maximum traffic symmetry) is plotted. However, no further improvement in latency is realized since the number of delivered frames in each transmission is still 2. When IBFD IEEE 802.11 is augmented by dual-frame aggregation, there is a 33% improvement in latency for each case of n compared to IBFD without aggregation. The reason is that in each transmission, 1 DL frame and 2 UL frames are delivered. When multi-frame aggregation is introduced, latency is reduced by 50% compared to IBFD without aggregation since 1 DL frame and 3 UL frames are now served during each transmission. Clearly, aggregation is necessary to improve latency in IBFD-WLAN, and original ρ values do not affect average latency, which decreases as a result of increasing the number of transmitted frames.

Constant ρ values are assumed in this scenario, and the analytical values for η are as calculated in Table 4.1. The analytical results simply match the simulated results as expected

Table 4.1: IBFD link utilization for deterministic ρ values

Aggregation Mode	$\rho_{original}$	γ	ρ_{new}	Φ	η
Pure IBFD (no aggregation)	0.3	1	0.3	0.3	65%
IBFD dual-frame aggregation	0.3	2	0.6	0.6	80%
IBFD multi-frame aggregation	0.3	3	0.9	0.9	95%

since deterministic ρ values are assumed. It is worth noting that η is not affected by the number of nodes in the network since only the size of useful traffic is relevant here. The results for η indicate how well the channel is utilized in the assumed IBFD-WLAN network. IBFD link utilization becomes more sophisticated in the next section for random ρ values.

4.8.3 Random Symmetry Ratio Values

In this section, a ρ value for each client STA is randomly assigned such that ρ is uniformly distributed over $\{0.1, 0.2, ..., 0.9\}$. New ρ assignments are updated in each simulation run. The average result of 200 independent runs is reported for each simulation scenario. For IBFD dual-frame aggregation, only STAs with $0.1 \leq \rho \leq 0.5$ double their loads while the rest of STAs with $0.6 \leq \rho \leq 0.9$ maintain their original frames. When IBFD multi-frame aggregation is used, STAs with $0.6 \leq \rho \leq 0.9$ transmit their original loads while the rest of STAs aggregate their loads according to Table 4.2, which shows aggregation rules for both dual-frame and multi-frame modes. Fig. 4.7 shows throughput results versus n. When $n = 2$, IBFD introduces an 85% increase in throughput compared to 112% increase when $n = 20$ (both comparisons are with the corresponding HD cases). The difference in improvement between the two cases is consistent with the case of deterministic ρ values in that there is much less data transmitted in the DL direction when n is high resulting in low throughput in the HD baseline case. When dual-frame aggregation is employed, there is an improvement of 11% in throughput for each case of n compared to the corresponding IBFD case without aggregation. For multi-frame aggregation, the increase in throughput is 24%. Thus, IBFD multi-frame aggregation provides superior performance as expected since more

Table 4.2: IBFD frame aggregation rules for random ρ values

$\rho_{current}$	Dual-Frame		Multi-Frame	
	γ	ρ_{new}	γ	ρ_{new}
0.1	2	0.2	10	1
0.2	2	0.4	5	1
0.3	2	0.6	3	0.9
0.4	2	0.8	2	0.8
0.5	2	1	2	1
0.6	1	0.6	1	0.6
0.7	1	0.7	1	0.7
0.8	1	0.8	1	0.8
0.9	1	0.9	1	0.9

UL transmission time is utilized.

Fig. 4.8 displays latency results versus n when ρ values are random. IBFD without aggregation reduces latency by 45% compared to the HD case when $n = 2$, but the improvement in latency decreases as the number of nodes increases until it reaches 33% when $n = 12$. Even though increasing the number of nodes increases latency as expected, improvement in latency due to IBFD transmission remains unaffected and stays at 33% as n increases. This behavior is consistent with the scenario of deterministic ρ values in that as n continues to increase, nodes in the HD network experience higher delays while waiting for the active transmission to finish. Dual-frame aggregation introduces 16% of reduction in latency when $n = 2$ compared to IBFD without aggregation, and the improvement saturates to 22% as n increases. Multi-frame aggregation initially introduces 31% improvement when $n = 2$ compared to IBFD without aggregation, and the improvement saturates to 47% for higher values of n. In both aggregation schemes, more reduction in latency is noted as n increases. This behavior can be explained by the fact that as the number of nodes increases, there are more STAs that can initially have low ρ values, which enable them to aggregate and transmit more frames. Therefore, the expected total number of transmitted frames in the UL direction increases as n increases, which further reduces the average latency.

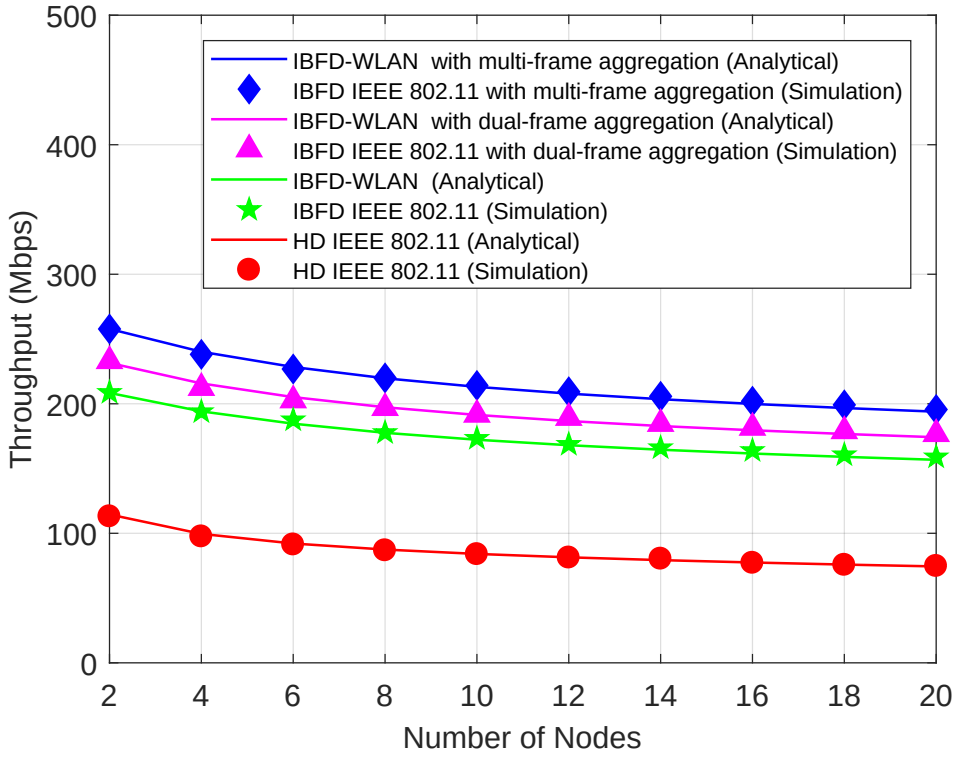

Figure 4.7: Throughput versus number of nodes (random ρ values, 200 runs).

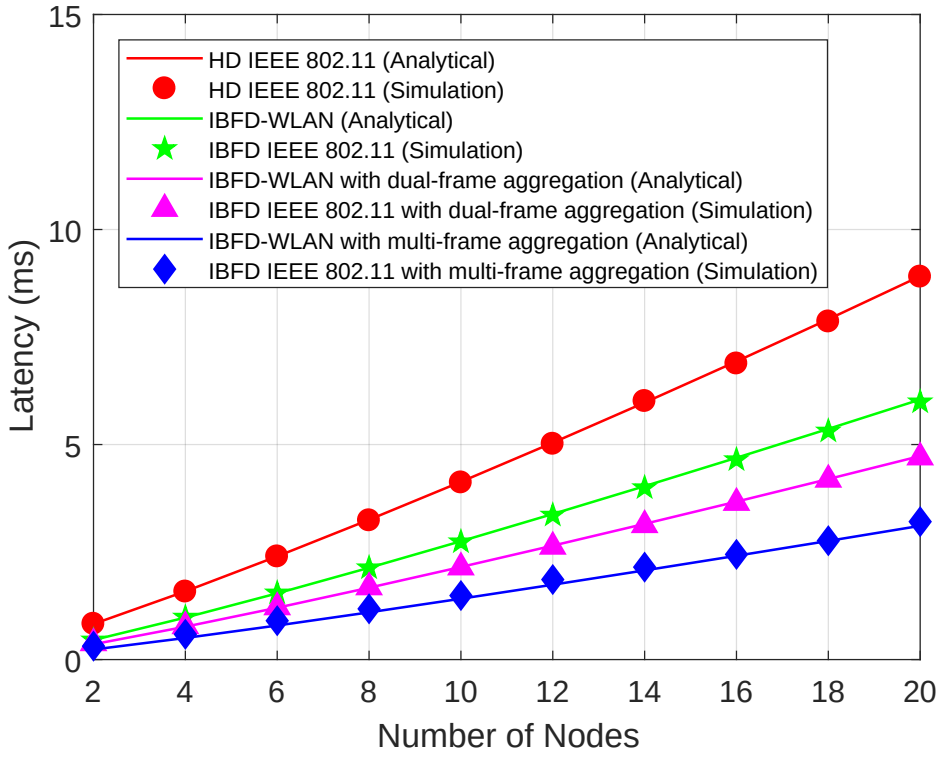

Figure 4.8: Throughput versus number of nodes (random ρ values, 200 runs).

Table 4.3: IBFD link utilization for random ρ values

Aggregation Mode	Analytical			Simulation		
	$E[\gamma]$	Φ	η	$E[\gamma]$	Φ	η
None	1	0.5000	75.00%	1	0.5044	75.22%
Dual-frame	1.5556	0.6667	83.34%	1.5608	0.6649	83.24%
Multi-frame	2.8889	0.8556	92.78%	2.8915	0.8545	92.72%

Since the value of ρ is equally likely to be one of the uniformally distributed values between 0.1 and 0.9, $E[\gamma]$ can be directly calculated based on the values in Table 4.2. In addition, analytical values for η in the case of random ρ values are readily obtained based on the calculated values of Φ, and the results are summarized in Table 4.3. Average simulation results from 200 runs are also reported for $E[\gamma]$, Φ, and η. It is noted that the values of η are directly proportional to the values of Φ as expected. When random ρ values are introduced into the system, simulation results for IBFD performance metrics are in strong agreement with the analytical results and still consistent with the case of deterministic ρ values.

4.9 Conclusion

In this chapter, an accurate model characterizing IEEE 802.11 DCF for IBFD-WLAN is presented. The model is based on a two-dimensional DTMC framework. The concepts of IBFD transmission and frame aggregation are combined to maximize throughput and minimize latency in WLANs. The proposed aggregation schemes increase the utilization of available UL transmission time that would otherwise be unused. Each client STA uses its own traffic information to make a localized decision about the option and size of aggregation. Aggregation is necessary to minimize latency in IBFD-WLANs. The proposed analytical model and related metrics are robust and produce values coinciding with the simulated results even when randomness is introduced in the system. Since no changes to IEEE 802.11 protocol were introduced in this chapter, the proposed IBFD frame aggregation schemes would be back-

ward compatible with future IEEE 802.11 releases. Network throughput, average latency, and link utilization are proposed as metrics to quantify potential enhancements resulting from introducing IBFD in WLANs.

Chapter 5

Power Consumption and Energy-Efficiency for IBFD WLANs

5.1 Motivation

Increasing energy-efficiency in IEEE 802.11 Wireless Local-Area Networks (WLANs) has become a priority due to the vast deployment of WiFi networks over recent years [53]. In this chapter, an analytical model is presented to quantify power consumption and energy-efficiency for In-Band Full-Duplex (IBFD) WLANs. Unlike Half-Duplex (HD) communications (i.e. Time-Division Duplexing or Frequency-Division Duplexing), IBFD techniques allow two wireless nodes to transmit and receive simultaneously on one frequency band (details can be found in [6]).

5.2 Contribution

While IBFD is a promising technique to improve several metrics in wireless networks, the effect on power consumption has not been sufficiently addressed. This chapter presents a mathematical model for power consumption in IBFD-WLANs, and the model is confirmed by simulation. Additionally, energy-efficiency in both HD and IBFD WLANs are compared in terms of successfully transmitted data per unit of energy. Finally, both power consumption and energy-efficiency are studied under different traffic assumptions in the collision-free mode when a WLAN consists of an AP and an STA.

5.3 System Model

This chapter assumes an infrastructure WLAN with an Access Point (AP) and $n-1$ associated client stations (STAs) adopting basic IEEE 802.11 Distributed Coordination Function (DCF) standard with one channel. Total frame loss happens when collisions occur. No errors at the PHY layer take place. All wireless nodes can detect one another with no hidden terminals. Each node always has a frame to transmit. The AP always has a load of the maximum MAC Protocol Data Unit ($\text{MPDU}_{\max}$). All STAs have equal Symmetry Ratio (SR) values as defined in [30]. If the traffic load is designated as (L), then SR is the ratio of the uplink to the downlink as follows

$$\rho \triangleq \frac{L_{UL}}{L_{DL}}. \tag{5.1}$$

PHY and MAC parameters are set according to the latest IEEE 802.11ac release [26] as indicated in Table 3.1.

5.4 HD IEEE 802.11 Power Consumption Model

Power consumption is based on the classical definition of power [54]

$$\text{Power} \triangleq \frac{\text{Energy}}{\text{Time}}. \tag{5.2}$$

As presented in [55], the energy consumed by a node in an HD WLAN depends on the state of the node. There are six mutually exclusive states a node can be in. The energy consumption ($\mathcal{E}$) in terms of power consumption (ω) and the probability for each state are given as follows

1. Idle (d) state

$$\mathcal{E}_{\text{d}} = \omega_{\text{d}}\sigma \tag{5.3}$$

$$Pr(\text{d}) = (1-\tau)^n \tag{5.4}$$

2. Successful transmission (S-TX) state

$$\mathcal{E}_{\text{S-TX}} = \omega_{\text{TX+CTRL}}\text{DATA}_{\text{TX}} + \omega_{\text{d}}(\text{DIFS+SIFS}) + \omega_{\text{RX+CTRL}}\text{ACK} \tag{5.5}$$

$$Pr(\text{S-TX}) = \tau(1-p) \tag{5.6}$$

3. Successful reception (S-RX) state

$$\mathcal{E}_{\text{S-RX}} = \omega_{\text{RX+CTRL}}\text{DATA}_{\text{RX}} + \omega_{\text{d}}(\text{DIFS+SIFS}) + \omega_{\text{TX+CTRL}}\text{ACK} \tag{5.7}$$

$$Pr(\text{S-RX}) = \tau(1-\tau)^{n-1} \tag{5.8}$$

4. Successful overhearing (S-$\overline{\text{RX}}$) state

$$\mathcal{E}_{\text{S-}\overline{\text{RX}}} = \omega_{\text{RX+CTRL}}(\text{DATA}_{\text{RX}} + \text{ACK}) + \omega_{\text{d}}(\text{DIFS+SIFS}) \tag{5.9}$$

$$Pr(\text{S-RX}) = (n-2)\tau(1-\tau)^{n-1} \tag{5.10}$$

5. Transmitting during a collision (C-TX) state

$$\mathcal{E}_{\text{C-TX}} = \omega_{\text{TX+CTRL}}\text{DATA}_{\text{TX}} + \omega_{\text{d}}(\text{DIFS+SIFS+ACK}) \tag{5.11}$$

$$Pr(\text{C-TX}) = \tau p \tag{5.12}$$

6. Overhearing a collision (C-$\overline{\text{RX}}$) state

$$\mathcal{E}_{\text{C-RX}} = \omega_{\text{RX+CTRL}}\text{DATA}_{\text{RX}} + \omega_{\text{d}}(\text{DIFS+SIFS+ACK}) \tag{5.13}$$

$$Pr(\text{C-}\overline{\text{RX}}) = (1-\tau)[1-(1-\tau)^{n-1} - (n-1)\tau(1-\tau)^{n-2}] \tag{5.14}$$

where τ is the probability of transmission, p is the conditional collision probability, and n is the number of nodes (details are in [29]).

The expected value of consumed energy by a node can be expressed in terms of the energy consumption and probability of each state as

$$\mathbb{E}[\text{energy}] = \sum_{i=1}^{6}(\text{energy in state } i) \cdot Pr(\text{state } i). \tag{5.15}$$

Finally, the average power consumption of a node is given by rewriting (5.2) as

$$\begin{aligned} \text{Power} &= \frac{\mathbb{E}[\text{energy}]}{\mathbb{E}[\text{time duration}]} \\ &= \frac{\sum_{i=1}^{6}(\text{energy in state } i)\cdot Pr(\text{state } i)}{(1-P_{tr})\sigma + P_{tr}P_sT_s + P_{tr}(1-P_s)T_c} \end{aligned} \tag{5.16}$$

where the probability that there is at least a transmission (P_{tr}), the probability of a successful transmission (P_s), the expected time of a successful transmission (T_s), and the expected time of a collision (T_c) are are given in [29] and refined in [46].

5.5 Analysis for IBFD-WLAN Power Consumption

A similar approach to the HD case is adopted here for an IBFD-WLAN. Several considerations must be taken into account. First, the AP properties in an IBFD system are different from those of STAs. Second, energy consumption for Self-Interference Cancellation (SIC) to enable IBFD communications must be added. Third, IBFD mechanisms must be factored into the expressions for each state.

5.5.1 The AP in an infrastructure IBFD-WLAN

For the AP in an IBFD-WLAN, there are 3 mutually exclusive states as follows

1. Idle (AP-d) state

$$\mathcal{E}_{\mathrm{d}}^{\mathrm{AP}} = \omega_{\mathrm{d}}\sigma \tag{5.17}$$

$$Pr(\text{AP-d}) = (1-\tau_{_{AP}})(1-\tau_{_{STA}})^{n-1} \tag{5.18}$$

2. Successful transmission/reception (AP-S-TXRX) state

$$\mathcal{E}^{\text{AP}}_{\text{S-TXRX}} = \omega_{\text{TX+CTRL}}(\text{DATA}_{\text{TX}} + \text{ACK}) + \omega_{\text{RX+SIC}}(\text{DATA}_{\text{RX}} + \text{ACK}) + \omega_{\text{d}}(\text{DIFS+SIFS}) \tag{5.19}$$

$$Pr(\text{AP-S-TXRX}) = \tau_{_{AP}}(1-\tau_{_{STA}})^{n-1} + (n-1)\tau_{_{STA}}(1-\tau_{_{STA}})^{n-2} \tag{5.20}$$

3. Transmitting/receiving a collision (AP-C-TXRX) state

$$\mathcal{E}^{\text{AP}}_{\text{C-TXRX}} = \omega_{\text{TX+CTRL}}\text{DATA}_{\text{TX}} + \omega_{\text{RX+SIC}}\text{DATA}_{\text{RX}} + \omega_{\text{d}}(\text{DIFS+SIFS+ACK}) \tag{5.21}$$

$$Pr(\text{AP-C-TXRX}) = 1 - Pr(\text{AP-d}) - Pr(\text{AP-S-TXRX}) \tag{5.22}$$

5.5.2 An STA in an infrastructure IBFD-WLAN

For each STA in an IBFD-WLAN, there are 5 mutually exclusive states as follows

1. Idle (STA-d) state

$$\mathcal{E}^{\text{STA}}_{\text{d}} = \omega_{\text{d}}\sigma \tag{5.23}$$

$$Pr(\text{STA-d}) = (1-\tau_{_{AP}})(1-\tau_{_{STA}})^{n-1} \tag{5.24}$$

2. Successful transmission/reception (STA-S-TXRX) state

$$\mathcal{E}^{\text{STA}}_{\text{S-TXRX}} = \omega_{\text{TX+SIC}}(\text{DATA}_{\text{TX}} + \text{ACK}) + \omega_{\text{RX+CTRL}}(\text{DATA}_{\text{RX}} + \text{ACK}) + \omega_{\text{d}}(\text{DIFS+SIFS}) \tag{5.25}$$

$$Pr(\text{STA-S-TXRX}) = \tau_{_{STA}}(1-p_{_{STA}}) + (1-\tau_{_{STA}})^{n-1}\frac{\tau_{_{AP}}}{(n-1)} \tag{5.26}$$

3. Successful overhearing (STA-S-$\overline{\text{RX}}$) state

$$\mathcal{E}^{\text{STA}}_{\text{S-}\overline{\text{RX}}} = \omega_{\text{RX+CTRL}}(\text{DATA}_{\text{RX}} + \text{ACK}) + \omega_{\text{d}}(\text{DIFS+SIFS}) \tag{5.27}$$

$$\begin{aligned} Pr(\text{STA-S-}\overline{\text{RX}}) &= (n-2)\tau_{_{STA}}(1-\tau_{_{STA}})^{n-2}(1-\tau_{_{AP}}) \\ &\quad + \frac{(n-2)}{(n-1)}\tau_{_{AP}}\Big[\tau_{_{STA}}(1-\tau_{_{STA}})^{n-2} + (1-\tau_{_{STA}})^{n-1}\Big] \end{aligned} \tag{5.28}$$

4. Transmitting/receiving a collision (STA-C-TXRX) state

$$\mathcal{E}^{\text{STA}}_{\text{C-TXRX}} = \omega_{\text{TX+SIC}}\text{DATA}_{\text{TX}} + \omega_{\text{RX+CTRL}}\text{DATA}_{\text{RX}} + \omega_{\text{d}}(\text{DIFS+SIFS+ACK}) \tag{5.29}$$

$$Pr(\text{STA-C-TXRX}) = \tau_{_{STA}}p_{_{STA}} \tag{5.30}$$

5. Overhearing a collision (STA-C-$\overline{\text{RX}}$) state

$$\mathcal{E}^{\text{STA}}_{\text{C-}\overline{\text{RX}}} = \omega_{\text{RX+CTRL}}\text{DATA}_{\text{RX}} + \omega_{\text{d}}(\text{DIFS+SIFS+ACK}) \tag{5.31}$$

$$\begin{aligned} Pr(\text{STA-C-}\overline{\text{RX}}) &= 1 - Pr(\text{STA-d}) - Pr(\text{STA-S-TXRX}) \\ &\quad - Pr(\text{STA-S-}\overline{\text{RX}}) - Pr(\text{STA-C-TXRX}) \end{aligned} \tag{5.32}$$

Detailed expressions for $\tau_{_{AP}}$, $\tau_{_{STA}}$, P_{tr}, P_s, T_s, and T_c in an IBFD-WLAN can be found in [56].

5.6 Results and Evaluation

Both analytical and simulation results are reported in this chapter. First, power consumption and energy-efficiency are analyzed when the traffic is fully symmetrical (i.e. $\rho = 1$) for both HD and IBFD systems. Then, the effect of symmetry on both power consumption and energy efficiency is presented through the two extreme cases of low symmetry ($\rho = 0.1$) and

Table 5.1: Power consumption values

Power Category	Value
Transmitter (ω_{TX})	2.6883 W
Receiver (ω_{RX})	1.5900 W
Idel State (ω_{d})	0.9484 W
Control Circuit (ω_{CTRL})	0.3000 W
Self-Interference Cancellation (ω_{SIC})	0.0650 W

Table 5.2: Energy consumption of each state in an HD WLAN

State	Energy Consumption
$\mathcal{E}_{\text{d}}$	8.5356 μJ
$\mathcal{E}_{\text{S-TX}}$	1.0818 mJ
$\mathcal{E}_{\text{S-RX}}$	0.7889 mJ
$\mathcal{E}_{\text{S-}\overline{\text{RX}}}$	0.7354 mJ
$\mathcal{E}_{\text{C-TX}}$	1.0360 mJ
$\mathcal{E}_{\text{C-}\overline{\text{RX}}}$	0.6896 mJ

high symmetry ($\rho = 0.9$). Lastly, the special case of $n = 2$ is analyzed in 3 different traffic scenarios. The calculated power consumption values for ω_{TX}, ω_{RX}, and ω_{d} in Table 5.1 are based on [57] (see Appendix D for details). Values of ω_{SIC} and ω_{CTRL} are stated in [58]. While ω_{SIC} accounts for both active and passive cancellation circuits, the majority of SIC is treated passively with minimal power consumption. Tables 5.2 and 5.3 respectively show the resulting energy consumption values for all states in both HD and IBFD WLANs.

5.6.1 Fully Symmetrical Traffic

Fig. 5.1 shows how the number of nodes affects the power consumption per node in both HD and IBFD networks. Both analytical and simulation results are reported when the traffic is assumed to be fully symmetrical. This is the best case scenario where the link is fully utilized in both uplink and downlink directions. In the HD case, the AP and every STA have identical power consumption since HD IEEE 802.11 yields the same power profile for every

Table 5.3: Energy consumption of each state in an IBFD-WLAN

State	Energy Consumption
$\mathcal{E}_{\mathrm{d}}^{\mathrm{AP}}$	8.5356 μJ
$\mathcal{E}_{\text{S-TXRX}}^{\mathrm{AP}}$	1.7377 mJ
$\mathcal{E}_{\text{C-TXRX}}^{\mathrm{AP}}$	1.5579 mJ
$\mathcal{E}_{\mathrm{d}}^{\mathrm{STA}}$	8.5356 μJ
$\mathcal{E}_{\text{S-TXRX}}^{\mathrm{STA}}$	1.7377 mJ
$\mathcal{E}_{\text{S-}\overline{\text{RX}}}^{\mathrm{STA}}$	0.7354 mJ
$\mathcal{E}_{\text{C-TXRX}}^{\mathrm{STA}}$	1.5579 mJ
$\mathcal{E}_{\text{C-}\overline{\text{RX}}}^{\mathrm{STA}}$	0.6896 mJ

node. The power consumption per node in an HD WLAN stabilizes at a constant value as the number of nodes increases since the dominant power consumption mode happens in states S-TX and C-TX, and the associated probabilities for both transmitting states reach a steady value quickly as the number of nodes increases. In the case of IBFD-WLAN, the results are reported for both the AP and an STA since they have different properties here. Power consumption is higher in IBFD-WLANs since there is simultaneous transmission and reception at both the AP and an STA when the channel is non-idle. The AP in an IBFD-WLAN has high power consumption since it is always transmitting (states AP-S-TXRX and AP-C-TXRX) regardless of how many STAs are in the network. This does not constitute an efficiency concern since APs are typically powered by AC electricity in residential WLANs. As the number of nodes increases, power consumption per STA gradually decreases to reach a constant value since the probability values of transmitting states (i.e. STA-S-TXRX and STA-C-TXRX) quickly stabilize as the number of nodes becomes high.

Fig. 5.2 shows analytical and simulation results of energy-efficiency in terms of Megabits/Joule resulting from dividing throughput by consumed power as in [58]. The results are reported for both HD and IBFD cases. IBFD-WLANs always have higher energy-efficiency since more data is transmitted. A key reason here is that only one node uses the link for data in HD

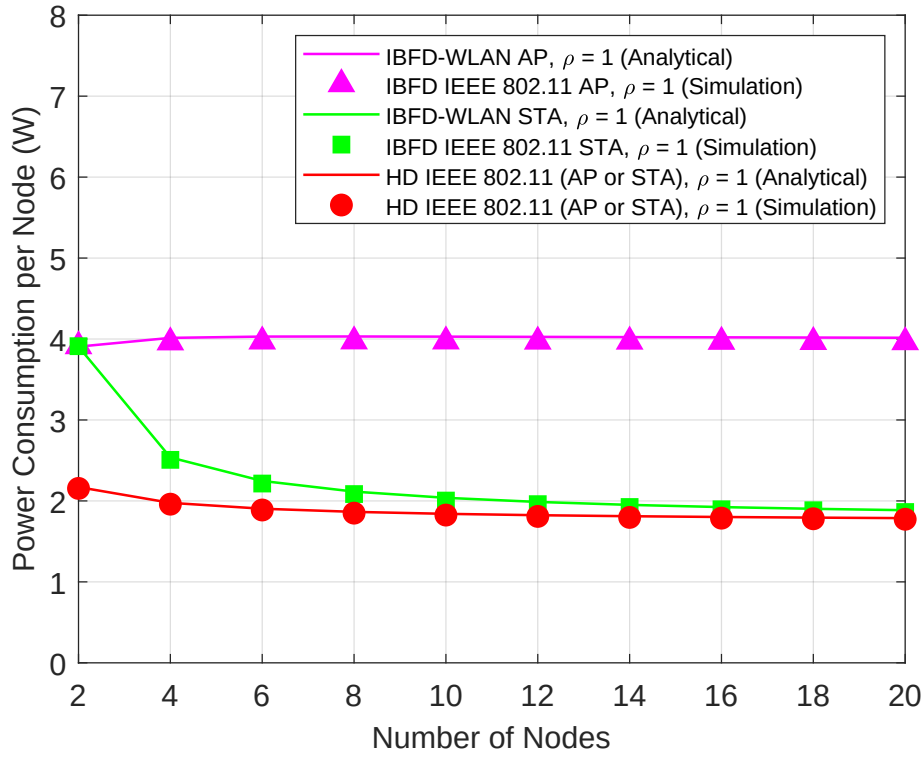

Figure 5.1: Power consumption per node in HD and IBFD WLANs when $\rho = 1$.

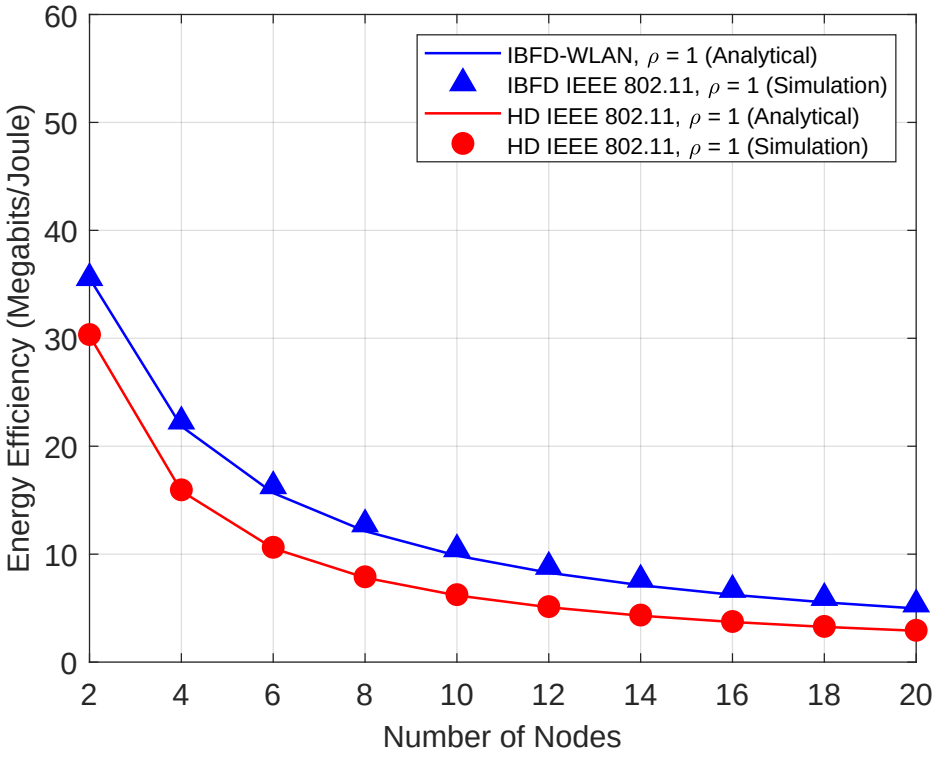

Figure 5.2: Energy-efficiency in HD and IBFD WLANs when $\rho = 1$.

networks while two transmitting nodes utilize the link for data in an IBFD-WLAN.

5.6.2 High Symmetry vs. Low Symmetry

Fig. 5.3 shows the results of power consumption per node in both HD and IBFD WLANs. High symmetry ($\rho = 0.9$) and low symmetry ($\rho = 0.1$) are considered. Similar patterns to the ones in Fig. 5.1 can be seen here. Power consumption is reduced when symmetry is low since lower power consumption is needed to transmit (and receive) smaller uplink traffic loads. For HD WLAN, the power consumption is slightly affected by the change of symmetry mode but remains lower than the corresponding IBFD case. Power consumption increases as symmetry increases because more power is needed to transmit a larger uplink payload.

Fig. 5.4 shows the energy-efficiency for the cases of high and low symmetry scenarios in both HD and IBFD WLANs. The key result in this figure is that energy-efficiency of low symmetry IBFD-WLAN is almost equal to the energy-efficiency of high symmetry HD WLAN. The low symmetry scenario is naturally inefficient due to the lower utilization of the uplink. Hence, it takes an extremely inefficient assumption (i.e. low symmetry) to reduce the high efficiency of an IBFD-WLAN to the upper limit of energy-efficiency in the HD case. This result is intuitive since an IBFD-WLAN with low symmetry has effectively only one fully utilized communications direction (i.e. downlink), which is equivalent to the fully utilized communications direction (i.e. either the uplink or downlink) in the HD WLAN with high symmetry. Even though more power is needed when there is a larger data load, both HD and IBFD networks show increase in efficiency when the traffic is highly symmetrical. The increase of efficiency in an IBFD-WLAN as symmetry increases shows that the increase of transmitted data is high enough to overcome the increase in consumed power.

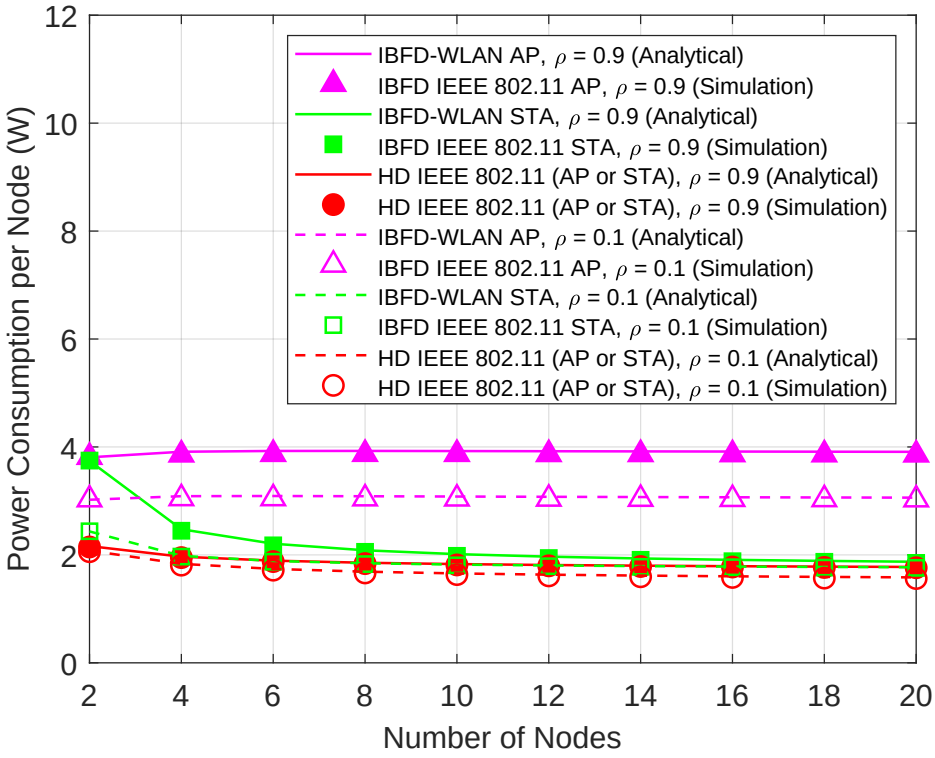

Figure 5.3: Power consumption per node in HD and IBFD WLANs.

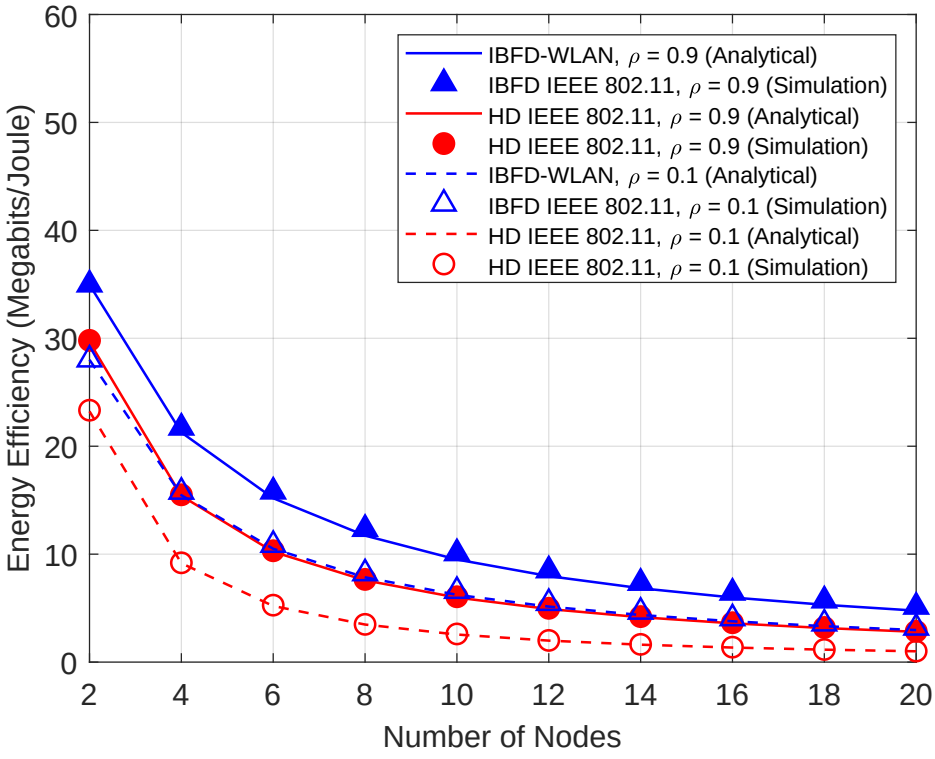

Figure 5.4: Energy-efficiency in HD and IBFD WLANs.

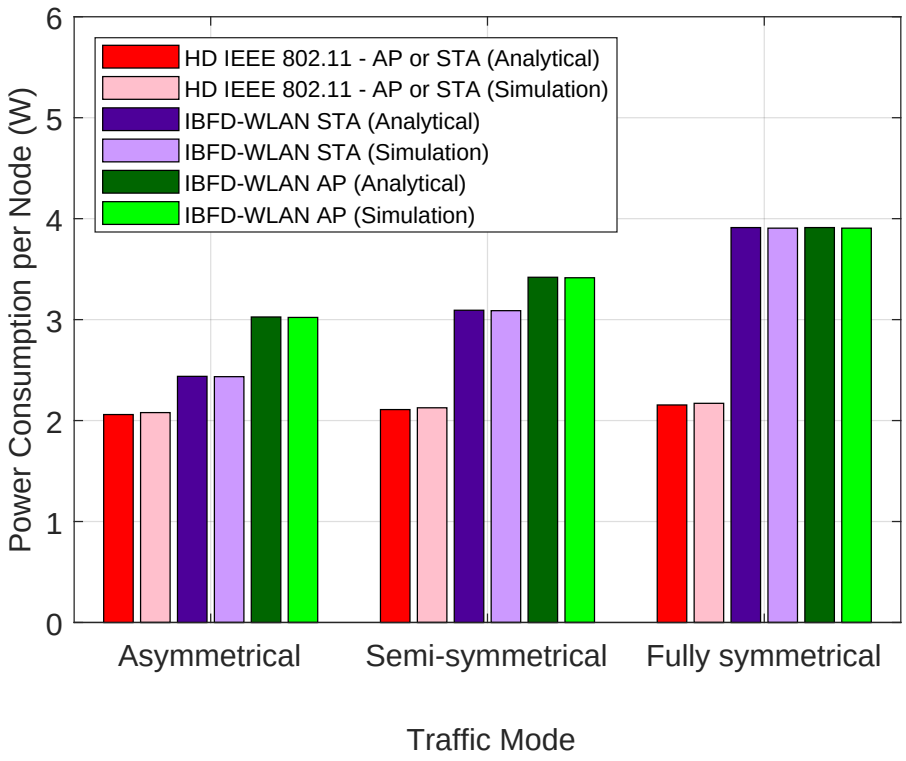

Figure 5.5: Power consumption for the AP and STA in HD and IBFD WLANs with $n = 2$.

5.6.3 Special Case: $n = 2$

Fig. 5.5 shows power consumption per node in both HD and IBFD WLANs when $n = 2$. In the case of IBFD-WLANs, the network becomes more efficient due to the elimination of collisions [47]. Therefore, this interesting case is considered here with asymmetrical traffic ($\rho = 0.1$), semi-symmetrical traffic ($\rho = 0.5$), and fully symmetrical traffic ($\rho = 1$). For the HD WLAN, the power consumption is slightly affected by the change of symmetry mode but remains lower than the corresponding IBFD case. In IBFD-WLANs, power consumption increases as symmetry increases because more power is needed to transmit (and receive) a larger uplink payload. The STA has higher power consumption in IBFD-WLANs than the corresponding HD case since it is simultaneously transmitting and receiving with IBFD. The power consumption of the AP in the IBFD case increases when the uplink load increases due to the increase in power consumption at the AP's receiver. In the fully symmetrical traffic

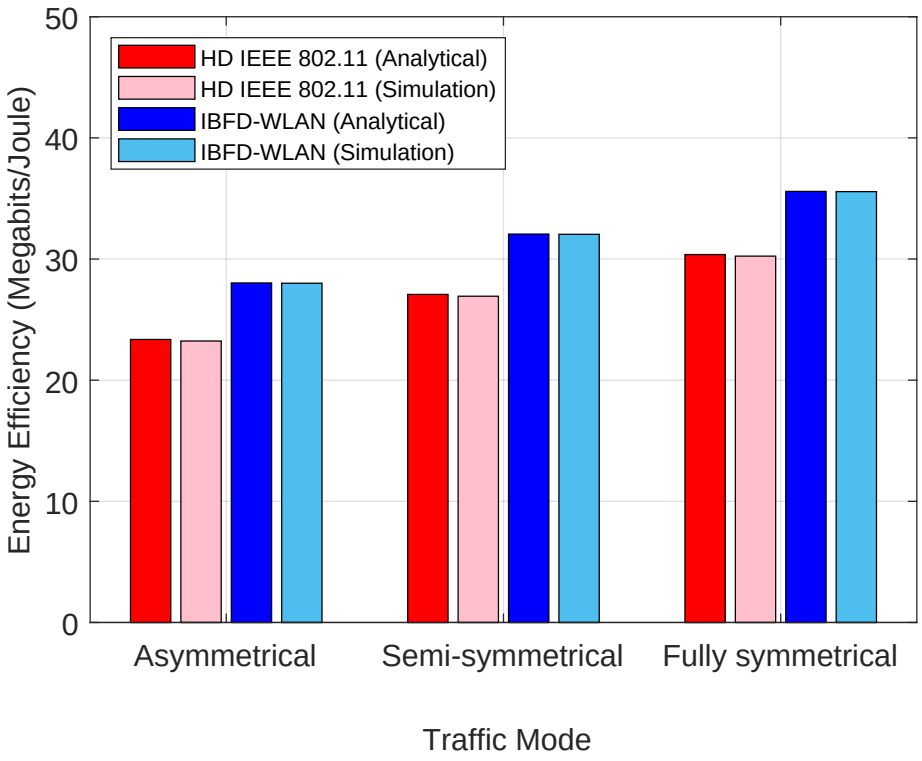

Figure 5.6: Energy-efficiency in HD and IBFD WLANs with $n = 2$.

scenario, the AP and the STA have the same power consumption in the IBFD case since they have the same probabilistic properties with no collision and no overhearing from either nodes as indicated in [47].

Fig. 5.6 shows energy-efficiency versus traffic symmetry when $n = 2$. In both HD and IBFD WLANs, energy-efficiency consistently increases as the the traffic becomes more symmetrical. The increase of energy-efficiency as the symmetry increases is due to the higher amount of useful data transmitted over the link.

5.7 Conclusion

An analytical model for power consumption and energy-efficiency in IBFD-WLANs is presented and confirmed by simulation. Even though power consumption is higher in IBFD-

WLANs compared to HD WLANs, IBFD networks still have higher energy-efficiency. The presented model is necessary to study future IBFD solutions for IEEE 802.11 networks.

Chapter 6

Conclusions

6.1 Summary

This dissertation examines the application of IBFD in WLANs adopting IEEE 802.11 standard. A novel and backward-compatible IBFD-MAC protocol is introduced to utilize features not realized in contemporary HD systems. Collisions are tolerated in special cases through the proposed IBFD CSMA/CT. Accurate mathematical models, which are confirmed by software simulation, are thoroughly derived in this dissertation for throughput gain, latency reduction, frame aggregation, link utilization, power consumption, and energy-efficiency in IBFD-WLANs. The dissertation quantifies potential benefits of IBFD for future IEEE 802.11 releases.

6.2 Future Outlook

Research in the area of IBFD is gaining increasing momentum. IBFD applications are proposed in several areas including vehicular communications, massive MIMO, millimeter

wave communications, small cells, military communications, energy harvesting, and real-time industrial networks [59, 60].

IBFD techniques will not be included in the forthcoming IEEE 802.11ax standard currently under development by High Efficiency WLAN Task Group (HEW-TG) [61]. However, IEEE 802.11 Full-Duplex Technical Interest Group (FD-TIG) was formed to study the feasibility of implementing IBFD methods in the IEEE 802.11 standard [62]. FD-TIG recently confirmed that implementing IBFD is beneficial in increasing throughput, enhancing latency, and reducing collisions [63]. Those benefits had already been confirmed analytically and by simulation throughout this dissertation. FD-TIG recently recommended that pursing IBFD solutions should continue in the newly established IEEE 802.11 Extremely High Throughput Study Group (EHT-SG) [64]. As a result, IBFD is officially under consideration to be a part of a future IEEE 802.11 release.

6.3 Future Work

While this dissertation primarily focuses on the MAC sub-layer for IBFD-WLANs, many exciting extensions for the presented work and beyond should be pursued. Possible future work can include

- Extending the IBFD-MAC protocol with SR_{th} policy to include more practical assumptions with regards to traffic configuration.
- Developing algorithms that identify the optimal value for SR_{th} in the IBFD-MAC protocol.
- Implementing distributed resource-allocation algorithms to assign channels based on individual traffic requirements of client STAs in IBFD-WLANs.

- Introducing metrics for performance analysis to further study trade-offs related to throughput, latency, energy-efficiency, and fairness.
- Modifying analytical work and simulation experiments to account for actual traffic patterns with non-saturated buffers.
- Building and testing experimental systems with practical assumptions to emulate realistic IBFD-WLANs.
- Revisiting fairness analyses like [65, 66, 67, 68] to consider the impact of IBFD on classical work in the context of wireless networks.
- Studying the possibility of implementing IBFD relays as WiFi range extenders without reducing the effective bandwidth as it is the case in commercial range extension devices.
- Optimizing IBFD systems using Game Theory (preliminary work is outlined in [69]).
- Investigating the use of IBFD solutions for backhaul links (e.g. the work in [70]).
- Studying the feasibility and quantifying the benefits of IBFD applications in the emerging area of Internet of Things (IoT) (related survey was recently published in [71]).
- Utilizing IBFD methods for Ultra-Reliable and Low Latency Communications (URLLC) as suggested in [72].

IBFD is still an emerging technique, and it has the potential to be useful for WLANs as well as many other applications with further research investigations and contributions.

Bibliography

[1] A. Goldsmith, *Wireless Communications*. Cambridge University Press, 2005.

[2] V. K. Garg, *Wireless Communications & Networking*, ser. The Morgan Kaufmann Series in Networking. Burlington: Morgan Kaufmann, 2007.

[3] A. Sabharwal, P. Schniter, D. Guo, D. W. Bliss, S. Rangarajan, and R. Wichman, "In-band full-duplex wireless: challenges and opportunities," *IEEE Journal on Selected Areas in Communications*, vol. 32, no. 9, pp. 1637–1652, Sep. 2014.

[4] D. Kim, H. Lee, and D. Hong, "A survey of in-band full-duplex transmission: from the perspective of PHY and MAC layers," *IEEE Communications Surveys Tutorials*, vol. 17, no. 4, pp. 2017–2046, 2015.

[5] Z. Zhang, K. Long, A. V. Vasilakos, and L. Hanzo, "Full-duplex wireless communications: challenges, solutions, and future research directions," *Proceedings of the IEEE*, vol. 104, no. 7, pp. 1369–1409, July 2016.

[6] L. Song, R. Wichman, Y. Li, and Z. Han, *Full-Duplex Communications and Networks*. Cambridge University Press, 2017.

[7] M. Duarte and M. Guillaud, "Engineering wireless full-duplex nodes and networks," GLOBECOM Industry Tutorial, Huawei France Research Center, San Diego, December 2015.

[8] D. Bharadia, E. McMilin, and S. Katti, "Full duplex radios," in *Proceedings of the ACM SIGCOMM 2013 Conference on SIGCOMM*, Hong Kong, China, 2013, pp. 375–386.

[9] E. Ahmed, A. M. Eltawil, and A. Sabharwal, "Self-interference cancellation with nonlinear distortion suppression for full-duplex systems," in *2013 Asilomar Conference on Signals, Systems and Computers*, Nov 2013, pp. 1199–1203.

[10] E. Ahmed and A. M. Eltawil, "All-digital self-interference cancellation technique for full-duplex systems," *IEEE Transactions on Wireless Communications*, vol. 14, no. 7, pp. 3519–3532, July 2015.

[11] M. Duarte, C. Dick, and A. Sabharwal, "Experiment-driven characterization of full-duplex wireless systems," *IEEE Transactions on Wireless Communications*, vol. 11, no. 12, pp. 4296–4307, December 2012.

[12] K. E. Kolodziej, B. T. Perry, and J. S. Herd, "In-band full-duplex technology: Techniques and systems survey," *IEEE Transactions on Microwave Theory and Techniques*, pp. 1–17, 2019.

[13] E. Ahmed, A. M. Eltawil, Z. Li, and B. A. Cetiner, "Full-duplex systems using multireconfigurable antennas," *IEEE Transactions on Wireless Communications*, vol. 14, no. 11, pp. 5971–5983, Nov 2015.

[14] M. Duarte, A. Sabharwal, V. Aggarwal, R. Jana, K. K. Ramakrishnan, C. W. Rice, and N. K. Shankaranarayanan, "Design and characterization of a full-duplex multiantenna system for WiFi networks," *IEEE Transactions on Vehicular Technology*, vol. 63, no. 3, pp. 1160–1177, March 2014.

[15] M. Jain, J. I. Choi, T. Kim, D. Bharadia, S. Seth, K. Srinivasan, P. Levis, S. Katti, and P. Sinha, "Practical, real-time, full duplex wireless," in *Proceedings of the 17th Annual International Conference on Mobile Computing and Networking*, ser. MobiCom '11. New York, NY, USA: ACM, 2011, pp. 301–312.

[16] M. Rodrig, C. Reis, R. Mahajan, D. Wetherall, and J. Zahorjan, "Measurement-based characterization of 802.11 in a hotspot setting," in *Proceedings of the 2005 ACM SIGCOMM Workshop on Experimental Approaches to Wireless Network Design and Analysis*, ser. E-WIND '05. New York, NY, USA: ACM, 2005, pp. 5–10.

[17] A. Schulman, D. Levin, and N. Spring, "On the fidelity of 802.11 packet traces," in *Passive and Active Network Measurement*, M. Claypool and S. Uhlig, Eds. Berlin, Heidelberg: Springer Berlin Heidelberg, 2008, pp. 132–141.

[18] K. M. Thilina, H. Tabassum, E. Hossain, and D. I. Kim, "Medium access control design for full duplex wireless systems: challenges and approaches," *IEEE Communications Magazine*, vol. 53, no. 5, pp. 112–120, May 2015.

[19] *Wireless LAN Medium Access Control (MAC) and Physical Layer (PHY) Specifications*, IEEE 802.11 Std., 2012.

[20] A. Gupta, J. Min, and I. Rhee, "Wifox: Scaling wifi performance for large audience environments," in *Proceedings of the 8th International Conference on Emerging Networking Experiments and Technologies*. New York, NY, USA: ACM, 2012, pp. 217–228.

[21] J. Jeong, S. Choi, and C. Kim, "Achieving weighted fairness between uplink and downlink in ieee 802.11 dcf-based wlans," in *Second International Conference on Quality of Service in Heterogeneous Wired/Wireless Networks (QSHINE'05)*, Aug 2005, pp. 10 pp.–22.

[22] X. Wang and S. A. Mujtaba, "Performance enhancement of 802.11 wireless LAN for asymmetric traffic using an adaptive MAC layer protocol," in *Proceedings IEEE 56th Vehicular Technology Conference*, vol. 2, Sep. 2002, pp. 753–757 vol.2.

[23] J. Kim, W. Kim, and J. Kim, "A new full duplex MAC protocol to solve the asymmetric transmission time," in *2015 IEEE Globecom Workshops (GC Wkshps)*, Dec 2015, pp. 1–5.

[24] C. Kim and C. Kim, "A full duplex MAC protocol for efficient asymmetric transmission in WLAN," in *2016 International Conference on Computing, Networking and Communications (ICNC)*, Feb 2016, pp. 1–5.

[25] Z. Ma, Q. Zhao, Y. Z. Zhang, and H. Dai, "AT-MAC: A novel full duplex MAC design for achieving asymmetric transmission," in *Mobile and Wireless Technologies*, vol. 391. Springer Singapore, May 2016, pp. 41–49.

[26] *Wireless LAN Medium Access Control (MAC) and Physical Layer (PHY) Specifications: Enhancements for Very High Throughput for Operation in Bands below 6 GHz*, IEEE 802.11ac Std., 2013.

[27] "Wi-Fi alliance publishes 7 for '17 Wi-Fi predictions," Jan. 2017.

[28] B. P. Crow, I. Widjaja, J. G. Kim, and P. T. Sakai, "IEEE 802.11 wireless local area networks," *IEEE Communications Magazine*, vol. 35, no. 9, pp. 116–126, Sep. 1997.

[29] G. Bianchi, "Performance analysis of the IEEE 802.11 distributed coordination function," *IEEE Journal on Selected Areas in Communications*, vol. 18, no. 3, pp. 535–547, March 2000.

[30] M. Murad and A. M. Eltawil, "A simple full-duplex MAC protocol exploiting asymmetric traffic loads in WiFi systems," in *2017 IEEE Wireless Communications and Networking Conference (WCNC)*, March 2017, pp. 1–6.

[31] "Cisco visual networking index," Feb. 2017.

[32] "The zettabyte era: trends and analysis," Jun. 2017.

[33] M. Luvisotto, A. Sadeghi, F. Lahouti, S. Vitturi, and M. Zorzi, "RCFD: A novel channel access scheme for full-duplex wireless networks based on contention in time and frequency domains," *IEEE Transactions on Mobile Computing*, vol. 17, no. 10, pp. 2381–2395, Oct 2018.

[34] H. Zuo, Y. Sun, S. Li, Q. Cao, Y. Chen, W. Shi, and X. Wang, "A distributed IBFD MAC mechanism and non-saturation throughput analysis for wireless networks," in *13th International Wireless Communications and Mobile Computing Conference (IWCMC)*, June 2017, pp. 1851–1856.

[35] Y. Liao, K. Bian, L. Song, and Z. Han, "Full-duplex MAC protocol design and analysis," *IEEE Communications Letters*, vol. 19, no. 7, pp. 1185–1188, July 2015.

[36] D. Marlali and O. Gurbuz, "Design and performance analysis of a full-duplex MAC protocol for wireless local area networks," *Ad Hoc Networks*, vol. 67, pp. 53 – 67, 2017.

[37] E. Askari and S. Aissa, "Single-band full-duplex MAC protocol for distributed access networks," *IET Communications*, vol. 8, no. 10, pp. 1663–1673, July 2014.

[38] A. Tang and X. Wang, "A-duplex: Medium access control for efficient coexistence between full-duplex and half-duplex communications," *IEEE Transactions on Wireless Communications*, vol. 14, no. 10, pp. 5871–5885, Oct 2015.

[39] R. Doost-Mohammady, M. Y. Naderi, and K. R. Chowdhury, "Performance analysis of CSMA/CA based medium access in full duplex wireless communications," *IEEE Transactions on Mobile Computing*, vol. 15, no. 6, pp. 1457–1470, June 2016.

[40] K. Lee and J. Yoo, "Performance of the full-duplex MAC protocol in non-saturated conditions," *IEEE Communications Letters*, vol. 21, no. 8, pp. 1827–1830, Aug 2017.

[41] J. Hu, B. Di, Y. Liao, K. Bian, and L. Song, "Hybrid MAC protocol design and optimization for full duplex Wi-Fi networks," *IEEE Transactions on Wireless Communications*, vol. 17, no. 6, pp. 3615–3630, June 2018.

[42] H. Zuo, Y. Sun, S. Li, Q. Cao, H. Xu, and G. Zhou, "A distributed medium access mechanism for in-band full-duplex wireless networks," in *2016 International Wireless Communications and Mobile Computing Conference (IWCMC)*, Sept 2016, pp. 958–963.

[43] H. J. Yang, H. W. Park, and H. Jin, "Performance analysis of infrastructure WLANs with multi-packet reception and full-duplex radio," in *2015 International Conference on Information and Communication Technology Convergence (ICTC)*, Oct 2015, pp. 1307–1311.

[44] Y. Liao, B. Di, K. Bian, L. Song, D. Niyato, and Z. Han, "Cross-layer protocol design for distributed full-duplex network," in *2015 IEEE Global Communications Conference (GLOBECOM)*, Dec 2015, pp. 1–6.

[45] R. Liao, B. Bellalta, and M. Oliver, "Modelling and enhancing full-duplex MAC for single-hop 802.11 wireless networks," *IEEE Wireless Communications Letters*, vol. 4, no. 4, pp. 349–352, Aug 2015.

[46] I. Tinnirello, G. Bianchi, and Y. Xiao, "Refinements on IEEE 802.11 distributed coordination function modeling approaches," *IEEE Transactions on Vehicular Technology*, vol. 59, no. 3, pp. 1055–1067, March 2010.

[47] M. Murad and A. M. Eltawil, "Collision tolerance and throughput gain in full-duplex IEEE 802.11 DCF," in *2018 IEEE International Conference on Communications (ICC)*, May 2018, pp. 1–6.

[48] G. Bianchi, S. Choi, and I. Tinnirello, "Performance study of IEEE 802.11 DCF and IEEE 802.11e EDCA," in *Emerging technologies in wireless LANs: theory, design, and deployment*, B. Bing, Ed. New York, NY: Cambridge University Press, 2008, ch. 4, p. 83.

[49] D. P. Bertsekas and R. G. Gallager, *Data Networks*. New Jersey, NJ: Prentice-Hall International, 1992.

[50] *Wireless LAN Medium Access Control (MAC) and Physical Layer (PHY) Specifications: Enhancements for Higher Throughput*, IEEE 802.11n Std., 2009.

[51] R. Karmakar, S. Chattopadhyay, and S. Chakraborty, "Impact of IEEE 802.11n/ac PHY/MAC high throughput enhancements on transport and application protocols - a survey," *IEEE Communications Surveys Tutorials*, vol. 19, no. 4, pp. 2050–2091, 2017.

[52] E. Perahia and R. Stacey, *Next Generation Wireless LANs 802.11n and 802.11ac*. New York, NY: Cambridge University Press, 2013.

[53] S.-L. Tsao and C.-H. Huang, "A survey of energy efficient MAC protocols for IEEE 802.11 WLAN," *Computer Communications*, vol. 34, no. 1, pp. 54–67, 2011.

[54] C. K. Alexander and M. N. O. Sadiku, *Fundamentals of Electric Circuits*. McGraw-Hill Education, 2017.

[55] M. Ergen and P. Varaiya, "Decomposition of energy consumption in ieee 802.11," in *2007 IEEE International Conference on Communications*, June 2007, pp. 403–408.

[56] M. Murad and A. M. Eltawil, "Performance analysis and enhancements for in-band full-duplex wireless local area networks," March 2019. [Online]. Available: https://arxiv.org/abs/1903.11720

[57] O. Lee, J. Kim, and S. Choi, "Wizizz: Energy efficient bandwidth management in IEEE 802.11ac wireless networks," in *2015 12th Annual IEEE International Conference on Sensing, Communication, and Networking (SECON)*, June 2015, pp. 136–144.

[58] M. Kobayashi, R. Murakami, K. Kizaki, S. Saruwatari, and T. Watanabe, "Wireless full-duplex medium access control for enhancing energy efficiency," *IEEE Transactions on Green Communications and Networking*, vol. 2, no. 1, pp. 205–221, March 2018.

[59] A. H. Gazestani, S. A. Ghorashi, B. Mousavinasab, and M. Shikh-Bahaei, "A survey on implementation and applications of full duplex wireless communications," *Physical Communication*, vol. 34, pp. 121 – 134, 2019.

[60] M. Luvisotto, F. Tramarin, and S. Vitturi, "Assessing the impact of full-duplex wireless in real-time industrial networks," in *IECON 2018 - 44th Annual Conference of the IEEE Industrial Electronics Society*, Oct 2018, pp. 4119–4124.

[61] B. Bellalta, "IEEE 802.11ax: Wireless networking in high-density WLANs," Webinar, Wireless Networking Group at Universitat Pompeu Fabra, Barcelona, March 2017.

[62] K. Oteri, "Rosemont meeting minutes," IEEE 802.11 Technical Interest Group on Full Duplex, Meeting Minutes IEEE 802.11-18/0574r0, March 2018.

[63] Y. Xin *et al.*, "Technical report on full duplex for 802.11," IEEE 802.11 Technical Interest Group on Full Duplex, Tech. Rep. IEEE 802.11-18/0498r8, September 2018.

[64] K. Oteri and Y. Xin, "San Diego meeting minutes," IEEE 802.11 Technical Interest Group on Full Duplex, Meeting Minutes IEEE 802.11-18/2076r0, November 2018.

[65] R. K. Jain, D.-M. W. Chiu, and W. R. Hawe, "A quantitative measure of fairness and discrimination," *Eastern Research Laboratory, Digital Equipment Corporation: Hudson, MA, USA*, pp. 2–7, 1984.

[66] F. P. Kelly, A. K. Maulloo, and D. K. H. Tan, "Rate control for communication networks: shadow prices, proportional fairness and stability," *Journal of the Operational Research Society*, vol. 49, no. 3, pp. 237–252, Mar 1998.

[67] J. Mo and J. Walrand, "Fair end-to-end window-based congestion control," *IEEE/ACM Transactions on Networking*, vol. 8, no. 05, pp. 556–567, Sep 2000.

[68] S. H. Low and D. E. Lapsley, "Optimization flow control-I: basic algorithm and convergence," *IEEE/ACM Transactions on Networking*, vol. 7, no. 6, pp. 861–874, Dec 1999.

[69] L. Song, Y. Li, and Z. Han, "Game-theoretic resource allocation for full-duplex communications," *IEEE Wireless Communications*, vol. 23, no. 3, pp. 50–56, June 2016.

[70] U. Siddique, H. Tabassum, and E. Hossain, "Adaptive in-band self-backhauling for full-duplex small cells," in *2015 IEEE International Conference on Communication Workshop (ICCW)*, June 2015, pp. 44–49.

[71] S. Wu, H. Guo, J. Xu, S. Zhu, and H. Wang, "In-band full duplex wireless communications and networking for IoT devices: Progress, challenges and opportunities," *Future Generation Computer Systems*, vol. 92, pp. 705 – 714, 2019.

[72] G. J. Sutton, J. Zeng, R. P. Liu, W. Ni, D. N. Nguyen, B. A. Jayawickrama, X. Huang, M. Abolhasan, Z. Zhang, E. Dutkiewicz, and T. Lv, "Enabling technologies for ultra-reliable and low latency communications: From PHY and MAC layer perspectives," *IEEE Communications Surveys Tutorials*, pp. 1–1, 2019.

Appendix A

Derivations of $b_{i,0}$ and $b_{0,0}$

Start with calculating $b_{1,0}$ in terms of $b_{0,0}$ based on Fig. 4.2

$$\begin{aligned}
b_{1,0} &= b_{0,0}\frac{p}{W_1} + b_{1,1}\cdot\alpha \\
&= b_{0,0}\frac{p}{W_1} + \alpha\cdot(b_{0,0}\frac{p}{W_1} + \alpha\cdot b_{1,2}) \\
&= b_{0,0}\frac{p}{W_1} + \alpha\cdot b_{0,0}\frac{p}{W_1} + \alpha^2\cdot b_{1,2} \\
&= b_{0,0}\frac{p}{W_1}(1+\alpha+\alpha^2+...+\alpha^{W_1-2}) + \alpha^{W_1-1}\cdot b_{1,W_1-1} \\
&= b_{0,0}\frac{p}{W_1}(1+\alpha+\alpha^2+...+\alpha^{W_1-2}) + \alpha^{W_1-1}\cdot b_{0,0}\frac{p}{W_1} \\
&= \frac{b_{0,0}\cdot p}{W_1}\sum_{j_1=0}^{W_1-1}\alpha^{j_1} \\
&= \frac{b_{0,0}\cdot p}{W_1}\cdot\frac{1-\alpha^{W_1}}{1-\alpha}
\end{aligned} \tag{A.1}$$

based on resolving the sum of the geometric series. Similarly, calculate $b_{2,0}$ and substitute for $b_{1,0}$ from (A.1)

$$\begin{aligned} b_{2,0} &= \frac{b_{1,0}\cdot p}{W_2}\sum_{j_2=0}^{W_2-1}\alpha^{j_2} = \frac{b_{0,0}\cdot p}{W_1}\cdot\frac{1-\alpha^{W_1}}{1-\alpha}\cdot\frac{p}{W_2}\cdot\frac{1-\alpha^{W_2}}{1-\alpha} \\ &= \frac{b_{0,0}\cdot p^2}{W_1\cdot W_2}\cdot\frac{(1-\alpha^{W_1})(1-\alpha^{W_2})}{(1-\alpha)^2}. \end{aligned} \tag{A.2}$$

Noticing the pattern in $b_{1,0}$ and $b_{2,0}$, $b_{i,0}$ can be written as

$$\Rightarrow b_{i,0} = b_{0,0}(\frac{p}{1-\alpha})^i\prod_{j=1}^{i}\frac{1-\alpha^{W_j}}{W_j}, 1\le i\le m. \tag{A.3}$$

For $b_{0,0}$, it can directly be deduced from Fig. 4.2 that

$$\begin{aligned} b_{0,0} &= \sum_{i=0}^{m} b_{i,0}\cdot(1-p)\cdot\frac{1}{W_0} + \sum_{i=0}^{m}\sum_{k=1}^{W_i-1} b_{i,k}\cdot\beta\cdot\frac{1}{W_0} + b_{m,0}\cdot p\cdot\frac{1}{W_0} + \alpha\cdot b_{0,1} \\ &= \tau\cdot(1-p)\cdot\frac{1}{W_0} + (1-\tau)\cdot\beta\cdot\frac{1}{W_0} + b_{m,0}\cdot p\cdot\frac{1}{W_0} + \alpha\cdot b_{0,1} \\ &= \underbrace{\frac{\tau(\alpha-p)+1-\alpha+p\cdot b_{m,0}}{W_0}}_{Z} + \alpha\cdot b_{0,1} \\ &= Z + \alpha\cdot(Z+\alpha\cdot b_{0,2}) = Z(1+\alpha)+\alpha^2\cdot b_{0,2} \\ &= Z(1+\alpha+\alpha^2+...+\alpha^{W_0-2}) + \alpha^{W_0-1}\cdot\underbrace{b_{0,W_0-1}}_{Z} \\ &= Z\sum_{j=0}^{W_0-1}\alpha^j = Z\cdot\frac{1-\alpha^{W_0}}{1-\alpha} \\ &= \frac{1-\alpha^{W_0}}{1-\alpha}\frac{\alpha-p}{W_0}\cdot\tau + \frac{1-\alpha^{W_0}}{W_0} + \frac{1-\alpha^{W_0}}{1-\alpha}\frac{p\cdot b_{m,0}}{W_0}. \end{aligned} \tag{A.4}$$

By substituting the expression for $b_{m,0}$ from (A.3) in (A.4), $b_{0,0}$ becomes

$$b_{0,0} = \frac{1-\alpha^{W_0}}{W_0}\left[\frac{\alpha-p}{1-\alpha}\cdot\tau+1\right] + \frac{1-\alpha^{W_0}}{(1-\alpha)W_0}\cdot p\cdot b_{0,0}(\frac{p}{1-\alpha})^m\prod_{j=1}^{m}\frac{1-\alpha^{W_j}}{W_j} \tag{A.5}$$

$$\Rightarrow b_{0,0} = \frac{\frac{1-\alpha^{W_0}}{W_0}\left[\frac{\alpha-p}{1-\alpha}\cdot\tau+1\right]}{1-(\frac{p}{1-\alpha})^{m+1}\prod_{j=0}^{m}\frac{1-\alpha^{W_j}}{W_j}}. \tag{A.6}$$

Appendix B

Derivation of P_s^{IBFD}

Based on the four cases of the conditional probabilities given for P_s^{IBFD}

$$\begin{aligned} P_s^{IBFD} &= \frac{\tau_{AP}(1-\tau_{STA})^{n-1}}{P_{tr}^{IBFD}} + \frac{(n-1)\tau_{STA}(1-\tau_{AP})(1-\tau_{STA})^{n-2}}{P_{tr}^{IBFD}} \\ &+ \frac{1}{n}\cdot\frac{1}{n-1}\cdot\frac{\tau_{AP}\tau_{STA}(1-\tau_{STA})^{n-2}}{P_{tr}^{IBFD}} + \frac{n-1}{n}\cdot\frac{1}{n-1}\cdot\frac{\tau_{AP}\tau_{STA}(1-\tau_{STA})^{n-2}}{P_{tr}^{IBFD}} \\ &= \frac{\tau_{AP}(\overline{\tau}_{STA})^{n-1}}{P_{tr}^{IBFD}} + \frac{(n-1)\tau_{STA}(\overline{\tau}_{AP})(\overline{\tau}_{STA})^{n-2}}{P_{tr}^{IBFD}} \\ &+ \frac{1}{n(n-1)}\cdot\frac{\tau_{AP}\tau_{STA}(\overline{\tau}_{STA})^{n-2}}{P_{tr}^{IBFD}} + \frac{1}{n}\cdot\frac{\tau_{AP}\tau_{STA}(\overline{\tau}_{STA})^{n-2}}{P_{tr}^{IBFD}}. \end{aligned} \tag{B.1}$$

According to equation (4.35),

$$P_{tr}^{IBFD} = 1 - [(1-\tau_{AP})(1-\tau_{STA})^{n-1}] = 1 - [(\overline{\tau}_{AP})(\overline{\tau}_{STA})^{n-1}] \tag{B.2}$$

$$\Rightarrow P_s^{IBFD} = \frac{\tau_{AP}(\overline{\tau}_{STA})^{n-1} + (n-1)\tau_{STA}(\overline{\tau}_{AP})(\overline{\tau}_{STA})^{n-2}}{1 - [(\overline{\tau}_{AP})(\overline{\tau}_{STA})^{n-1}]} \tag{B.3}$$

$$+ \frac{\tau_{AP}\tau_{STA}(\overline{\tau}_{STA})^{n-2}}{(n-1)\big\{1 - [(\overline{\tau}_{AP})(\overline{\tau}_{STA})^{n-1}]\big\}}.$$

Appendix C

Flow Chart of IEEE 802.11 DCF

The following flow chart illustrates parts of IEEE 802.11 DCF mechanisms. It is useful to construct a software simulator like the one used in this dissertation.

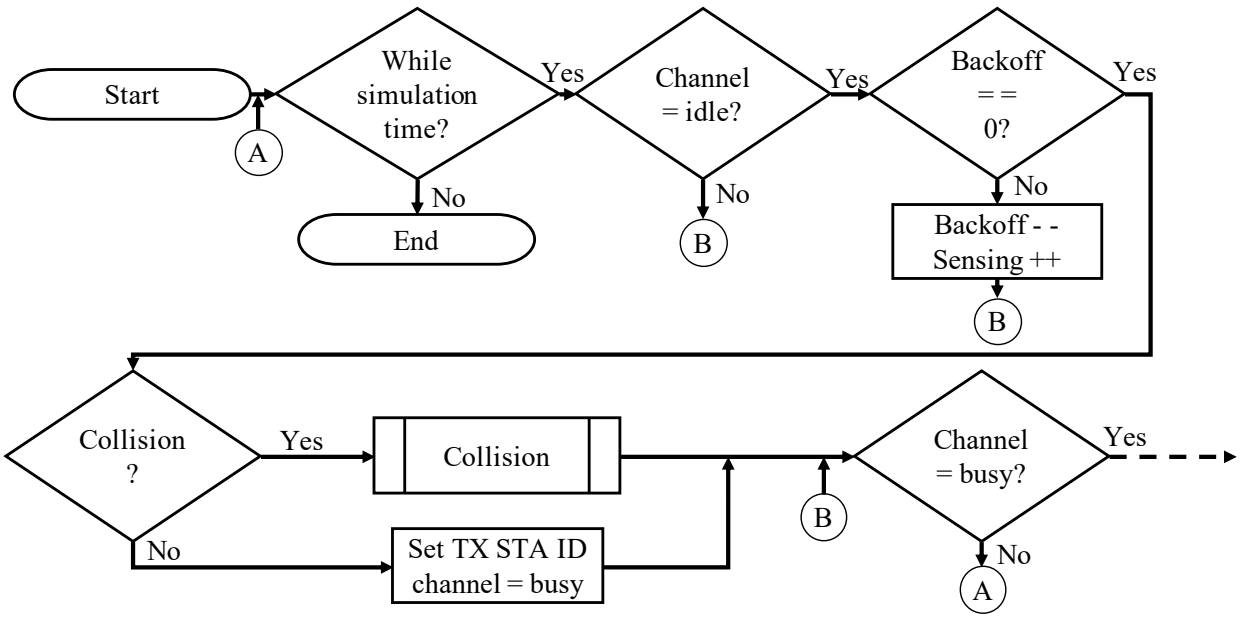

Figure C.1: Flow Chart of IEEE 802.11 DCF - Part 1 of 3

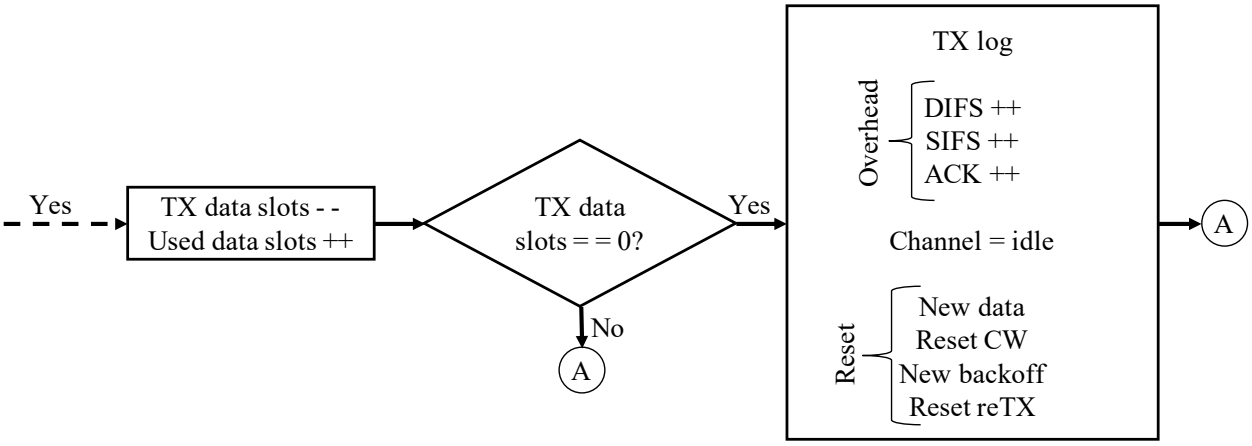

Figure C.2: Flow Chart of IEEE 802.11 DCF - Part 2 of 3

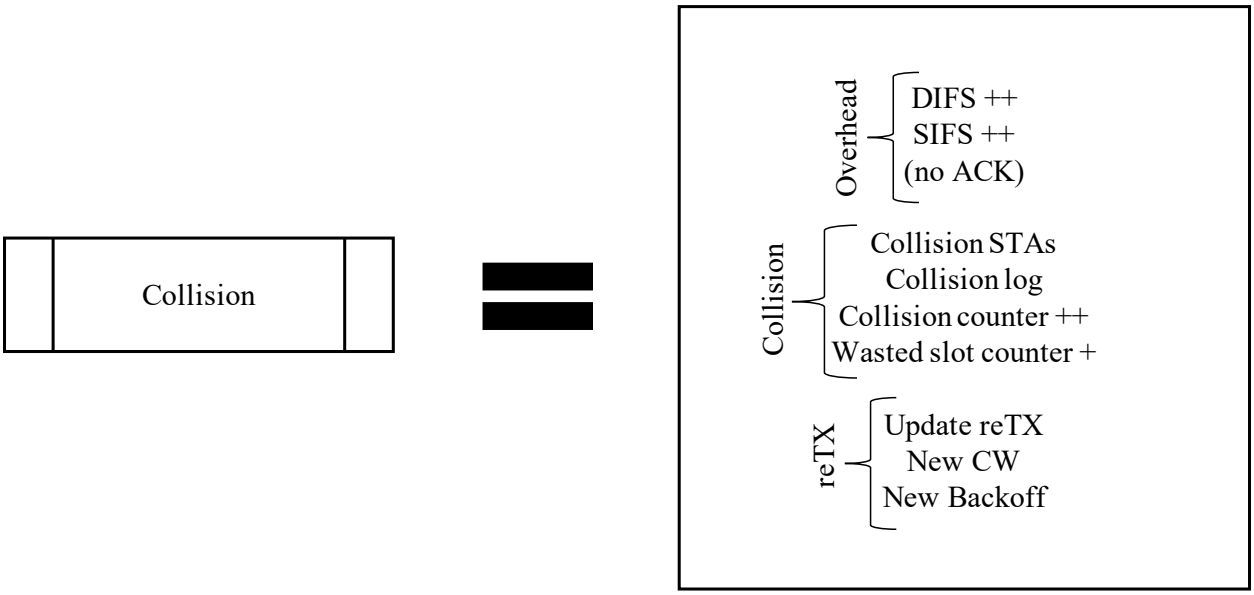

Figure C.3: Flow Chart of IEEE 802.11 DCF - Part 3 of 3

Appendix D

Power Calculations for IEEE 802.11ac

Using the model presented in [57],

$$\begin{aligned}
\omega_{\text{TX}} &= B(\beta_1 N_{tx} + \beta_2 N_{ss} \cdot \log_2 B + f_{tx}(N_{ss})) + \beta_3 N_{tx} + \beta_4 r + \beta_5 P_t + P_f \\
&= 80(0.022 \times 2 + 0.038 \times 2 \times \log_2(80) + 1.68) \\
&+ 802.2 \times 2 + 0.001 \times 234 + 4.352 \times 100 + 472.1 \\
&= \underline{2.6338\text{W}}
\end{aligned}$$

$$\begin{aligned}
\omega_{\text{RX}} &= B(\alpha_1 N_{rx} + \alpha_2 N_{rx} \cdot \log_2 B + f_{rx}(N_{ss})) + \alpha_3 N_{rx} + \alpha_4 r + P_f \\
&= 80(0.035 \times 2 + 0.48 \times 2 \times \log_2(80) + 4.4) + 82.4 \times 2 + 0.47 \times 234 + 472.1 \\
&= \underline{1.5900\text{W}}
\end{aligned}$$

$$\begin{aligned}\omega_{\mathrm{d}} &= i_1 N_{rx} B + i_2 N_{rx} + P_f \\ &= 1.978 \times 2 \times 80 + 79.9 \times 2 + 472.1 \\ &= \underline{0.9484\mathrm{W}}\end{aligned}$$